D4.8 SPECTRUM REGULATION ANALYSIS FOR 6G NTN SCENARIOS

Revision: v.1.0

Work package	WP4
Task	Task 4.3
Due date	31/12/2025
Submission date	12/01/2026
Deliverable lead	TH-SIX
Version	0.1
Authors	LETURC Xavier (TH-SIX), TONG Sorya (TH-SIX), PANAITOPOL Dorin (TH-SIX), KHALIFA Ebraam (QCOM), FU Xiaotian (ERIF), GHASEMIFARD Fatemeh (ERIS)
Reviewers	
Abstract	One of the goals of the 6G-NTN project is to combine terrestrial networks (TN) and non-terrestrial networks (NTN) seamlessly for improved user experience, latency and availability across the globe. It is thus necessary to examine the different coexistence scenarios and offer interference mitigation solutions for each case. The deliverable D4.8 is updated from D4.7 with coexistence simulation results between TN and NTN operating on adjacent frequencies in the Q/V and the C-bands, and between two NTN operating at different orbits. The coexistence studies follow the 3GPP procedure, and provide as outputs requirements for the adjacent channel leakage ratio (ACLR) and adjacent channel selectivity (ACS) of the satellite and the NTN user equipments.
Keywords	6G, NTN, Interference mitigation, Coexistence scenarios, Spectrum allocation

Grant Agreement No.: 101096479
Call: HORIZON-JU-SNS-2022
Topic: HORIZON-JU-SNS-2022-STREAM-B-01-03
Type of action: HORIZON-JU-RIA

Document Revision History

Version	Date	Description of change	List of contributor(s)
V0.1	14/10/2025	Version ready for internal review	TH-SIX, QCOM, ERIS
V1.0	12/01/2026	Approved for submission	Alessandro Vanelli-Coralli (UniBo)

DISCLAIMER

Project funded by

Schweizerische Eidgenossenschaft
Confédération suisse
Confederazione Svizzera
Confederaziun svizra

Swiss Confederation

Federal Department of Economic Affairs, Education and Research EAER
State Secretariat for Education, Research and Innovation SERI

6G-NTN (*6G Non Terrestrial Network*) project has received funding from the **Smart Networks and Services Joint Undertaking (SNS JU)** under the European Union's **Horizon Europe research and innovation programme** under Grant Agreement No 101096479.

COPYRIGHT NOTICE

Project co-funded by the European Commission in the Horizon Europe Programme		
Nature of the deliverable:	**R***	
Dissemination Level		
PU	*Public, fully open, e.g. web (Deliverables flagged as public will be automatically published in CORDIS project's page)*	✓
SEN	*Sensitive, limited under the conditions of the Grant Agreement*	
Classified R-UE/ EU-R	*EU RESTRICTED under the Commission Decision No2015/ 444*	
Classified C-UE/ EU-C	*EU CONFIDENTIAL under the Commission Decision No2015/ 444*	
Classified S-UE/ EU-S	*EU SECRET under the Commission Decision No2015/ 444*	

* R: Document, report (excluding the periodic and final reports)

DEM: Demonstrator, pilot, prototype, plan designs

DEC: Websites, patents filing, press & media actions, videos, etc.

DATA: Data sets, microdata, etc.

DMP: Data management plan

ETHICS: Deliverables related to ethics issues.

SECURITY: Deliverables related to security issues

OTHER: Software, technical diagram, algorithms, models, etc.

EXECUTIVE SUMMARY

This deliverable is the third out of three planned deliverables (D4.4, D4.7, D4.8) related to spectrum regulation analysis for 6G-NTN (6G-Non-Terrestrial Networks) scenarios (Task 4.3) addressing objective 9 from the 6G-NTN project's Description of the work.

This document first provides an analysis of spectrum regulation of the 6G-NTN spectrum bands and their utilization.

Then, results from a coexistence study between Terrestrial Network (TN) and Non-Terrestrial Network (NTN) operating on adjacent frequencies in both the Q/V and the C-band are provided. This study has been performed on several scenarios for different orbits for the satellite, and for different satellite elevations for each band. The results enable to provide recommendations regarding the adjacent channel leakage ratio (ACLR) and adjacent channel selectivity (ACS) parameters of the satellite and the NTN user equipment (UE) in these bands. Moreover, additional coexistence techniques were simulated for the more challenging coexistence scenario in the Q/V-band.

Finally, results from a coexistence study between two NTN layers operating in the Q/V-band are provided. This study had been performed under two assumptions: either the two satellites operate on the same frequency band, or on adjacent frequency bands. The obtained results enable to provide recommendations for the exclusion angle between the two satellite boresight as a function of the two satellites ACLR and ACS.

Co-funded by the European Union

TABLE OF CONTENTS

LIST OF FIGURES

LIST OF TABLES

ABBREVIATIONS

3GPP	3rd Generation Partnership Project
AAS	Active Antenna Systems
ABS	Almost Blank Subframes
ACIR	Adjacent Channel Interference Ratio
ACLR	Adjacent Channel Leakage Ratio
ACS	Adjacent Channel Selectivity
ACU	Antenna Control Unit
ATA	Advanced TPC algorithm
A-ESIM	Aeronautical-Earth Station In Motion
BF-OFDM	Block Filtered-Orthogonal Frequency Division Multiplexing
BS	Base Station
BTA	Basic TPC algorithm
BUC	Block Up-Converter
BW	BandWidth
BWP	BandWidth Part
CA	Carrier Aggregation
CC	Carrier Components
CDF	Cumulative Distribution Function
CEPT	European Conference of Postal and Telecommunications Administrations
CFR	Code of Federal Regulations
CHO	Conditional HandOver
CIR	Carrier-to-Interference Ratio
CL	Coupling Loss
CNIR	Carrier-to-Noise-and-Interference Ratio
CNR	Carrier-to-Noise Ratio
CoMP	Coordinated Multi-Point
CQI	Channel Quality Indicator
CS	Coordinated Scheduling
CSI	Channel State Information
DC	Down Converter
DL	Down Link
DP	Duplexer
DPS	Dynamic Point Selection
DUEL	Deterministic UE Location
ECC	Electronic Communications Committee
eICIC	Enhanced Inter-Cell Interference Coordination
EIRP	Effective Isotropic Radiated Power
ePDCCH	enhanced Physical Downlink Control Channel
EPFD	Equivalent Power Flux Density Limit
ESIM	Earth Station In Motion
FCC	Federal Communications Commission
FDD	Frequency Division Duplex
FeICIC	Further enhanced Inter-Cell Interference Coordination
FFR	Fractional Frequency Reuse
FR	Frequency Range

FRF	Frequency Reuse Factor
FSS	Fixed-Satellite Service
GEO	Geosynchronous Equatorial Orbit
gNB	gNodeB
GSO	Geostationary Satellite Orbit
G/T	antenna Gain to noise Temperature
HetNet	Heterogeneous Networks
HFR	Hard Frequency Reuse
HPA	High Power Amplifier
HPBW	Half Power Beam Width
ICI	Inter-Cell Interference
ICIC	Inter-Cell Interference Coordination
IF	Intermediate Frequency
IM	Interference Measurement
IRC	Interference Rejection Combiner
ISD	Inter-Site Distance
ISL	Inter-Satellite Link
ITU	International Telecommunication Union
ITU-R	ITU Radiocommunication Sector
IUI	Inter-User Interference
JR	Joint Reception
JT	Joint Transmission
LA	Link Adaptation
LEO	Low Earth Orbit
L-ESIM	Land-ESIM
LHCP	Left-Handed Circular Polarisation
LNA	Low Noise Amplifier
LOS	Line Of Sight
LTE	Long Term Evolution
MAC	Medium Access Control
MBS	Multicast and Broadcast Services
MCS	Modulation and Coding Scheme
MFCN	Mobile/Fixed Communications Networks
MIMO	Multiple-Input Multiple-Output
MMSE	Minimum Mean Square Error
MS	Mobile Station
NF	Noise Figure
NGSO	Non-Geostationary Satellite Orbit
NLOS	Non-Line Of Sight
NR	New Radio
NTN	Non-Terrestrial Network
NZP CSI-RS	Non-Zero-power CSI Reference Signal
OpenAMIP	Open Antenna to Modem Interface Protocol
OpenBMIP	Open BUC Modem Interface Protocol
PA	Power Amplifier
PCC	Primary Carrier Components
PCell	Primary Cell
PDCCH	Physical Downlink Control Channel

PDSCH	Physical Downlink Shared Channel
PFD	Power Flux Density
PHY	PHYsical layer
PL	Path Loss
PRB	Physical Resource Block
PUSCH	Physical Uplink Shared CHannel
RB	Resource Block
RE	Resource Element
RF	Radio Frequency
RHCP	Right-Handed Circular Polarisation
RMa	Rural Macro
RP	Reception Point
RP-ABS	Reduced Power Almost Blank Sub frames
RRM	Radio Resource Management
RS	Reference Signal
RUEL	Random UE Location
SAN	Satellite Access Network
SCC	Secondary Carrier Components
SCell	Secondary Cell
SF	Scaling Factor
SINR	Signal-to-Interference-plus-Noise Ratio
SNR	Signal-to-Noise Ratio
SNS	Smart Networks and Services
TAB	Transceiver Array Boundary
TDD	Time Division Duplex
TN	Terrestrial Network
TP	Transmission Point
TPC	Transmit Power Control
TR	Technical Report
TS	Technical Specification
TSG-RAN	Technical Specification Groups-Radio Access Network
TSG-SA	Technical Specification Groups-System Aspects
UC	Up Converter
UE	User Equipment
UL	Up Link
ULA	Uniformly Distributed Array
UMa	Urban Macro
UMi	Urban Micro
URLLC	Ultra-Reliable Low Latency Communications
UT	User Terminal
UTC	Coordinated Universal Time
VMR	Vehicle Mounted Relay
VSAT	Very Small Aperture Terminal
WRC	World Radiocommunication Conferences

1 INTRODUCTION

Through the use of satellite networks, 6G NTN will allow devices to access connectivity with increased availability across the globe, enabling new use cases. Those devices include handheld User Equipment (UE), mounted UE, etc., please refer to section 2.5 for some examples of UEs considered in the project, or Deliverable 2.2 for a complete view.

6G-NTN project aims to combine terrestrial and non-terrestrial networks seamlessly, targeting ubiquitous connectivity, lower latency for TN-NTN mobility and efficient use of networks. It is thus necessary to examine the coexistence scenarios envisaged in novel spectrum regulations to address both 6G NTN and 6G TN challenges and implement spectrum management techniques and interference mitigation solutions for each case.

The present deliverable outlines preliminary analysis and use cases in order to identify potential novel spectrum allocation. Moreover, NTN-TN adjacent band coexistence analysis is essential for:

- Definition of Radio Frequency (RF) core requirements of NTN (Adjacent Channel Leakage Ratio (ACLR), Adjacent Channel Selectivity (ACS), etc.);
- Introduction of new NTN bands.

1.1 SCOPE AND OBJECTIVES

The objectives are:

- To propose and validate new spectrum coexistence scenarios and methods to support efficient spectrum utilisation from various incumbents;
- To evaluate the interference scenarios considered by novel spectrum regulations to address the 6G NTN challenges.

In order to fulfil these objectives, the planned work for the T4.3 task includes:

- NTN-TN coexistence scenarios identification to specifically address Q/V and C frequency bands;
- Channel model identification;
- Simulations & evaluation of different coexistence methods;
- Identify NTN related (RF/ Radio Resource Management (RRM)) requirements, and increase the NTN end-user throughput through spectrum sharing and multiple NTN/TN access point connectivity.

This deliverable is also in line with 3GPP Rel-19 5G NR (New Radio) NTN proposed topics related to:

- TSG-RAN (Technical Specification Groups-Radio Access Network):
  - Improve the service experience
    - Coverage enhancements (DownLink (DL) and possibly UpLink (UL))
    - NTN/TN Mobility enhancement in connected mode (e.g., Conditional HandOver (CHO))

- New Notification/Alert message for UE terminating calls with UE in poor Signal-to-Noise Ratio (SNR) conditions preventing paging message reception

- New capabilities (band agnostic)
  - Support of Regenerative payloads (i.e., with Inter-Satellite Link (ISL))
  - Support of Multicast and Broadcast Services (MBS)
  - Asynchronous multi-connectivity (e.g., between two satellite access i.e., Non-Geostationary Satellite Orbit (NGSO) and Geostationary Satellite Orbit (GSO); possibly between NTN/TN) for above 10 GHz only
  - Support for alleviating discontinuous coverage (mitigating coverage holes during deployment/operation of constellation)

➲ TSG-SA (Technical Specification Groups-System Aspects)

- Improve delay
  - Store and Forward Satellite operation for delay-tolerant communication services
  - UE-Satellite-UE communication (without going through the ground network)
- Improve service capability
  - Dual steer NTN/TN
  - MBS via NTN
  - Vehicle Mounted Relay (VMR) in NTN

According to the 3GPP roadmap for 6G, a 6G study phase is envisioned in Rel-20 and 6G normalisation phase is expected in Rel-21 assuming 18 months release plan. This 3GPP roadmap depicted in ***Figure 1*** is therefore aligned with 6G-NTN Smart Networks and Services (SNS) timeline, whose end is in the end of 2025.

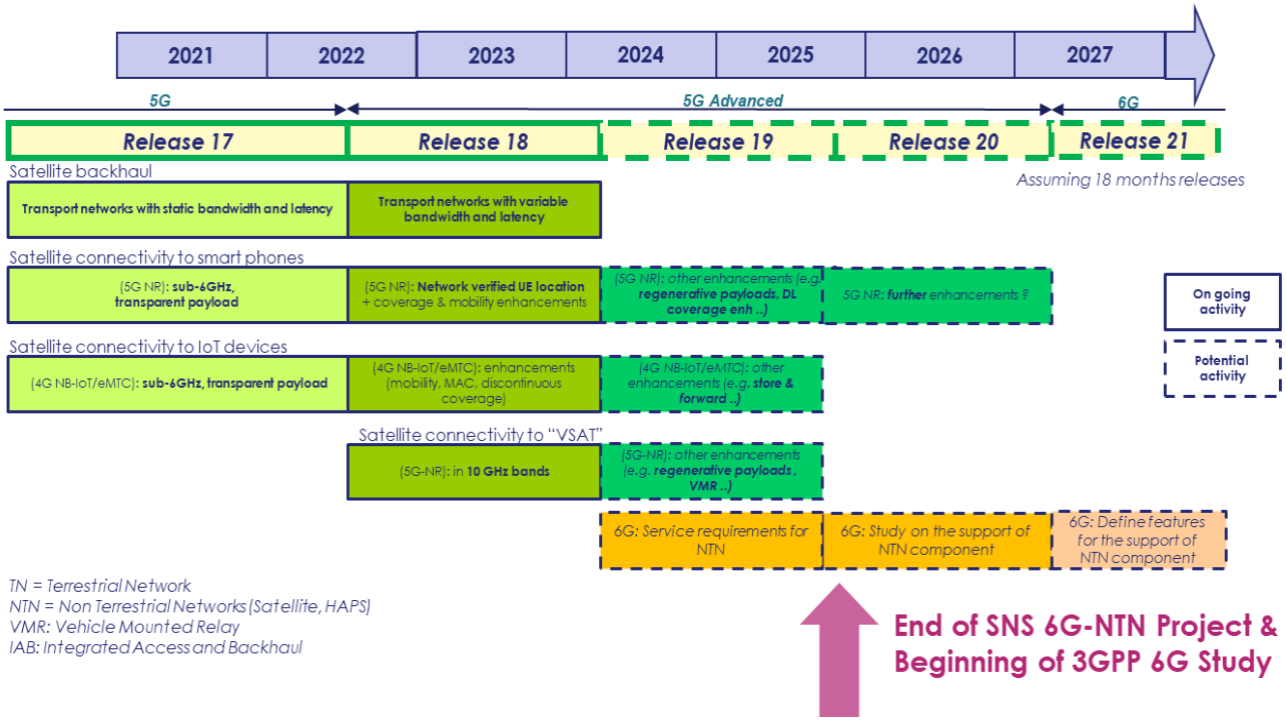

Figure 1: *3GPP Roadmap for 6G*

1.2 RELATION TO OTHER WORK PACKAGES IN 6G-NTN

The present deliverable is dedicated to T4.3, which is one of the tasks in Work Package WP4. The work of T4.3 is coordinated with other WPs for inputs, namely:

- WP2: D2.5 '*Report on Regulatory requirements*' (T2.5) for inputs on frequency bands and regulation
- WP3: D3.1 '*Report on 3D multi layered NTN architecture*' (T3.1) and subsequent deliverables for inputs on the 6G-NTN architecture.

1.3 STRUCTURE OF THE DOCUMENT

As this deliverable expands upon the previous ones (D4.4 and D4.7), some existing sections have been kept unchanged while other sections related to coexistence simulations results have been added. This deliverable is structured as follows:

- Section 2 offers an overview on channel model and spectrum allocation for both terrestrial and non-terrestrial components of the 6G NTN architecture. This section had been updated since the last version of the deliverable with up-to-date spectrum regulation analysis in Section 2.2.
- Section 3 introduces the different frequency bands use cases and respective coexistence scenarios that will be further studied in Q/V and C frequency bands.
- Section 4 reports the different parameters for NTN UE (User Equipment).
- Section 5 reports the different parameters for TN BS (Base Station) and UE, including the values for TN Adjacent Channel Leakage Ratio (ACLR) and Adjacent Channel Selectivity (ACS) in Q/V-band.

- Section 6 describes the parameters for NTN SAN (Satellite Access Network).
- Section 7 reports the parameters for TN BS.
- Section 8 provides a state-of-the-art for strategies for coexistence and interference mitigation techniques.
- Section 9 introduces the metrics and purpose for the NTN and TN calibration done in this deliverable.
- Section 10 presents the NTN calibration methodology and results for Q/V-band.
- Section 11 presents the TN calibration methodology and results for Q/V-band.
- Section 12 adds further precisions on parameters and methodologies adopted for coexistence scenarios.

The previous Sections were already available in the previous version of this deliverable, i.e. in D4.7. The following new sections are related to the coexistence simulation results between TN and NTN and between several NTN layers:

- Section 13 provides a complete description of the coexistence simulation methodology. The objective is to ensure a self-contained section that could be read (almost) independently from the other ones (with appropriate references) such that a reader interested only on the coexistence results could directly go to this section before going trough the numerical results in the following sections.
- Section 14 provides the coexistence results between TN and NTN in the Q/V-band.
- Section 15 provides the coexistence results between TN and NTN in the C-band.
- Section 16 provides the coexistence simulation results between two satellite layers, which is conducted in the Q/V-band.
- Section 17 provides the conclusions of the document.
- Section 18 is an appendix where various mathematical derivations are relegated, as well as the details of a technical discussion with WP3 related to definition of parameters for the C-band.

All partners contributed to the coexistence simulation study in the Q/V-band in Section 14. TH-SIX simulated the additional coexistence techniques required by one scenario in the Q/V-band (Section 14.3). TH-SIX provided the simulation results from Section 15 and Section 16.

Part of the material presented in this document has been published in [36], which provides results related to the link budget computation in the Q/V-band and in the C-band, and in [37], which provides part of the coexistence results between a GEO and a LEO satellite in the Q/V-band, i.e., part of the material from Section 16.

2 CHANNEL MODEL AND SPECTRUM ALLOCATION

2.1 INTRODUCTION

Before starting the discussion on coexistence scenarios and related parameters, it is first necessary to define the considered frequency bands for this study. In this section, we will explain choices for frequency bands and the international regulations they may be subjected to concerning spectrum allocation.

We provide in what follows an overview on relevant information concerning NTN and TN networks in 3GPP.

2.2 SPECTRUM ALLOCATION, EXISTING BANDS AND STATE-OF-THE-ART

Table 1 provides the up-to-date list of NTN operating bands in FR1 and FR2, as well as the duplex mode. It also indicates in blue the E-UTRA operating bands for satellite access. This table has been obtained by concatenation of information from [1] and [39].

Table 1: *NTN operating bands in FR1 and FR2. The E-UTRA operating bands for satellite access are also provided in blue*

NTN satellite operating band	UL operating band SAN receive / UE transmit $F_{UL,low}$ – $F_{UL,high}$	DL operating band SAN transmit / UE receive $F_{DL,low}$ – $F_{DL,high}$	Specification	Duplex mode
n256	1980 – 2010 MHz	2170 – 2200 MHz	NR Rel-17	FDD
n255	1626.5 – 1660.5 MHz	1525 – 1559 MHz	NR Rel-17	FDD
n512[4]	27.5 – 30.0 GHz	17.3 – 20.2 GHz	NR Rel-18	FDD
n511[5]	28.35 – 30.0 GHz	17.3 – 20.2 GHz	NR Rel-18	FDD
n510[6]	27.5 – 28.35 GHz	17.3 – 20.2 GHz	NR Rel-18	FDD
n254	1610 – 1626.5 MHz	2483.5 – 2500 MHz	NR Rel-18	FDD
256	1980 – 2010 MHz	2170 – 2200 MHz	LTE Rel-18	FDD
255	1626.5 – 1660.5 MHz	1525 – 1559 MHz	LTE Rel-18	FDD
254	1610 – 1626.5 MHz	2483.5 – 2500 MHz	LTE Rel-18	FDD
253[7]	1668 – 1675 MHz	1518 – 1525 MHz	LTE Rel-18	FDD

n253	1668 – 1675 MHz	1518 – 1525 MHz	NR Rel-19	FDD
n252	2000 – 2020 MHz	2180 – 2200 MHz	NR Rel-19	FDD
252	2000 – 2020 MHz	2180 – 2200 MHz	LTE Rel-19	FDD
n251	1626.5 – 1660.5 MHz	1518 – 1559 MHz	NR Rel-19	FDD
n250	1668 – 1675 MHz	1518 – 1559 MHz	NR Rel-19	FDD
249[8]	1616 – 1626.5 MHz	1616 – 1626.5 MHz	LTE Rel-19	TDD
246[9]	N/A	1467 – 1492 MHz	LTE Rel-19	SDO
n248	14.0 – 14.5 GHz	10.7 – 12.75 GHz[2,3]	NR Rel-19	FDD
n509	14.0 – 14.5 GHz	10.7 – 12.75 GHz[2,3]	NR Rel-19	FDD
n247	13.75 – 14.0 GHz	10.7 – 12.75 GHz[2,3]	NR Rel-19	FDD
n508	13.75 – 14.0 GHz	10.7 – 12.75 GHz[2,3]	NR Rel-19	FDD

NOTE 1: Operating band n200 is a reserved value.

NOTE 2: For region 2, the downlink is limited to 10700 – 12700 MHz.

NOTE 3: For the US, the downlink is limited to 10700 – 12200 MHz for Mobile VSAT.

NOTE 4: This band is applicable in the countries subject to or referring to CEPT ECC Decision(05)01 and ECC Decision (13)01.

NOTE 5: This band is applicable in the countries subject to or referring to FCC 47 CFR part 25.

NOTE 6: This band is applicable for Earth Station operations in the USA subject to FCC 47 CFR part 25. FCC rules currently do not include ESIM operations in this band (47 CFR 25.202).

NOTE 7: UE assigned to channels and allocated frequency resources in the lower portion of Band 253 may experience blocking or harmful interference from terrestrial networks in adjacent or nearby frequencies when operating in the proximity with terrestrial base stations.

NOTE 8: Band 249 is defined only for NB-IoT operation.

NOTE 9: Band 246 only applies for LTE-based 5G Broadcast over Geosynchronous Satellite in region 3.

In addition, World Radiocommunication Conferences (WRC) decisions should also be taken into account [5]:

- WRC-15 authorised Earth Station in Motion (ESIM) operations in 19.7-20.2 GHz (space-to-Earth) and 29.5-30.0 GHz (Earth-to-space) under certain conditions, and for GSO systems only.

- WRC-19 authorised ESIM operations in 17.7-19.7 GHz (space-to-Earth) and 27.5-29.5 GHz (Earth-to-space) under certain conditions, and for Geostationary Satellite Orbit (GSO) systems only.
- WRC-23 Agenda item 1.16 on Non-Geostationary Satellite Orbit (NGSO) ESIM Ka Band aims to study and develop technical, operational and regulatory measures, as appropriate, to facilitate the use of the frequency bands 17.7-18.6 GHz and 18.8-19.3 GHz and 19.7-20.2 GHz (space-to-Earth) and 27.5-29.1 GHz and 29.5-30 GHz (Earth-to-space) by non-GSO Fixed-Satellite Service (FSS) ESIM, while ensuring due protection of existing services in those frequency bands, in accordance with Resolution 173 (WRC-19).

For the bands further investigated as part of the 6G-NTN project please refer to deliverable D2.5 '*Report on Regulatory requirements*' in the 6G-NTN project related to band regulations and current spectrum allocation.

2.3 RELEVANT 3GPP NTN INFORMATION

For relevant NTN 3GPP information, please refer to TR 38.811 [6], TR 38.821 [7] and TR 38.863 [3]. For instance, TR 38.821 describes the relationship between Signal-to-Interference-plus-Noise Ratio (SINR)/Carrier-to-noise-and-interference ratio (CNIR) and G/T (antenna Gain to noise Temperature), noise figures as well as other parameters.

Carrier-to-noise-and-interference ratio (CNIR) of transmission link between satellite and UE can be derived by carrier-to-noise ratio (CNR) and carrier-to-interference ratio (CIR) as follows:

$$\mathrm{CNIR\ [dB]} = -10\log_{10}\left(10^{-0.1\mathrm{CNR\ [dB]}} + 10^{-0.1\mathrm{CIR\ [dB]}}\right)$$

The formula for CNR calculation is:

$$\mathrm{CNR\ [dB]} = \mathrm{EIRP\ [dBW]} + \frac{G}{T}\mathrm{[dB/K]} - k\ \mathrm{[dBW/K/Hz]} - PL_{FS}\ \mathrm{[dB]} - PL_{A}\ \mathrm{[dB]} - PL_{SM}\ \mathrm{[dB]} - PL_{SL}[dB] - PL_{AD}\ \mathrm{[dB]} - B\ \mathrm{[dBHz]}$$

where:

- EIRP is Effective Isotropic Radiated Power,
- G/T is antenna-gain-to-noise-temperature,
- k is Boltzmann constant and equals to -228.6 dBW/K/Hz,
- PL_{FS} is free space path loss,
- PL_{A} is atmospheric path loss due to gases and rain fades,
- PL_{SM} is shadowing margin,
- $PL_{SL}[dB]$ is scintillation loss,
- PL_{AD} is additional loss, for example degradation due to feeder links in case of non-regenerative systems,
- B is channel bandwidth.

Antenna-gain-to-noise-temperature G/T can be derived by:

$$G/T\ \mathrm{[dB]} = G_R\ \mathrm{[dBi]} - N_f\ \mathrm{[dB]} - 10\log_{10}\left(T_0\ \mathrm{[K]} + (T_a\ \mathrm{[K]} - T_0\ \mathrm{[K]})10^{-0.1N_f\ \mathrm{[dB]}}\right)$$

where G_R is receive antenna gain, N_f is noise figure, T_0 is ambient temperature and T_a is antenna temperature.

Receive antenna gain G_R can be obtained by

$$G_R\ [\text{dBi}] = \begin{cases} G_{R,e}[\text{dBi}] + 10\log_{10}(N_{R,a}) - L_p[\text{dB}], & \text{array antenna} \\ 10\log_{10}\left(\eta \cdot \pi^2 \cdot \frac{D[m]^2}{\lambda[m]^2}\right), & \text{parabolic antenna} \end{cases}$$

where $G_{R,e}$ is receive antenna element gain, $N_{R,a}$ is the number of receive antenna elements, L_p is polarisation loss, η is the antenna aperture efficiency (a dimensionless parameter with typical values for parabolic antennas from 0.55 to 0.70), D is the equivalent antenna diameter, and λ is the wavelength.

EIRP can be calculated by

$$\text{EIRP}\ [\text{dBW}] = P_T\ [\text{dBW}] - L_C\ [\text{dB}] + G_T\ [\text{dBi}]$$

where P_T is antenna transmit power, L_C is cable loss, and G_T is transmit antenna gain and can be derived by

$$G_T\ [\text{dBi}] = \begin{cases} G_{T,e}\ [\text{dBi}] + 10\log_{10}(N_{T,a}), & \text{array antenna} \\ 10\log_{10}\left(\eta \cdot \pi^2 \cdot \frac{D[m]^2}{\lambda[m]^2}\right), & \text{parabolic antenna} \end{cases}$$

where $G_{T,e}$ is transmit antenna element gain and $N_{T,a}$ is the number of transmit antenna elements.

CIR can be computed similarly as for CNR, but this time by taking into account the interference power instead of the useful transmitted power for wanted communication.

In this case, EIRP of the interferer depends on the transmitted power of the interferer and the antenna gain of the interferer.

Moreover, the path loss of the interferer may be different from the path loss of the useful signal, depending on the scenario. In practice, the antenna gain is a function of the direction of communication and therefore, the antenna gain of the interferer will be different from the antenna gain in the direction of the wanted communication.

With respect to link budget parameters, it is proposed that 6G-NTN project should follow similar methodology as in TR 38.863 [3], with the adaptations required for Q/V-Band with channel models/link budget parameters described in TR 38.811 [6] and TR 38.821 [7].

2.4 RELEVANT 3GPP TN INFORMATION

The relevant information from 3GPP TR 38.901 “Study on channel model for frequencies from 0.5 to 100 GHz” [8] are path loss models and Line of Sight (LOS) probability. Two deployment scenarios are considered: Rural Macro (RMa) and Urban Macro (UMa), each further differentiated between NLOS (Non-Line Of Sight) and LOS scenarios.

2.4.1 Path Loss model

Table 2 summarizes the Path loss models, and ***Figure 2*** illustrates the distance definitions for outdoor User Terminal (UT) [1]and ***Figure 3*** for indoor UT. Note that the shadowing follows a log-normal distribution, whose standard deviation for each scenario is provided in ***Table 2***.

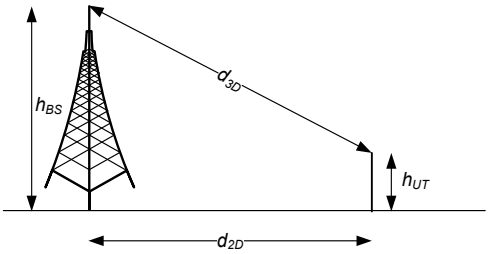

Figure 2: *Definition of d_{2D} and d_{3D} for outdoor UT.*

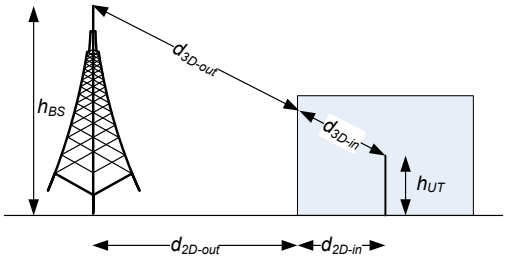

Figure 3: *Definition of $d_{2D\text{-}out}$, $d_{2D\text{-}in}$ and $d_{3D\text{-}out}$, $d_{3D\text{-}in}$ for indoor UT.*

Table 2: *Path loss models*

Scenario	Path loss [dB], f_c is in GHz and d is in m, see note 6	Shadow fading std [dB]	Applicability range, antenna height default values
RMa LOS	$PL_{\text{RMa-LOS}} = \begin{cases} PL_1 & 10\text{m} \le d_{2D} \le d_{BP} \\ PL_2 & d_{BP} \le d_{2D} \le 10\text{km} \end{cases}$, see note 5 $PL_1 = 20\log_{10}(40\pi d_{3D} f_c / 3) + \min(0.03h^{1.72}, 10)\log$ $-\min(0.044h^{1.72}, 14.77) + 0.002\log_{10}(h)d_{3D}$ $PL_2 = PL_1(d_{BP}) + 40\log_{10}(d_{3D} / d_{BP})$	$\sigma_{SF} = 4$ $\sigma_{SF} = 6$	$h_{BS} = 35\text{m}$ $h_{UT} = 1.5\text{m}$ $W = 20\text{m}$ $h = 5\text{m}$ *h = avg. building height* *W = avg. street width* *The applicability ranges:* $5\text{m} \le h \le 50\text{m}$ $5\text{m} \le W \le 50\text{m}$ $10\text{m} \le h_{BS} \le 150\text{m}$ $1\text{m} \le h_{UT} \le 10\text{m}$
RMa NLOS	$PL_{\text{RMa-NLOS}} = \max(PL_{\text{RMa-LOS}}, PL'_{\text{RMa-NLOS}})$ for $10\text{m} \le d_{2D} \le 5\text{km}$ $PL'_{\text{RMa-NLOS}} = 161.04 - 7.1\log_{10}(W) + 7.5\log_{10}(h)$ $-(24.37 - 3.7(h/h_{BS})^2)\log_{10}(h_{BS})$ $+(43.42 - 3.1\log_{10}(h_{BS}))(\log_{10}(d_{3D}) - 3)$ $+20\log_{10}(f_c) - (3.2(\log_{10}(11.75h_{UT}))^2 - 4.97)$	$\sigma_{SF} = 8$	
UMa LOS	$PL_{\text{UMa-LOS}} = \begin{cases} PL_1 & 10\text{m} \le d_{2D} \le d'_{BP} \\ PL_2 & d'_{BP} \le d_{2D} \le 5\text{km} \end{cases}$, see note 1 $PL_1 = 28.0 + 22\log_{10}(d_{3D}) + 20\log_{10}(f_c)$ $PL_2 = 28.0 + 40\log_{10}(d_{3D}) + 20\log_{10}(f_c)$ $-9\log_{10}((d'_{BP})^2 + (h_{BS} - h_{UT})^2)$	$\sigma_{SF} = 4$	$1.5\text{m} \le h_{UT} \le 22.5\text{m}$ $h_{BS} = 25\text{m}$

[1] Please notice that UE and UT are used interchangeably throughout the document.

UMa NLOS	$PL_{\text{UMa-NLOS}} = \max(PL_{\text{UMa-LOS}}, PL'_{\text{UMa-NLOS}})$ for $10\text{m} \le d_{2D} \le 5\text{km}$ $PL'_{\text{UMa-NLOS}} = 13.54 + 39.08\log_{10}(d_{3D}) + 20\log_{10}(f_c) - 0.6(h_{\text{UT}} - 1.5)$	$\sigma_{\text{SF}} = 6$	$1.5\text{m} \le h_{\text{UT}} \le 22.5\text{m}$ $h_{\text{BS}} = 25\text{m}$ *Explanations: see note 3*

Note 1:Breakpoint distance d'$_{BP}$ = 4 h'$_{BS}$ h'$_{UT}$ f_c/c, where f_c is the centre frequency in Hz, c = 3.0×10^8 m/s is the propagation velocity in free space, and h'$_{BS}$ and h'$_{UT}$ are the effective antenna heights at the BS and the UT, respectively. The effective antenna heights h'$_{BS}$ and h'$_{UT}$ are computed as follows: h'$_{BS}$ = h_{BS} – h_E, h'$_{UT}$ = h_{UT} – h_E, where h_{BS} and h_{UT} are the actual antenna heights, and h_E is the effective environment height. For UMa h_E=1m with a probability equal to 1/(1+C(d_{2D}, h_{UT})) and chosen from a discrete uniform distribution uniform(12,15,…,(h_{UT}-1.5)) otherwise. With C(d_{2D}, h_{UT}) given by $C(d_{2D}, h_{UT}) = 0$ if $h_{UT} < 13$ m and $C(d_{2D}, h_{UT}) = \left(\frac{h_{UT}-13}{10}\right)^{1.5} g(d_{2D})$ otherwise, where $g(d_{2D}) = 0$ if $d_{2D} < 18$ m, and $g(d_{2D}) = \frac{5}{4}\left(\frac{d_{2D}}{100}\right)^3 e^{-\frac{d_{2D}}{150}}$ otherwise.

Note that h_E depends on d_{2D} and h_{UT} and thus needs to be independently determined for every link between BS sites and UTs. A BS site may be a single BS or multiple co-located BSs.

Note 2:The applicable frequency range of the Path Loss (PL) formula in this table is 0.5 < f_c < f_H GHz, where f_H = 30 GHz for RMa and f_H = 100 GHz for all the other scenarios. It is noted that RMa path loss model for >7 GHz is validated based on a single measurement campaign conducted at 24 GHz.

Note 3:UMa NLOS path loss is from TR36.873 with simplified format and $PL_{UMa\text{-}LOS}$ = Path loss of UMa LOS outdoor scenario.

Note 4:Break point distance d_{BP} = 2π h_{BS} h_{UT} f_c/c, where f_c is the centre frequency in Hz, c = 3.0 × 10^8 m/s is the propagation velocity in free space, and h_{BS} and h_{UT} are the antenna heights at the BS and the UT, respectively.

Note 5:f_c denotes the center frequency normalised by 1GHz, all distance related values are normalised by 1m, unless it is stated otherwise.

2.4.2 LOS probability

Table 3 provides the LOS probabilities.

***Table 3**: LOS probability*

Scenario	LOS probability (distance is in m)
RMa	$\Pr_{\text{LOS}} = \begin{cases} 1 & ,d_{\text{2D-out}} \le 10\text{m} \\ \exp\left(-\frac{d_{\text{2D-out}} - 10}{1000}\right) & ,10\text{m} < d_{\text{2D-out}} \end{cases}$
UMa	$\Pr_{\text{LOS}} = \begin{cases} 1 & ,d_{\text{2D-out}} \le 18\text{m} \\ \left[\frac{18}{d_{\text{2D-out}}} + \exp\left(-\frac{d_{\text{2D-out}}}{63}\right)\left(1 - \frac{18}{d_{\text{2D-out}}}\right)\right]\left(1 + C'(h_{\text{UT}})\frac{5}{4}\left(\frac{d_{\text{2D-out}}}{100}\right)^3 \exp\left(-\frac{d_{\text{2D-out}}}{150}\right)\right) & ,18\text{m} < d_{\text{2D-out}} \end{cases}$ where $C'(h_{\text{UT}}) = \begin{cases} 0 & ,h_{\text{UT}} \le 13\text{m} \\ \left(\frac{h_{\text{UT}} - 13}{10}\right)^{1.5} & ,13\text{m} < h_{\text{UT}} \le 23\text{m} \end{cases}$

Note: The LOS probability is derived with assuming antenna heights of 3m for indoor, 25m for UMa

2.5 CHANNEL MODEL REFERENCES INCLUDING UE-UE CHANNEL MODELS IN Q/V-BAND

To align with the simulation assumptions from 3GPP RAN4 as in R4-2313890 [9] and 3D multilayer architecture (WP3), the following NTN UE scenarios can be considered as in **Table 4** which reflects the different antenna heights for different NTN UE types.

Deliverable D2.2 ‘‘*User requirements’* of the 6G-NTN project separates NTN UEs into three main types: handheld (consumer or professional), drone (light or heavy) and mounted NTN UEs (First responder stationary or Vehicular Mounted Moving (e.g., trains, cars, maritime vessel, first responders)).

In terms of characteristics, these would correspond to different terminal classes in terms of transmission power, antenna gain and altitude. For these reasons, we have regrouped these different NTN UE types into three types of NTN UE according to their common altitude group: Fixed VSAT (Very Small Aperture Terminal), A-ESIM (Aeronautical-Earth Station In Motion) and L-ESIM (Land-Earth Station In Motion).

At least for first responder missions, one can identify two classes: one corresponding to a fixed VSAT and the other one corresponding to moving VSAT, mounted on a vehicle.

Drones are part of the A-ESIM category while handheld and Vehicular Mounted Moving NTN UEs can be considered part of L-ESIMs in terms of altitude. The maritime ESIM can also be associated to an altitude of 22.5m or less, depending on the height of the vessel.

Table 4: NTN UE scenario

NTN UE scenario	Fixed VSAT	A-ESIM	L-ESIM
Altitude	22.5m	3-14km	1.5m

Several propagation models within TN, NTN and the cross path loss propagation between TN and NTN can be seen in ***Table 5***.

Table 5: *propagation models with respect to link type*

Link	Propagation model
TN BS to Fixed VSAT on roof	Free space path loss
TN BS to L-ESIM at 1.5 m	UMa as in 3GPP TR 38.803
TN BS to TN UE	UMa as in 3GPP TR 38.803
TN UE to Fixed VSAT on roof	UMa as in 3GPP TR 38.803 (BS is to be replaced with VSAT)
TN UE to L-ESIM	UMi (Urban Micro)
Satellite to TN BS/UE	3GPP TR 38.821
Satellite to VSAT/ESIM	3GPP TR 38.821
TN BS to Satellite	3GPP TR 38.821
Note1: For the propagation models which use the 3GPP TR 38.821 [7], to use same assumptions as in [7] and consider the atmospheric losses and the scintillation losses. Note2: TN BS height is 25m	

3 FREQUENCY BANDS AND COEXISTENCE SCENARIOS

3.1 FREQUENCY BANDS

The following frequency bands below are explored in the 6G-NTN project:

- **The Q/V-band** has been identified as potential candidate for the service link as part of 6G NTN, with the following frequency ranges for both NGSO and GSO satellite services:
  - DL: 37.5 – 42.5 GHz (Q-band);
  - UL: 47.2 – 50.2 GHz and 50.4 – 51.4 GHz (V-band).

  Please also note that TN mobile service allocated bands (currently) are:
  - DL & UL: 37.0 – 43.5 GHz;
  - DL/UL in some countries (e.g., Brazil): 45.5 – 47 GHz and 47.2 – 48.2 GHz.
- **The C-band** is a new NTN frequency band opportunity for direct connectivity to smartphones and cars that is considered in the 6G-NTN project:
  - DL NTN satellite communications could potentially use TN TDD (Time Division Duplex) frequency bands n77 (3,300 – 4,200 MHz) / n78 (3,300 – 3,800 MHz).
  - UL NTN satellite communications could potentially use the upper frequency spectrum (around 6 GHz) or lower frequency spectrum (e.g., UL n255 or UL n256).

Taking into account these constraints, the following operational band usage scenario has been identified for study in Q/V-band:

Table 6: *considered band usage scenario for Q/V-band*

Q/V-band scenario #	Scenario Name	UL freq. (channel bandwidth (BW))	DL band (channel BW)	Comments
1	FR2 – Q/V	47 GHz (400 MHz)	37 GHz (400 MHz)	UE = flat panel antenna

Several operational band usage scenarios have been identified for study in C-band and are detailed in ***Table 7***. The most promising scenarios are filled by pink.

Table 7: *Considered band usage scenario for C-band*

C-band scenario #	Scenario Name	UL freq. (channel BW)	DL band (channel BW)	Comments
1	FR1 – Hybrid S/C-band FDD	2000 MHz (15 MHz) **(See Note 1, Note 3)**	3700 MHz (100 MHz)	Combination of C for DL (advantage in throughput), and lower band for UL (advantage in link budget) Anticipated challenges: availability of UL band may vary locally (could range from 1.4 GHz to 2.4 GHz)

2	FR1 – Lower C-band TDD **(See Note 2)**	3700 MHz (100 MHz)	3700 MHz (100 MHz)	TDD implementation = in line with duplex mode of 3GPP n77/n78 Anticipated challenges: synchronisation, guard time impact on capacity
3	**FR1 – Lower C-band FDD**	4000 MHz (100 MHz) **(See Note 4)**	3500 MHz (100 MHz) **(See Note 5)**	Representative of duplex FDD fully implemented in C-band Anticipated challenges: Duplexer is needed in the UE (not the case currently in 3GPP n77/n78 TDD)
4	**FR1 – Upper C-band UL/DL 6/4 GHz FDD**	6500 MHz (100 MHz) **(See Note 3, Note 6)**	3700 MHz (100 MHz)	FDD implementation matching ITU current satellite UL/DL allocations Anticipated challenges: UE UL link budget; spectrum availability TBD due to the lack of global support for 3GPP n96/n104 (TDD)

Note 1: S band has been already considered in the 3GPP coexistence scenarios.

Note 2: For satellite access, only FDD mode will be considered, explaining why scenario 2 is not identified as high priority.

Note 3: In the description of work, 6 GHz and 2 GHz have been considered for UL instead of C-band.

Note 4: Please note that according to ITU Radio regulation, 4 GHz band has FSS DL allocation. Thus, there is a lack of authorisation to operate UL at this frequency. One way to mitigate this issue would be for 6G NTN UEs to operate on non-interference basis w.r.t. GSO Earth Station reception to ensure long term protection of GSO FFS DL.

Note 5: For the coexistence simulations, we only need the carrier frequency, not the explicit band. For these reasons, we selected a 3.5 GHz carrier for DL.

Note 6: Lack of global support for NTN due to spectrum availability.

Scenario 1 uses S-band that is already considered in the 3GPP coexistence scenarios. Thus, the added value gained by studying it is lower compared to other scenarios using frequency ranges that have not been studied yet in 3GPP for NTN.

Scenario 2 is a TDD band. However, for satellite access, only FDD mode will be considered.

Considering the above notes, scenarios 3 and 4 are the most promising ones, as they have the advantage of being FDD and have not yet been the object of study by 3GPP for NTN.

3.2 COEXISTENCE SCENARIOS

3.2.1 Coexistence scenario 1. Aggressor and victim combination (Q/V-band) in adjacent bands

Table 8 below describes the eight different coexistence scenarios to be considered and the scope of the coexistence simulations. For instance, scenario n°1 where the NTN UL (VSAT UE transmitter in Q/V-band) is the aggressor and TN UL (gNodeB (gNB) receiver in Q/V-band) is the victim. Frequency carrier for this scenario has been identified at 47 GHz. For this scenario, TN gNB ACS is fixed while NTN VSAT UE ACLR is a tuneable parameter. These scenarios are also depicted in

Figure 4 (scenarios 1 to 4) and ***Figure 5*** (scenarios 5 to 8).

Similar analysis can be done for different coexistence scenarios.

Table 8: *Q/V-band coexistence scenarios in adjacent band*

No.	Combination	Aggressor	Victim	Notes	Scope of Coexistence Simulation
1	TN with NTN	NTN UL	TN UL	i1, with f_c=47 GHz for simulation purposes	ACLR NTN UE to be varied/defined ACS TN gNB fixed
2	TN with NTN	TN UL	NTN UL	i2, with f_c=47 GHz for simulation purposes	ACLR TN UE fixed ACS NTN SAN to be varied/defined
3	TN with NTN	NTN UL	TN DL	i3, with f_c=47 GHz for simulation purposes	ACLR NTN UE to be varied/defined ACS TN UE fixed
4	TN with NTN	TN DL	NTN UL	i4, with f_c=47 GHz for simulation purposes	ACLR TN gNB fixed ACS NTN SAN to be varied/defined
5	TN with NTN	TN DL	NTN DL	i5, with f_c=37 GHz for simulation purposes	ACLR TN gNB fixed ACS NTN UE to be varied/defined
6	TN with NTN	NTN DL	TN DL	i6, with f_c=37 GHz for simulation purposes	ACLR NTN SAN to be varied/defined ACS TN UE fixed
7	TN with NTN	NTN DL	TN UL	i7, with f_c=37 GHz for simulation purposes	ACLR NTN SAN to be varied/defined ACS TN gNB fixed
8	TN with NTN	TN UL	NTN DL	i8, with f_c=37 GHz for simulation purposes	ACLR TN UE fixed ACS NTN UE to be varied/defined

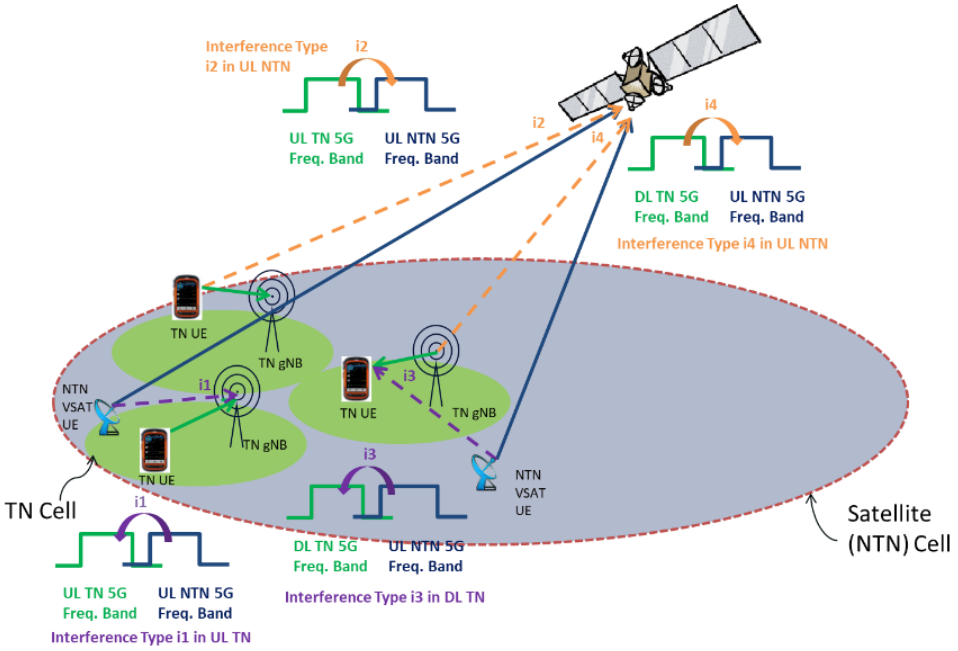

Figure 4: *Coexistence scenarios 1-4 (e.g. Q/V-band).*

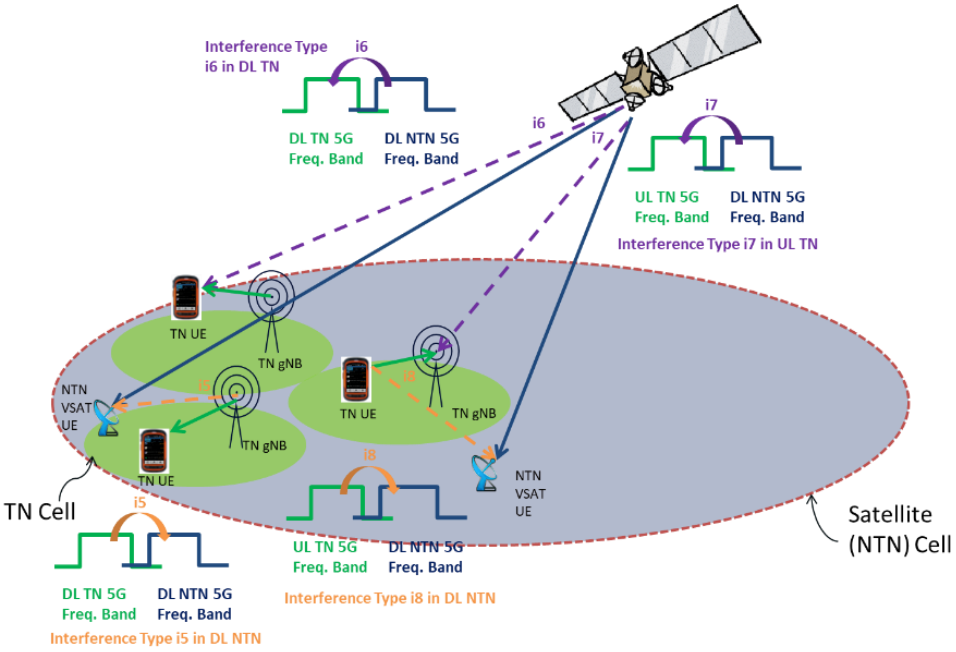

Figure 5: *Coexistence scenarios 5-8 (e.g. Q/V-Band)*

3.2.2 Coexistence scenario 2. Aggressor and victim combination (C-band) in adjacent bands

As explained in Section 3.1, for C-band we will continue with band usage scenarios 3 and 4 for the rest of the study.

From band usage scenario 3 (DL 3.5 GHz, UL 4 GHz) the following coexistence scenarios in ***Table 9*** can be derived. Scenarios 7 and 8 will be studied in priority since the other scenarios are already considered by 3GPP TR38.863 [3].

Table 9: *c-band coexistence scenarios in adjacent band for frequency band scenario 3*

No	Combination	Aggressor	Victim	Notes	Scope of Coexistence Simulation	Comment
1	TN with NTN	NTN UL	TN UL	i1, with f_c=4GHz for simulation purposes	ACLR NTN UE to be varied/defined ACS TN gNB fixed	**Considered by 3GPP TR38.863. S-band requirement (ACLR) should cover this coexistence scenario**
2	TN with NTN	TN UL	NTN UL	i2, with f_c=4GHz for simulation purposes	ACLR TN UE fixed ACS NTN SAN to be varied/defined	**Considered by 3GPP TR38.863. S-band requirement (ACS) should cover this coexistence scenario**
3	TN with NTN	NTN UL	TN DL	i3, with f_c=4GHz for simulation purposes	ACLR NTN UE to be varied/defined ACS TN UE fixed	**Considered by 3GPP TR38.863. S-band requirement (ACLR) should cover this coexistence scenario**
4	TN with NTN	TN DL	NTN UL	i4, with f_c=4GHz for simulation purposes	ACLR TN gNB fixed ACS NTN SAN to be varied/defined	**Considered by 3GPP TR38.863. S-band requirement (ACS) should cover this coexistence scenario**

5	TN with NTN	TN DL	NTN DL	i5, with f_c=3.5GHz for simulation purposes	ACLR TN gNB fixed ACS NTN UE to be varied/defined	**Considered by 3GPP TR38.863. S-band requirement (ACS) should cover this coexistence scenario**
6	TN with NTN	NTN DL	TN DL	i6, with f_c=3.5GHz for simulation purposes	ACLR NTN SAN to be varied/defined ACS TN UE fixed	**Considered by 3GPP TR38.863. S-band requirement (ACLR) should cover this coexistence scenario**
7	**TN with NTN**	**NTN DL**	**TN UL**	**i7, with f_c=3.5GHz for simulation purposes**	**ACLR NTN SAN to be varied/defined** **ACS TN gNB fixed**	**HIGH PRIORITY**
8	**TN with NTN**	**TN UL**	**NTN DL**	**i8, with f_c=3.5GHz for simulation purposes**	**ACLR TN UE fixed** **ACS NTN UE to be varied/defined**	**HIGH PRIORITY**

The reason for excluding previous coexistence scenarios (1 to 6) is due to the fact that 3GPP already considered S-band coexistence with n1 FDD and n34 TDD. We do not expect worse coexistence scenarios and more stringent requirements for C-band as compared to S-band since the carrier frequency is higher and therefore the path loss will increase, thus decreasing the interference.

The remaining coexistence scenarios 7 & 8 have not been considered by 3GPP in previous works because the NTN DL (n256) was far away from the TN TDD UL band (n34).

From band usage scenario 4 (DL 3.7 GHz, UL 6.5 GHz), the following coexistence scenarios can be derived, with scenarios 1 2, 3 and 4 to be studied in priority:

Table 10: *c-band coexistence scenarios in adjacent band for frequency band scenario 4*

No	Combination	Aggressor	Victim	Notes	Scope of Coexistence Simulation	Comments
1	TN with NTN	NTN UL	TN UL	i1, with f_c=6.5GHz for simulation purposes	ACLR NTN UE to be varied/defined ACS TN gNB fixed	**LOWER PRIORITY**
2	TN with NTN	TN UL	NTN UL	i2, with f_c=6.5GHz for simulation purposes	ACLR TN UE fixed ACS NTN SAN to be varied/defined	**LOWER PRIORITY**
3	TN with NTN	NTN UL	TN DL	i3, with f_c=6.5GHz for simulation purposes	ACLR NTN UE to be varied/defined ACS TN UE fixed	**LOWER PRIORITY**

4	TN with NTN	TN DL	NTN UL	i4, with f_c=6.5GHz for simulation purposes	ACLR TN gNB fixed ACS NTN SAN to be varied/defined	**LOWER PRIORITY**
5	TN with NTN	TN DL	NTN DL	i5, with f_c=3.7 GHz for simulation purposes	ACLR TN gNB fixed ACS NTN UE to be varied/defined	**Considered by 3GPP TR38.863. S-band requirement (ACS) should cover this coexistence scenario**
6	TN with NTN	NTN DL	TN DL	i6, with f_c=3.7 GHz for simulation purposes	ACLR NTN SAN to be varied/defined ACS TN UE fixed	**Considered by 3GPP TR38.863. S-band requirement (ACLR) should cover this coexistence scenario**
7	TN with NTN	NTN DL	TN UL	i7, with f_c=3.7 GHz for simulation purposes	ACLR NTN SAN to be varied/defined ACS TN gNB fixed	**Already considered in Table 9**
8	TN with NTN	TN UL	NTN DL	i8, with f_c=3.7 GHz for simulation purposes	ACLR TN UE fixed ACS NTN UE to be varied/defined	**Already considered in Table 9**

Similar reasoning as previous table has been done to justify the choices of discarding scenarios 5 to 8.

4 PARAMETERS FOR NTN UE

4.1 KA & Q/V NTN UE ARCHITECTURE

A reference UE architecture for Ka and Q/V-band is proposed in Figure 6, where:

- **UC:** Up-Converter;
- **PA:** Power Amplifier(s);
- **LNA:** Low Noise Amplifier(s);
- **DC:** Down-Converter;
- **DP:** Duplexer;
- **ACU:** Antenna Control Unit;
- **Antenna:** Active, Electronically or Hybrid Steered.

The UC and the Tx PA can be part of a BUC (Block Up-Converter). In this case, the BUC is part of the Transmission chain, and it includes a Tx power amplifier.

The Rx LNA and the DC can be part of an LNB (Low-Noise Block down-converter). In this case, the LNB is part of the Reception chain, and it includes a low noise amplifier.

RF represents the Radio Frequency region and IF the Intermediate Frequency region.

The interface between UE modem and BUC can be considered (for example) OpenBMIP (Open BUC Modem Interface Protocol) and could control the amplifier power and band selection. The interface between UE modem and ACU can be considered (for example) OpenAMIP (Open Antenna to Modem Interface Protocol) and could help to control the steering/switching of the antenna with respect to the satellite tracking. Parabolic/dish antenna design or active antenna design can be used. Steering can be performed electronically, mechanically or via a combination of both. Other interfaces or potential implementations are not excluded.

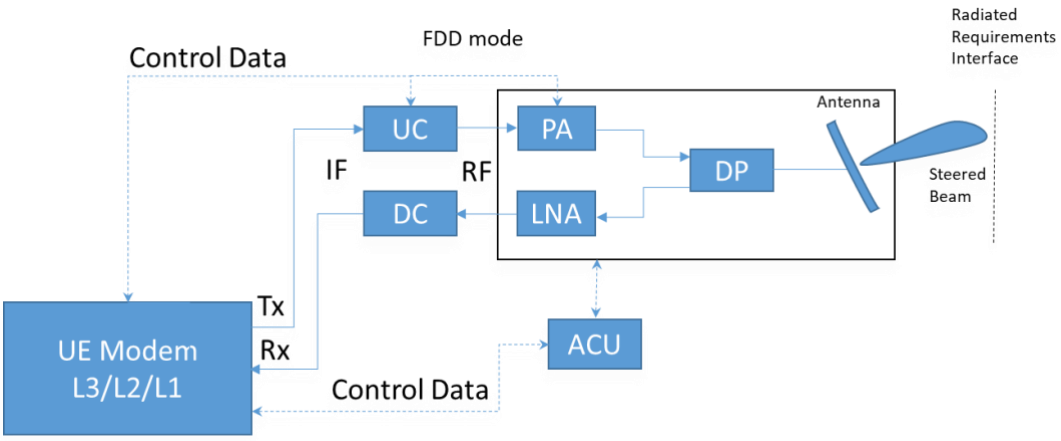

Figure 6: *Generalised NTN UE terminal reference architecture for above 10 GHz*

Note 1: The Up-Converter and the Tx Power Amplifier are part of the Transmission chain.

Note 2: The Rx Low-Noise Amplifier and the Down-Converter are part of the Reception chain.

It is assumed for the NTN capable UE operating in above 10 GHz that:

- the generated Rx/Tx beams are able to track the serving satellite as well as at least another neighbouring satellite;
- the rally time of (Rx and/or Tx) beam pointing between 2 satellites is considered negligible.

4.2 NTN UE GENERAL ASPECTS

All NTN UE antenna parameters have been adapted from TR 38.821 [7] by considering the following parameters adapted to Q/V satellite band:

- Downlink frequency: 37 GHz
- Uplink frequency: 47 GHz
- 15 cm antenna aperture diameter (2*a=15cm) **

**** Antenna aperture diameter subject to change according to budget link and other constraints.**

The Technical Report TR 38.811 [6] provides typical RF parameters shown in ***Table 11***.

Table 11: *Typical minimum RF characteristics of NTN UE*

Parameter	Very Small Aperture NTN UE Terminal (fixed or mounted on moving platforms)
Transmit Power	2 W (33 dBm)
Antenna type	15 cm equivalent aperture diameter (circular polarisation)
Antenna gain	Tx: 35.2 dBi Rx: 32.9 dBi
Noise figure	2 dB
Output loss	1.5 dB
EIRP	36.7 dBW
G/T (NOTE 1)	7.6 dB/K
Polarisation (NOTE 2)	Circular
NOTE 1: For the computation of G/T or figure of merit, following formula applies in dB: $G/T = Ga - NF - 10*LOG\ (T_o+(T_a-T_o)/(10^{0.1*NF}))$ **where:** - **Antenna Gain : Ga in dBi** - **Ambient Temperature : T_0 (usually 290 K)** - **Antenna temperature : T_a** - **Noise Figure: NF in dB including feeder loss**	

4.3 NTN UE ANTENNA PARAMETERS

4.3.1 Circular aperture antenna

The following normalised antenna pattern corresponding to a theoretical parabolic (reflector) antenna with circular aperture can be considered for coexistence analysis:

$$F(u) = \frac{2J_1(u)}{u}$$

where:

- $J_1(x)$ is the Bessel function of first type and first order with argument *x,*
- θ is the angle in a $(\theta; \varphi)$ spherical coordinates system,
- $u = \frac{\pi D}{\lambda} \sin(\theta)$,
- *D* is the antenna diameter,
- λ is the wavelength.

The normalised antenna pattern, expressed in decibels, is given by the following relation:

$$10 \log\left(F(u)\right)^2$$

With the linear form given by the following relation:

$$\left(F(u)\right)^2 = \left(\frac{2J_1(u)}{u}\right)^2$$

This is equivalent to TR 38.811 [6]:

$$\begin{cases} 1 & \text{for } \theta = 0 \\ 4\left|\frac{J_1(ka\sin(\theta))}{ka\sin(\theta)}\right|^2 & \text{for } 0 < |\theta| \leq 90° \end{cases}$$

where:

- $J_1(x)$ is the Bessel function of the first kind and first order with argument *x*;
- a is the radius of the antenna's circular aperture;
- $k = 2\pi f/c$ is the wave number;
- f is the frequency of operation;
- c is the speed of light in a vacuum and θ is the angle measured from the bore sight of the antenna's main beam.

Note that $k \times a$ equals to the number of wavelengths on the circumference of the aperture and is independent of the operating frequency.

Figure 7 shows the antenna pattern of an NTN UE transmit antenna reflector 0.15 m diameter and operating at 47000 MHz. This corresponds to a circular aperture, for example parabolic or dish antenna.

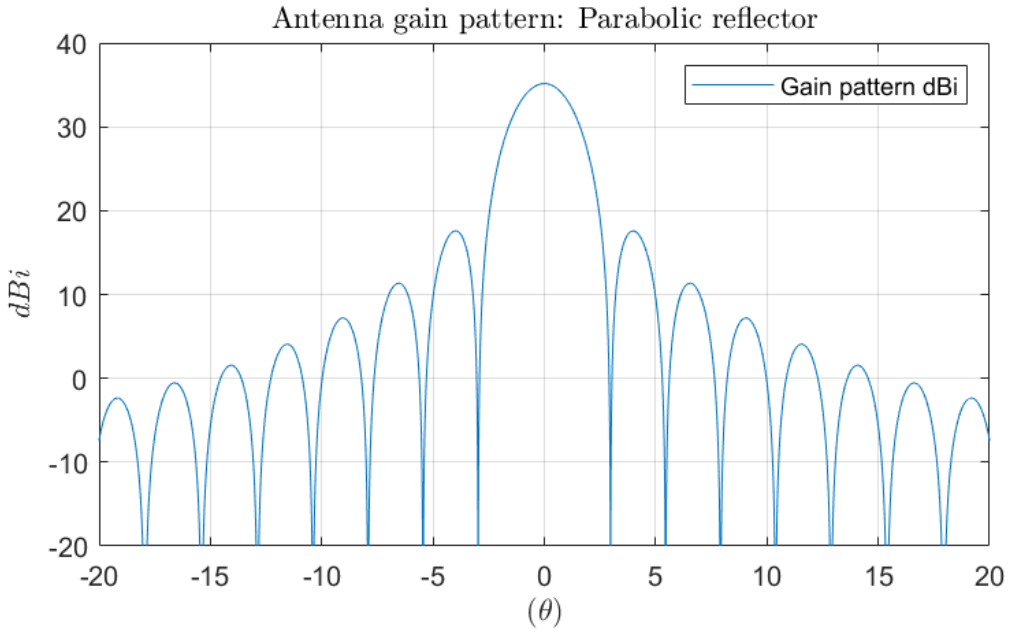

Figure 7: *Antenna gain pattern of an NTN UE transmit parabolic antenna operating at 47000 MHz*

4.3.2 Phased-array antenna model 1

A phased-array antenna with a square aperture of side length D and tapered illumination over the aperture is considered. The antenna pattern at $\phi = 0$ is described by the following relation:

$$F(u) = \left(\frac{\pi}{2}\right)^2 \frac{\cos u}{\left(\frac{\pi}{2}\right)^2 - u^2}$$

where:

- θ is the angle in a $(\theta; \phi)$ spherical coordinates system,
- $u = \frac{\pi D}{\lambda} \sin(\theta - \theta_0)$,
- θ_0 is the steering angle,
- λ is the wavelength,
- D is the side length.

The normalised antenna pattern, expressed in decibels, is given by the following relation:

$$\left(F(\theta, \phi)\right)_{dB} = 10\, log\left(F(\theta, \phi)\right)^2$$

The antenna gain can be evaluated with the following relation:

$$G(\theta_0) = \eta \frac{4\pi \times D^2}{\lambda^2} \cos\theta_0$$

where η is the antenna efficiency.

Antenna efficiency for UE antenna was computed using the following proposed values: 60% in Tx (DL) and 57% in Rx (UL).

Figure 8 shows the antenna gain pattern of an NTN UE transmit antenna with D=0.15 m, operating at 47000 MHz.

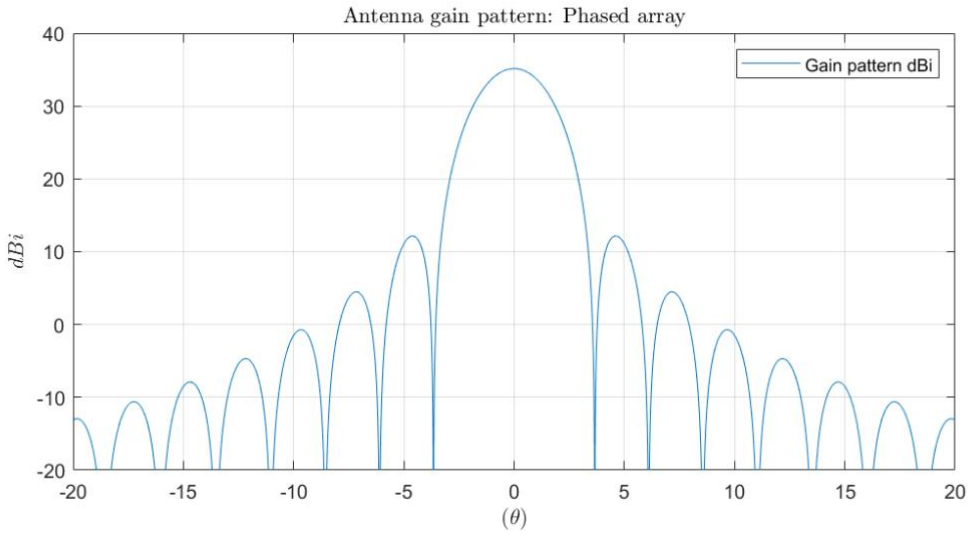

Figure 8: *Antenna gain pattern of an NTN UE transmit phased array antenna operating at 47000 MHz*

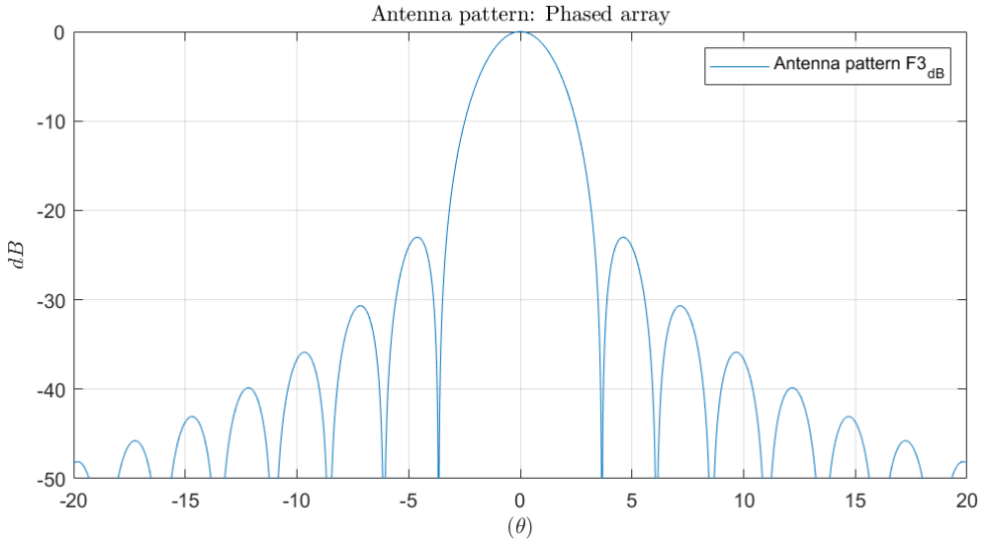

Figure 9*: Antenna pattern of an NTN UE transmit phased array antenna operating at 47000 MHz*

4.3.3 Phased-array antenna model 2

A more realistic phased-array antenna model (as alternative to model 1 presented in Section 4.3.2) can be found in [30]:

$$F(\theta,\phi) = \left[\frac{\sin\left(M\frac{\pi d_x}{\lambda}(\sin(\theta)\cos(\phi) - \sin(\theta_0)\cos(\phi_0)\right)}{M\sin\left(\frac{\pi d_x}{\lambda}(\sin(\theta)\cos(\phi) - \sin(\theta_0)\cos(\phi_0)\right)}\right] \times \left[\frac{\sin\left(N\frac{\pi d_y}{\lambda}(\sin(\theta)\sin(\phi) - \sin(\theta_0)\sin(\phi_0)\right)}{N\sin\left(\frac{\pi d_y}{\lambda}(\sin(\theta)\sin(\phi) - \sin(\theta_0)\sin(\phi_0)\right)}\right]$$

where:

- M : Number of radiating elements in the x direction

- N : Number of radiating elements in the *y* direction
- d_x: Distance between radiating elements in the *x* direction
- d_y: Distance between radiating elements in the *y* direction
- λ: Wavelength
- (θ_0, φ_0): Beam steering angular direction

An alternative relation for the phase array antenna (considering that a rectangular aperture corresponds to a *sin(x)/x* type of antenna pattern) can also be written as follows:

$$F(\theta,\phi) = \left[\frac{\sin\left(\frac{\pi D_x}{\lambda}(\sin(\theta)\cos(\phi) - \sin(\theta_0)\cos(\phi_0)\right)}{\frac{\pi D_x}{\lambda}(\sin(\theta)\cos(\phi) - \sin(\theta_0)\cos(\phi_0)}\right] \times \left[\frac{\sin\left(\frac{\pi D_y}{\lambda}(\sin(\theta)\sin(\phi) - \sin(\theta_0)\sin(\phi_0)\right)}{\frac{\pi D_y}{\lambda}(\sin(\theta)\sin(\phi) - \sin(\theta_0)\sin(\phi_0)}\right]$$

where:

- $D_x = D_y = 0.15\ m$*:* diameter of the NTN UE transmit antenna reflector;
- $d_x/\lambda = d_y/\lambda = 1/2$.

4.4 NTN UE TRANSMIT AND RECEIVE PERFORMANCES

The NTN UE transmit and receive performances are summarised in ***Table 12*** considering a circular reflector antenna operating in Q/V-band.

4.4.1 Option 1

Table 12 provides the parameters of NTN UE used for the coexistence analysis in Q/V-band for both uplink and downlink. As a consequence, some parameters are not applicable, for instance the transmit power when the UE acts as a receiver is N/A.

Table 12: *NTN UE Parameters option 1*

NTN UE Parameters	Unit	Tx (Uplink)	Rx (Downlink)
Polarisation		Circular	Circular
Low Frequency	(MHz)	47 000	37 000
Efficiency	(%)	60%	57%
On-axis antenna gain at F_c	(dBi)	35.2	32.9
Output power	(W)	2	N/A
Output power	(dBW)	3,0	N/A
Output loss	(dB)	-1,5	N/A
EIRP	(dBW)	**36.7**	N/A
Receiver noise figure	(dB)	N/A	2
Feeder loss	(dB)	N/A	-1
Sky temperature	(K)	N/A	30
Ground temperature	(K)	N/A	10
Antenna temperature	(K)	N/A	40
G/T figure of merit	(dB/K)	N/A	**7.6**
NOTE1: T_a = T_Sky + T_Ground NOTE2: The antenna temperatures are based on e.g. ITU-R Rec. P372 [10] and Rec. P618. NOTE3: T_sky is computed using [ITU-R Rec. P.618-14] [11] as expressed below			

According to ITU-R Rec. P.618-14 [11], the sky noise temperature at a ground station antenna may be estimated by:

$$T_{sky} = T_{mr}\left(1 - 10^{\left(-\frac{A}{10}\right)}\right) + 2.7 \times 10^{-\frac{A}{10}}$$

where:

- T_{sky} is the sky noise temperature (K) at the ground station antenna
- A refers to the total atmospheric attenuation excluding scintillation fading (dB)
- T_{mr} is the atmospheric mean radiating temperature (K).

As attenuation increases, the emission noise also increases. For earth stations with low-noise front-ends, this increase of noise temperature may have a greater impact on the resulting signal-to-noise ratio than the attenuation itself.

In general, antenna efficiency depends on the antenna manufacturer design. Herein, the proposed values are indicative and consistent with Q/V-band definition for UL and DL respectively. Moreover, in order to simplify the definition of NTN UE, one can compute an equivalent receiver NF at ambient temperature, and therefore the second option could be defined in the next section.

4.4.2 Option 2

Another way to more succinctly describe the different NTN UE parameters would be to introduce an equivalent receiver Noise Figure at ambient temperature, as provided in ***Table 13***.

Table 13: *NTN UE Parameters option 2*

NTN UE Parameters	Unit	Tx (Uplink)	Rx (Downlink)
Polarisation		Circular	Circular
Frequency	(MHz)	47 000	37 000
Efficiency	(%)	60%	57%
On-axis antenna gain at F_c	(dBi)	**35.2**	**32.9**
Output power at antenna input	(W)	2	N/A
Output power at antenna input	(dBW)	3,0	N/A
Output loss	(dB)	-1.5	N/A
Peak EIRP (on-axis)	(dBW)	**36.7**	N/A
Equivalent Receiver Noise Figure	(dB)	N/A	**3**
Feeder loss	(dB)	N/A	-1

Moreover, the system temperature can be computed using:

$$T_{sys} = T_{sky} + T_{ground} + T_0\left(10^{-\frac{L}{10}} - 1\right) + T_0 * \left(10^{\frac{NF}{10}} - 1\right) * 10^{-\frac{L}{10}},$$

with Gain over Thermal (G/T) parameter computed as:

$$\frac{\mathrm{G}}{\mathrm{T}} = \mathrm{G_{Rx}} - 10 * \log 10\left(\mathrm{T_{sky}} + \mathrm{T_{ground}} + \mathrm{T_0} * \left(10^{-\frac{\mathrm{L}}{10}} - 1\right) + \mathrm{T_0} * \frac{10^{\frac{\mathrm{NF}}{10}} - 1}{10^{\frac{\mathrm{L}}{10}}}\right).$$

The equivalent receiver NF can be then obtained with:

$$\mathrm{NF_{equivalent}} = 10 * \log_{10}\left(1 + \frac{\mathrm{T_{sys}} - \mathrm{T_{sky}} - \mathrm{T_{ground}}}{\mathrm{T_0}}\right).$$

The NF can be derived as well as a function of front-end loss and LNA as presented in 3GPP R4-2312120 [12] and R4-2309508 [13]:

$$N_f[\mathrm{dB}] = 10\log_{10}\left(\frac{T_S - T_a}{T_0} + 1\right)$$

where

$$T_s = T_a + (L-1)T_0 + LT_R + L(f-1)\frac{T_0}{G_R}.$$

5 PARAMETERS FOR TN BS AND UE

5.1 Q/V-BANDS

Table 14 and

Table 15 provide the parameters used for Q/V-bands TN BS and UE, respectively, and come from 3GPP TR 38.803 [14]. More precisely, ***Table 14*** provides general information regarding the used frequencies and the channel bandwidth as well as regarding the network layout and the UE deployments. On the other hand,

Table 15 is dedicated to the transmitter and receiver parameters (e.g. transmit power, antenna gains).

Table 14*: TN NR parameters for Q/V-bands*

TN parameters	NR
Carrier frequency in GHz	37 GHz / 47 GHz
Size of each nominal channel BW in MHz	200 MHz
Network layout	hexagonal grid, 19 macro –sites, 3 sectors per site with wrap around (57 sectors)
ISD (InterSite Distance) in m	200 m (UMa)
Minimum BS-UE distance in m	35 m
System loading and activity	Full buffer 100%
Network location	TN as victim: Randomly generated in NTN central beam
Number of scheduled UE per cell (DL)	1
Number of scheduled UE per cell (UL)	1
UE TX power range in dBm	-40 to 23
Building penetration loss	In Path loss model, TR 38.901 [8]
Handover margin in dB	3
UE indoor ratio	All outdoor, UE indoor ratio 0%
BS-UE path-loss model	UMa as in TR 38.803 [14]
UE distribution	Uniform
Evaluation metrics	5% Throughput loss, referring to TR 38.803 section 5.2.7 [14]

Table 15: *TN BS (Urban macro) and UE parameters for Q/V-bands*

TN parameters	BS (Urban macro)	UE
Antenna height in m	25 m	1.5 m
Antenna Pattern	For AAS, see TR 38.803 Section 5.2.3 [14]	
Element Gain in dBi	8	5
H and V 3dB beamwidth of single element in degree	65º for H 65º for V	90º for H 90º for V
H and V front-to-back ratio in dB	30 for both H/V	25 for both H/V
Antenna polarisation	Linear ±45º	Linear ±45º
Antenna array configuration (Row × Column)	8 x 16 elements	2 x 2 elements

Horizontal/Vertical radiating element spacing	0.5 of wavelength for H, 0.5 of wavelength for V	0.5 of wavelength for H, 0.5 of wavelength for V
Max TX power in dBm	43 dBm	23 dBm
Mechanical down tilt in degree	10	-
Noise Figure	11 dB	11 dB
ACLR in dB	26 dB	16 dB
ACS in dB	22 dB	22 dB

The assumptions for ACLR and ACS values are given for TN operating at 37 and 47 GHz.

5.2 C-BAND

The parameters for the C-band TN BS and UE side can be similar to the TN parameters that are used in (3GPP TR 38.828 [15]), as highlighted in ***Table 16*** and ***Table 17*** respectively.

Table 16: *TN NR parameters for C-band*

TN parameters	**NR**
Carrier frequency in GHz	4 GHz
Size of each nominal channel BW in MHz	100 MHz
Network layout	hexagonal grid, 19 macro sites, 3 sectors per site with wrap around (57 sectors)
ISD in m	450 m (UMa)
Minimum BS-UE distance in m	35 m
System loading and activity	Full buffer 100%
Network location	TN as victim: Randomly generated in NTN central beam
Number of scheduled UE per cell (DL)	1
Number of scheduled UE per cell (UL)	1
UE TX power range in dBm	-40 to 23
Building penetration loss	In Path loss model, TR 38.901 [8]
Cell selection margin in dB	3
UE indoor ratio	All outdoor, UE indoor ratio 0%
BS-UE path-loss model	UMa as in TR 38.803 [14]
UE distribution	Uniform
Evaluation metrics	5% Throughput loss, referring to TR 38.803 section 5.2.7 [14]

Table 17: *TN BS (Urban macro) and UE parameters for C-band*

TN parameters	**BS**	**UE**
Antenna height in m	20 m	1.5 m
Antenna Pattern	For AAS, see TR 38.803 Section 5.2.3 [14]	
Element Gain in dBi	5	0 (omni)
H and V 3dB beamwidth of single element in degree	65º for H 65º for V	-

H and V front-to-back ratio in dB	30 for both H/V	-
Antenna polarisation	Linear ±45º	-
Antenna array configuration (Row × Column)	8 x 8 elements	-
Horizontal/Vertical radiating element spacing	0.5 of wavelength for H, 0.8 of wavelength for V	-
Max TX power in dBm	49 dBm	23 dBm
Mechanical down tilt in degree	10	-
Noise Figure	5 dB	9 dB

5.3 TN UE TRANSMIT POWER CONTROL

For uplink scenario, TPC (Transmit Power Control) model specified in Section 9.1 of TR 36.942 [16] is applied for both NTN and TN with the following power control scheme:

$$P_t = P_{\max} \min\left\{1, \max\left[R_{\min}, \left(\frac{CL}{CL_{x-ile}}\right)^{\gamma}\right]\right\}$$

where:

- $\mathrm{P_{max}} = \max(\mathrm{P_{UE\,Tx}})$, i.e., 23 dBm for TN UE, and 33 dBm for NTN UE.
- $\mathrm{CL_{x-ile}} = -\mathrm{SNR_{target}} + \mathrm{P_{max}} - \mathrm{ThermalNoise} - \mathrm{NF} - 10 * \log_{10}(\mathrm{BW})$, considering SNR target is 15dB and BW is actual UL BW. NF is the Noise Figure of either BS or SAN according to context.
- $\mathrm{R_{min}} = min\,(Power\ reduction\ ratio)$, i.e., -63 dB for TN UE, and -63 dB by assuming NTN UE min Tx power as -30dBm as starting point for NTN UE.
- γ = 1.

6 PARAMETERS FOR NTN SAN

6.1 Q/V-BAND SATELLITE ANTENNA PATTERN

Table 18 provide two normalised antenna patterns corresponding to a circular aperture theoretical antenna pattern that can be considered for SAN parameterisation and related coexistence studies. The difference between these two options is illustrated later in this section.

Table 18: *Two possible options for Q/V-band satellite antenna pattern*

Options	Equations
Option 1	$F(\theta) = \frac{2\,J_1(u)}{u}$
Option 2	$F(\theta) = \frac{2}{3}\left[\frac{2\,J_1(u)}{u} + \frac{4\,J_2(u)}{u^2}\right]$

where:

- $J_i(x)$ is the Bessel function of first type and i^{th} order with argument *x*
- θ is the angle in a $(\theta;\varphi)$ spherical coordinates system,
- $u = \frac{\pi D}{\lambda}\sin(\theta)$
- *D* is Antenna diameter
- λ is the Wavelength

The theoretical antenna pattern can be applied to a circular aperture, either for a passive antenna or for an active antenna. Figure 10 shows an example with the normalised antenna pattern of a satellite transmit antenna as a function of *u* parameter with D/λ=333 (corresponding to e.g., D=2.124 m and λ= 0.0064 m).

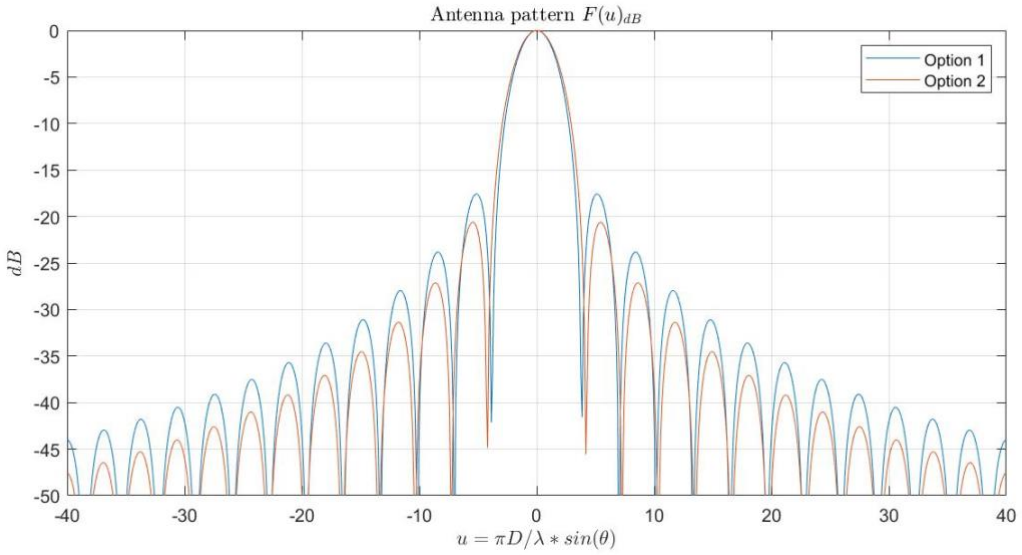

Figure 10: *Antenna pattern as a function of u parameter, with D/λ=333*

Moreover, the half-power beam-width ($2\theta_{-3dB}$) is given by the relations provided in Table 19.

Table 19: *half-power beam-width of the two options*

Options	$2\theta_{-3dB}$ Value
Option 1	$2\theta_{-3dB} = 2 * Arc\sin\left(1.616 \times \frac{\lambda}{\pi D}\right)$
Option 2	$2\theta_{-3dB} = 2 * Arc\sin\left(1.720 \times \frac{\lambda}{\pi D}\right)$

which results in equivalent values. For instance:

- Option 1 results in $2\theta_{-3dB} = 0.0031$ rad, i.e., 0.1770 deg.
- Option 2 results in $2\theta_{-3dB} = 0.0033$ rad, i.e., 0.1884 deg.

Based on discussion with other partners, the preferred option for subsequent simulations is option 1.

6.2 Q/V-BAND SAN TRANSMIT AND RECEIVE PARAMETERS

Table 20 provides the satellite beam diameter at nadir obtained using option 1 from the previous section, for the three types of satellite orbits that are considered in this project: Geosynchronous Equatorial Orbit (GEO), Low Earth Orbit (LEO) at an altitude of 1200 km and LEO at 600 km altitude.

Table 20: *SAN 3 dB beamwidth and resulting beam diameter at NADIR for the three satellite orbits considered in the project*

SAN parameters	GEO	LEO-1200 km	LEO-600 km
Satellite altitude (km)	35786	1200	600
3 dB beamwidth (deg)	0.1884	1.884	1.884

Satellite beam diameter at nadir (km)	117.7	39.5	19.7

One can notice that the values from TR 38.821 [7] for Ka-band (110, 40 and 20 km beam diameter respectively) are slightly different from the values proposed for Q/V-band (117.7, 39.5 and 19.7 km beam diameter respectively).

Moreover, ***Table 21*** provides the set of SAN parameters considered for Q/V band in DL (37 GHz).

Table 21: *Q/V-Band DownLink (i.e., ~37 GHz for DL) for different satellite orbits*

SAN parameters	GEO	LEO-1200 km	LEO-600 km
Equivalent satellite antenna aperture (m)	2.7	0.27	0.27
Satellite EIRP density (dBW/MHz)	45	18	15
Satellite Tx max Gain (dBi)	58.5	38.5	38.5

Equivalent satellite antenna aperture is corresponding to the antenna diameter in TR 38.811 6.4.1 [6] where a = D.

Table 22 proposes a set of SAN parameters for Q/V-Band in UL (47 GHz).

Table 22: *Q/V-Band UpLink (i.e., ~47 GHz for UL) for different satellite orbits*

SAN parameters	GEO	LEO-1200 km	LEO-600 km
Equivalent satellite antenna aperture (m)	2.1	0.21	0.21
G/T max (dB/K)	**31.8**	**11.8**	**11.8**
Satellite RX max Gain (dBi)	58.5	38.5	38.5
Earth temperature (K)	290	290	290
Satcom Repeater Noise Figure (dB)	**4**	**4**	**4**

An example of antenna pattern is shown in ***Figure 11*** considering the parameters in ***Table 23***.

Table 23: *Antenna parameters*

Parameter	Unit	Value
Frequency	[MHz]	Q/V Uplink
λ	[m]	0.0064 m
D	[m]	2.1 m
Efficiency	N/A	0.65
G_{max}	[dBi]	60.4
$2\theta_{-3dB}$	[°]	0.1770deg (Option 1) 0.1884 deg (Option 2)
D/λ	N/A	333

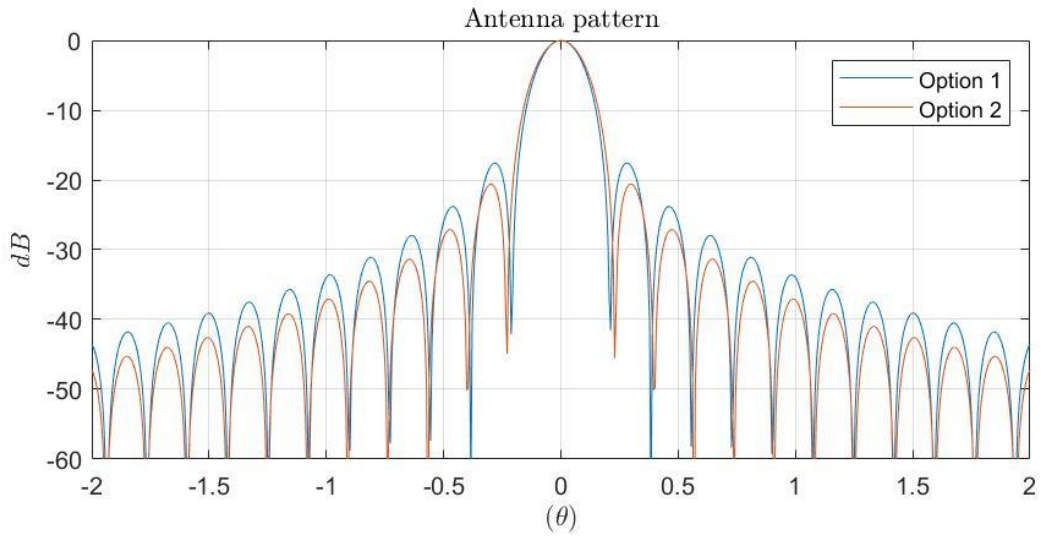

Figure 11: *Q/V-band transmit antenna pattern as a function of theta angle (°), with D/λ=333*

6.3 C-BAND SAN SATELLITE ANTENNA PATTERN

Similar antenna pattern as for the S-band can be reused [6] [7], with lower antenna size for GEO (22 to 12m), same antenna size for LEO (2m for both LEO-600km and LEO-1200km) and carrier frequency adapted for C-band (3.5 GHz instead of 2 GHz as in the case of S-band). Based on this setup, the antenna gains, the antenna beam diameter and the G/T can slightly change from S-band to C-band as presented in the next section. However, the satellite EIRP density has not been changed due to total transmission power limitation of the payload.

6.4 C-BAND SAN TRANSMIT AND RECEIVE PARAMETERS

Table 24 provides the SAN parameters for the C-band. The S-band SAN parameters from TR 38.821 are also provided comparison purposes.

Table 24: *DL and UL SAN parameters for simulations in C-band*

Satellite orbit		GEO	LEO-1200	LEO-600
Satellite altitude		35786 km	1200 km	600 km
Satellite antenna pattern		Section 6.4.1 in [2]	Section 6.4.1 in [2]	Section 6.4.1 in [2]
PAYLOAD CHARACTERISTICS FOR DL TRANSMISSIONS				
Equivalent satellite antenna aperture (Note 1)	S-band (i.e. 2 GHz)	22 m	2 m	2 m
Satellite EIRP density		59 dBW/MHz	40 dBW/MHz	34 dBW/MHz
Satellite Tx max Gain		51 dBi	30 dBi	30 dBi
3dB beamwidth		0.4011 deg	4.4127 deg	4.4127 deg
Satellite beam diameter (Note 2)		250 km	90 km	50 km
Equivalent satellite antenna aperture (Note 1)	C-band (i.e. 3.5 GHz for DL)	**12 m**	**2 m (and 1.2 m)**	**2 m (and 1.2 m)**
Satellite EIRP density		59 dBW/MHz	40 dBW/MHz	34 dBW/MHz
Satellite Tx max Gain		**50.5 dBi**	**35 dBi (30.5 dBi if 1.2 m)**	**35 dBi (30.5 dBi if 1.2 m)**
3dB beamwidth		**0.4207 deg**	**2.5247 deg (4.2084 deg if 1.2 m)**	**2.5247 deg (4.2084 deg if 1.2 m)**
Satellite beam diameter (Note 2)		**263 km**	**53 km (88 km if 1.2 m)**	**26.5 km (44 km if 1.2 m)**
PAYLOAD CHARACTERISTICS FOR UL TRANSMISSIONS				

Equivalent satellite antenna aperture (Note1)	S-band (i.e. 2 GHz)	22 m	2 m	2 m
G/T		19 dB K-1	1.1 dB K-1	1.1 dB K-1
Satellite Rx max Gain		51 dBi	30 dBi	30 dBi
Equivalent satellite antenna aperture (Note1)	C-band (i.e. 3.5 GHz for UL)	**12 m**	**2 m (also tested 1.2 m but G/T too small)**	**2 m (also tested 1.2 m but G/T too small)**
G/T		**21.87 dB K-1**	**6.87 dB K-1 (1.87 dB K-1 if 1.2 m)**	**6.87 dB K-1 (1.87 dB K-1 if 1.2 m)**
Satellite RX max Gain		**50.5 dBi**	**35 dBi (30.5 dBi if 1.2 m)**	**35 dBi (30.5 dBi if 1.2 m)**
NOTE 1: This value is equivalent to the antenna diameter in Sec. 6.4.1 of [2]. NOTE 2: This beam size refers to the Nadir pointing of the satellite NOTE 3: All these satellite parameters are applied per beam. NOTE 4: The EIRP density values are considered identical for all frequency re-use factor options. NOTE 5: The EIRP density values are provided assuming the satellite HPA is operated with a back-off of [5] dB.				

7 TN BS ANTENNA AND BEAM FORMING PATTERN MODELLING

7.1 C-BAND

Table 25 describes the Active antenna systems (AAS) patterns and parameters that are used, and ***Table 26*** provides the beam-forming related equations, which follow TR 38.921 [17].

Table 25: *Parameters of the parameterised array antenna model*

Parameter	Symbol	Unit
Front to back ratio	A_m	dB
Side lobe suppression	SLA_v	dB
Horizontal HPBW (Half Power Beam Width)	φ_{3dB}	Degrees
Vertical HPBW	θ_{3dB}	Degrees
Array element peak gain	$G_{E,max}$	dBi
Number of radiating elements rows and columns	(M, N)	Integer
Horizontal element separation	d_h	m
Vertical element separation	d_v	m
Electrical down-tilt angle	θ_{etilt}	Degrees
Electrical scan angle	φ_{escan}	Degrees

Table 26: *Array antenna model details for AAS (TR 38.921)*

Description	Equation	Unit
Peak normalised element radiation pattern	$A(\theta,\varphi) = -\min\left[-\left(-\min\left[12\left(\frac{\varphi}{\varphi_{3dB}}\right)^2, A_m\right] - \min\left[12\left(\frac{\theta-90}{\theta_{3dB}}\right)^2, SLA_v\right]\right), A_m\right]$	dB
Peak gain normalised element radiation pattern	$A_E(\theta,\varphi) = G_{E,max} + A(\theta,\varphi)$	dBi
Composite array radiation pattern	$\boldsymbol{A_A(\theta,\varphi) = A_E(\theta,\varphi) + 10\log_{10}\left(\left\lvert\sum_{m=1}^{M}\sum_{n=1}^{N} w_{m,n}v_{m,n}\right\rvert^2\right)}$, where $\boldsymbol{v_{m,n} = \exp\left(j2\pi\left((m-1)\frac{d_v}{\lambda}\cos(\theta) + (n-1)\frac{d_h}{\lambda}\sin(\theta)\sin(\varphi)\right)\right)}$ $\boldsymbol{w_{m,n} = \frac{1}{\sqrt{MN}}\exp\left(j2\pi\left((m-1)\frac{d_v}{\lambda}\sin(\theta_{etilt}) - (n-1)\frac{d_h}{\lambda}\cos(\theta_{etilt})\sin(\varphi_{escan})\right)\right)}$	dBi

Table 27: *AAS antenna parameters for C-band (TR 38.921)*

	Urban Macro	Suburban Macro
Base Station Antenna Characteristics		
Antenna pattern	TR 38.921 [17]	
Element gain $G_{E,max}$ (dBi)	5.5	6.4
φ_{3dB} / θ_{3dB} (degree)	90º / 90º	90º / 65º
Horizontal/vertical front-to-back ratio A_m (dB)	30 for both H/V	30 for both H/V
Antenna polarisation	Linear ±45º	Linear ±45º
Antenna array configuration (M, N)	16 × 8 elements	16 × 8 elements
Horizontal /Vertical (d_h/ d_v) radiating element spacing	0.5λ / 0.5λ	0.5λ / 0.7λ
Array Ohmic loss (dB)	2	2
Conducted power (before Ohmic loss) per antenna element (dBm)	22	22
Base station maximum coverage angle in the horizontal plane (degrees)	120	120
Base station vertical coverage range (degrees)	90-120	90-100
Mechanical downtilt (degrees)	10	6

7.2 Q/V-BAND

Coexistence aspects and radio frequency requirements for the new radio (5G NR) access technology with frequency up to 100 GHz are an object of study by TR 38.803 [14]. Therefore, the 6G NTN Q/V-band parameters are still applicable as part of the frequency ranges studied in TR 38.803.

TR 38.803 [14] describes a general antenna model using a uniform rectangular panel array, comprising $M_g N_g$ panels, is illustrated in Figure 12.

- M_g is the number of panels in a column
- N_g is the number of panels in a row
- Antenna panels are uniformly spaced in the horizontal direction with a spacing of $d_{g,H}$ and in the vertical direction with a spacing of $d_{g,V}$.
- On each antenna panel, antenna elements are placed in the vertical and horizontal direction, where N is the number of columns, M is the number of antenna elements with the same polarisation in each column.
- Antenna numbering on the panel illustrated in Figure 12 assumes observation of the antenna array from the front (with x-axis pointing towards broad-side and increasing y-coordinate for increasing column number).
- The antenna elements are uniformly spaced in the horizontal direction with a spacing of d_H and in the vertical direction with a spacing of d_V.
- The antenna panel is either single polarised (P=1) or dual polarised (P=2).

The rectangular panel array antenna can be described by the following tuple (M_g, N_g, M, N, P).

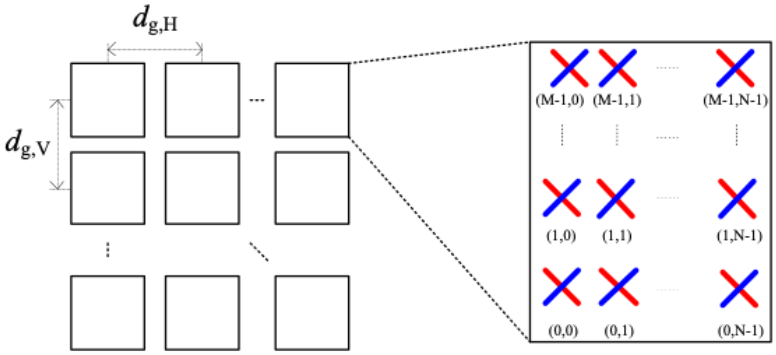

Figure 12: *General antenna model*

For a uniformly distributed array (ULA) antenna, as shown in Figure 13, the radiation elements are placed uniformly along the vertical **z**-axis in the Cartesian coordinate system. The **x-y** plane constructs the horizontal plane. A signal acting at the array elements is in the direction of **u**. The elevation angle of the signal direction is denoted as θ (defined between 0° and 180°, 90° represents perpendicular angle to the array antenna aperture) and the azimuth angle is denoted as φ (defined between -180° and 180°).

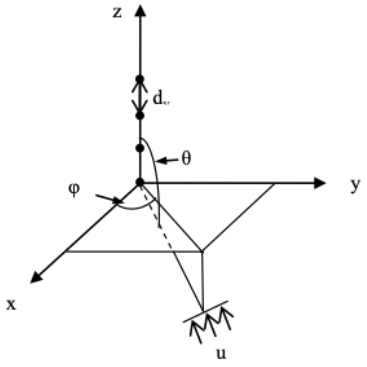

Figure 13: Antenna array geometry

The linear phase progression-based beamforming is assumed, as described in ***Table 27***. The beamforming-related equations used to compute the gains are provided in ***Table 28***.

Table 28: *Composite antenna pattern*

Parameter	Values
Composite Array radiation pattern in dB $A_A(\theta,\varphi)$	For beam i: $A_{A,Beami}(\theta,\varphi) = A_E(\theta,\varphi) + 10\log_{10}\left(\left\|\sum_{m=1}^{N_H}\sum_{n=1}^{N_V} w_{i,n,m}\cdot v_{n,m}\right\|^2\right)$ the super position vector is given by: $v_{n,m} = \exp\left(i\cdot 2\pi\left((n-1)\cdot\frac{d_V}{\lambda}\cdot\cos(\theta)+(m-1)\cdot\frac{d_H}{\lambda}\cdot\sin(\theta)\cdot\sin(\varphi)\right)\right),$ $n = 1,2,\ldots N_V; m = 1,2,\ldots N_H;$ the weighting is given by: $w_{i,n,m} = \frac{1}{\sqrt{N_H N_V}}\exp\left(i\cdot 2\pi\left((n-1)\cdot\frac{d_V}{\lambda}\cdot\sin(\theta_{i,etilt})-(m-1)\cdot\frac{d_H}{\lambda}\cdot\cos(\theta_{i,etilt})\cdot\sin(\varphi_{i,escan})\right)\right)$

In this simulation, there is one beam formed using all the antenna elements. Each beam is directed to one scheduled UE.

Note the above gives the correct antenna array radiation pattern, however the correct gain is only achieved if the element pattern $A_A(\theta,\varphi)$ is selected for the exact element spacing. For other element spacings, the element pattern $A_A(\theta,\varphi)$ must be separately calculated such that it is correct for the element spacing ($d_{g,H}$ and $d_{g,V}$). If $A_A(\theta,\varphi)$ is not linked to the element spacing then the calculated absolute gain may diverge from the correct value in a manner that varies as the beam is steered.

The correct composite array radiation pattern directivity (D) is given by:

$$D_A(\theta,\varphi) = 10\log\left(\frac{4\pi\left(|A_A(\theta,\varphi)|^2\right)}{\int_{-\pi}^{\pi}\int_{0}^{\pi}|P(\theta,\varphi)|^2\sin(\theta)d\theta d\varphi}\right),$$

The composite array radiation pattern gain can then be calculated as:

$$G_A(\theta,\varphi) = D_A(\theta,\varphi)L$$

where L is the Loss associated with the antenna. This is currently included in the estimate for element gain $A_E(\theta,\varphi)$, and is 1.8dB.

The antenna gains without beamforming is computed according to ***Table 29*** (the beamforming-related gain is computed according to ***Table 28***).

Table 29: *BS antenna modelling for Urban macro scenario*

Parameter	Values
Antenna element vertical radiation pattern (dB)	$A_{E,V}(\theta'') = -\min\left\{12\left(\frac{\theta''-90°}{\theta_{3\text{dB}}}\right)^2, SLA_V\right\}, \theta_{3\text{dB}} = 65°, SLA_V = 30\,\text{dB}$
Antenna element horizontal radiation pattern (dB)	$A_{E,H}(\varphi'') = -\min\left\{12\left(\frac{\varphi''}{\varphi_{3\text{dB}}}\right)^2, A_m\right\}, \varphi_{3\text{dB}} = 65°, A_m = 30\,\text{dB}$
Combining method for 3D antenna element pattern (dB)	$A''(\theta'',\varphi'') = -\min\left\{-\left[A_{E,V}(\theta'') + A_{E,H}(\varphi'')\right], A_m\right\}$
Maximum directional gain of an antenna element $G_{E,max}$	8 dBi
(M_g, N_g, M, N, P) note	For 30GHz: (1, 1, 8, 16, 2)
(d_v, d_h)	(0.5λ, 0.5λ)
Note:	**An additional 3dB gain is added to the total beamforming gain to account for the two polarisation directions. Boresight direction is horizontal**

8 STATE OF THE ART ON STRATEGIES FOR COEXISTENCE

This section provides a literature review on strategies for coexistence of communication systems using adjacent bands. Selected techniques will be described and the coexistence scenario under consideration will be stated where relevant.

This section therefore aims to identify TN/NTN UE, TN BS & SAN algorithms and techniques for improved coexistence and interference reduction scenarios such as GSO protection, isolation of beams, and side-lobe power level reduction for different frequency bands (e.g., C and Q/V-bands).

For instance, strategies for coexistence are needed for adjacent channel coexistence to derive NTN and/or TN core requirements (ACLR, ACS) or NTN-TN joint-optimisation techniques.

Coordination between different systems may also be considered:

- NTN-TN coordination, such as terrestrial systems protection/Power Flux Density limit for the satellite system,
- NTN-NTN coordination, such as GSO-NGSO coordination e.g., service link and/or feeder link, shut off the station if required and/or GSO protection depending on frequency bands, equivalent PFD (Power Flux Density) /EPFD (Equivalent Power Flux Density) limits.

Previous mentioned techniques may be applied at the level of PHY (Physical) layer or MAC (Medium Access Control) / RRM.

8.1 COEXISTENCE VIA COMPLIANCE TO STANDARDS

3GPP introduces as part of its standards a set of requirements for transmitters and receivers with the intent of enabling the operation in adjacent bands. The main requirements (cited from TN BS specification for FR1) are

- Adjacent Channel Leakage power Ratio (ACLR) – defined in [18] as “the ratio of the filtered mean power centred on the assigned channel frequency to the filtered mean power centred on an adjacent channel frequency”.
- Adjacent Channel Selectivity (ACS) – defined in [18] as “a measure of the receiver's ability to receive a wanted signal at its assigned channel frequency at the antenna connector for BS type 1-C or TAB (Transceiver Array Boundary) connector for BS type 1-H in the presence of an adjacent channel signal with a specified centre frequency offset of the interfering signal to the band edge of a victim system.”

Implementation differences may exist with respect to FR1 or FR2 ranges for TN (for instance 2-O type is considered), or FR1 (for instance 1-C type currently not considered) and above 10 GHz ranges for NTN (for instance 2-O type is considered). However, compliance to the standard generally speaking implies that the base station and UEs abide to limits for both ACLR and ACS, and that the throughput degradation for systems operating in adjacent bands is limited to 5%.

8.2 ISSUES RELATED TO SYNCHRONISED TDD OPERATION

While NTN systems typically operate in FDD mode, most terrestrial systems in frequencies above 3 GHz operate with TDD duplexing. With respect to NTN-related scenarios, this configuration does not occur and it might be considered only for TN-TN setup. However, the synchronised TN TDD operation may represent a difficult interference scenario for NTN since all the synchronised TN BS will transmit at the same time towards the satellite, therefore increasing the received interference from adjacent bands (if satellite and terrestrial systems use different adjacent bands).

For TN systems, special care must be taken to avoid the effects of cross-link interference. That may be thought of as the interference that occurs when two systems operate in opposite directions for the same time interval (slot).

Measurement results for the impact of misalignment of TDD slot patterns in adjacent bands are reported in [19]. The authors note that when the two adjacent systems use the same TDD format (synchronised operation), the interference impact on throughput and experienced delay is negligible. On the other hand, when the slot formats diverge (unsynchronised operation), such that cross-link interference occur, significant degradation ensues.

Coordination to avoid TDD slot format misalignment is recommended.

ECC Report 296 [20] proposes a “toolbox” with options to support Administrations and operators in identifying the most appropriate synchronisation regulatory framework at national level. The key elements from the “toolbox” regarding Synchronised operation are summarised hereafter.

Synchronised operation avoids any BS-BS and MS-MS (Mobile Station) interference therefore allowing coexistence between adjacent networks without the need for guard bands or additional filters. This operating mode simplifies network deployment because no additional interference mitigation is required. However, in order to implement this, within each deployment area/region, all MFCN (Mobile/Fixed Communications Networks) licensees operating in the same band (not limited to the licensees with adjacent blocks) should use:

- A common phase clock reference (e.g., UTC (Coordinated Universal Time)), with proper accuracy/performance constraints that depend on the underlining technology, and permanent monitoring and agreed remedies in case of accuracy loss. Those aspects and challenges are detailed in ECC Report 216 [25];

- A compatible frame structure to avoid simultaneous UL/DL transmission, which determines a specific DL/UL transmission ratio and frame length. The chosen frame structure will contribute to the network performance (e.g., latency, spectral efficiency, throughput and coverage). The feasibility and performance impacts of synchronised operation between different radio technologies have to be assessed on a case-by-case basis depending on the specific technologies. As assessed in [20], the synchronised operation of 5G-NR and LTE (Long Term Evolution)-TDD may imply a cost in terms of user plane latency and performance, especially with regards to 5G URLLC (Ultra-Reliable Low Latency Communications) latency targets. Agreements on synchronised operation between operators will be simplified when the same type of services are targeted with the associated desired user plane latency and performance targets.

8.3 INTERFERENCE MITIGATION VIA LINK ADAPTATION

Besides TDD slot format alignment, the authors in [19] suggest that a system that is suffering interference may adapt its link adaptation policies, introducing more robustness in coding to avoid retransmissions. This has the drawback of reducing peak throughput. However, there are other solutions to improve link adaptation performance.

Interference Measurement (IM) plays a significant role in Channel Quality Indicator (CQI) which is reported in Channel State Information (CSI) feedback. Thus, accurate IM can effectively improve Link Adaptation (LA) performance and further increase system capacity as well as coverage.

Two IM methods, non-zero-power CSI reference signal (NZP CSI-RS) method and CSI-IM method, are investigated and compared following 5G NR protocols in paper [21]. Besides, an interference limited scenario which particularly focuses on cell-edge users is considered in the paper. This inter-cell-interference has similarities with inter-technology interference. As a result, IM techniques are worth studying for the TN-NTN coexistence interference cancellation.

As studied in paper [21], both methods are compatible with non-pre-coded and pre-coded transmission. NZP CSI-RS method measures the interference in a residual manner, which means that IM is calculated by subtracting the product of estimated channel and transmitted RSs from the received signal.

NZP CSI-RS is allocated to the same and non-overlapped Resource Elements (REs) for serving and interfering gNBs in non-pre-coded transmission and pre-coded transmission, respectively. To the contrary, UE can measure interference directly using CSI-IM method as CSI-IM resources contain zero power REs.

Furthermore, the authors of [21] achieve higher quality channel measurement in CSI-IM method by allocating CSI-IM or ZP CSI-RS resources overlapped with NZP CSI-RS resources of interfering gNBs. Simulation results show that NZP CSI-RS method has the best throughput performance in non-pre-coded transmission scenario especially without outer loop link adaptation. On the other hand, CSI-IM method outperforms NZP CSI-RS in pre-coded interference measurement. Furthermore, NZP CSI-RS method consumes fewer overhead resources and provides relatively good performance, while CSI-IM method can estimate interference per gNB anticipated to be used for advanced receiver algorithms.

8.4 INTERFERENCE REJECTION COMBINING TECHNIQUES

With the advent of MIMO (Multiple-Input Multiple-Output), it is possible for a receiver to use additional degrees of freedom to null or mitigate interference signals. This is also called Interference Rejection Combining (IRC) technique. Paper [22] provides a study on IRC approach applied to LTE uplink transmission.

Another approach for IRC is Minimum Mean-Squared Error Interference Rejection Combining (MMSE-IRC). In [23] it is shown that MMSE-IRC performs well in the presence of interferers. It has the drawback of requiring channel estimates for the interference paths towards the victim.

MMSE-IRC addressing inter-cell interference (ICI) and intra-cell inter-user interference (IUI) is analysed for 5G NR system in [24]. Compared with conventional MMSE, MMSE-IRC shows significant performance improvement.

8.5 TN UE TO NTN INTERFERENCE MITIGATION TECHNIQUES

The interference level from TN UE to NTN SAN or NTN UE depends on the position of the satellite or the NTN UE with respect to the TN UE. For example, if the main lobe from the TN UE is directed towards a NTN satellite, then the NTN UL can experience large amount of interference. ***Figure 14*** illustrates two examples: an interference-free example on the left, with the TN UE main lobe beam pointing in a direction different from the NTN satellite, and on the right an interfering example with the TN UE main lobe beam directed towards the NTN satellite, resulting into a high level of interference on the NTN UL.

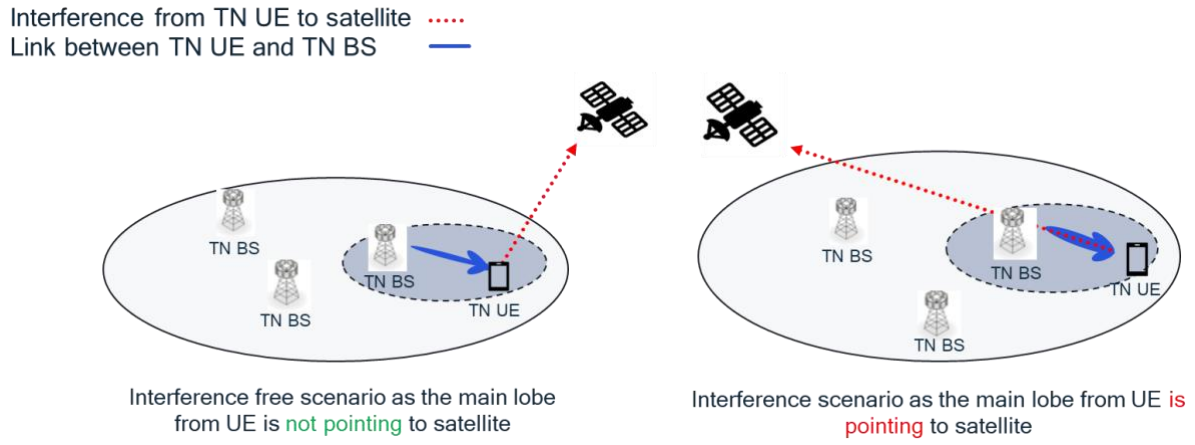

Figure 14: *Example of interference-free (left) and interference (right) scenarios from TN UE to NTN satellite*

Different solutions can be proposed to mitigate the interference from the TN UE to the NTN, for example by using advanced receiver at baseband which can mitigate or eliminate the interference signals [26].

Furthermore, several methods can be done in the TN UE if the position of the satellite or the NTN UE is well known to the TN UE. These methods can include but not limited to:

- Power reduction method: the target here is to keep the interference lower than the threshold and that can be done by reducing the transmit power from the UE in the direction to the satellite.
- Frequency method: the target here is to apply frequency re-use or to apply different frequency allocation between TN and NTN
- Spatial method: the target here is to use the advanced beamforming techniques to reduce the unintentional interference towards the NTN. That can include reduction in the antenna gain or beam nulling towards the NTN

8.6 KNOWN TN TECHNIQUES TO BE APPLIED FOR NTN

Several techniques are discussed in ***Table 30*** and the conclusions have been summarised in Section 8.7.

Table 30: *Known Tn techniques to be applied for NTN*

Mechanism	Overview	Comments
HFR: Hard Frequency Reuse scheme	-The whole frequency band can be partitioned into a configurable number disjoined sub-bands or BWP (Bandwidth Part) -Adjacent cells of different service areas edges are allocated with different disjointed sub-bands / BWPs -The Frequency Reuse Factor (FRF) equals the number of sub-bands / BWPs - Within a service area, an additional partitioning in (frequency, time) resource such as PRB or (sub-Carrier, sub-frames) is required. - Since these sub-bands / BWPs are allocated to cell isolated in space, they can be re-used as a configurable number of colours, pattern based -Inter-Cell Interference should be reduced between neighbouring satellite cells.	Feasible for satellite communication
CA (Carrier Aggregation) with carrier scheduling schemes	The principle of these coordination schemes is to allocate disjointed (orthogonal) Carrier Components (CCs) in FDD mode, to neighbouring cells. - CA scheduling grant and resource on the same carrier. In this case, the available spectrum is divided into parts, Primary Carrier Components (PCCs) and Secondary Carrier Components (SCCs). The interfering cells will use different frequency spectrum parts (either PCC or SCC). - CA based Cross-carrier scheduling It is an enhancement of the previous scheme. The scheduling grant and the resource allocated for data are not necessarily on the same carrier, which may keep operational the control of the scheduling grant in case of interference on the carrier associated to data. - CA based HetNet (Heterogeneous Networks) using PDCCH (Physical Downlink Control Channel). In this case, The PDCCH of a Secondary Cell (SCell) does not interfere with the PDCCH of the Primary Cell (PCell), since an extended PDCCH is allocated with the PRBs that the PDSCH (Physical Downlink Shared Channel) may use and not those ones of the PDCCH. - CA based HetNet using ePDCCH (enhanced PDCCH) channel with ICIC (Inter-Cell Interference Coordination). In this case, the extended PDCCH of the SCell cannot interfere with the extended PDCCH of the PCell, for a given frequency / band because they are not allocated on the same PRBs.	May be difficult to implement for satellite purposes due to tight synchronisation and interference management between different carriers
ICIC scheme	Inter-Cell Interference Coordination scheme: The principle of this coordination scheme is to allocate disjointed (orthogonal) PRB (Physical Resource Block) to neighbouring cells. This is actually a hybrid coordination scheme in time and frequency domains.	Feasible for satellite purposes, requires ISL(Inter-Satellite Link)/Xn

	Requires Time & Frequency synchronisation between gNBs.	interface between satellites
ABS based eICIC (enhanced ICIC)	Almost Blank Subframes based enhanced ICIC coordination schemes: The principle is to allocate (to schedule) disjoint (orthogonal) structures (sub-frame, sub-carrier) to neighbouring cells. It relies on transmission with Power Coordination in the time and frequency domains, per sub-frame, sub-carrier basis: -Zero Power sub-frames based eICIC; -RP-ABS based eICIC (Reduced Power Almost Blank Sub frames). The technique requires Time & Frequency synchronisation between gNBs.	Feasible for satellite purposes, requires ISL/Xn interface between satellites
CoMP (Coordinated Multi-Point) schemes and Interference nulling based CoMP	Downlink CS/CBS-CoMP (DL_CS_CoMP): Downlink Coordinated Scheduling per sub-frame, sub-carrier, potentially beam basis, with respect to JT/DPS (Joint Transmission/Dynamic Point Selection) schemes. The transmission is done from one TP (Tx Point) at once. The interfering transmission TP is steered towards the null space, for interference mitigation purposes.	May be difficult to implement for satellite purposes due to tight synchronisation and interference management between different transmission points
	Uplink CS/CBS-CoMP (UL_CS_CoMP): Uplink Coordinated Scheduling per sub-frame, sub-carrier, potentially beam basis. It relies both on scheduling & pre-coding selection decisions, per sub-frame, sub-carrier, potentially beam basis. UE data is transmitted to 1 RP (Rx point) at once. The interfering transmission UE is steered towards the null space. This technique is not suited for Handset UE with omnidirectional antenna (e.g. C-band) but to UE with antenna steering and therefore VSAT type, which might be applicable for Q/V-band.	
	Downlink Joint Transmission CoMP (DL_JT_CoMP). Relies on simultaneous Data Transmission from multiple TP.	
	Downlink DPS (Dynamic Point Selection) CoMP muting (DL_DPS_CoMP): Relies on Dynamic Transmission Points Selection, per sub-frame basis. It may be combined to JT. PRB pairs are selected within sub-frame.	
	Uplink Joint Reception CoMP (UL_JR_CoMP): It relies on multiple simultaneous Reception Points (RP) of UE transmitted by the PUSCH (Physical Uplink Shared Channel) and RP selection per sub-frame basis.	
Transmitter based FeICIC (Further eICIC)	The Transmitter mutes PDSCH resource elements that experiences strong interference from other TP (Transmission Points within cells).	Is normally used together with ICIC
Receiver based FeICIC	The Receiver subtracts the dominant interferer.	Is normally used together with ICIC
MIMO techniques	Spatial diversity, as provided by MIMO, can contribute to mitigate interferences.	To be analysed with respect to diversity of satellite channel model
	MMSE-IRC: Minimum Mean Square Error (MMSE) and Interference Rejection Combiner (IRC).	Technique to be further used in futur studies

	Beamforming based.	Technique to be further used in future studies for both UE and satellite
Waveform Design Based	5G NR allows for any filtering technique at the transmitter side, as long as it is transparent for the receiver (TR 38.802 [27]). Block Filtered-Orthogonal Frequency Division Multiplexing (BF-OFDM) as described in [28] provides several advantages, in the context of spectrum sharing: -High out-of-band rejections: each sub-band of BF-OFDM benefits from a filtering stage; therefore, the spectrum leakage in adjacent bands is very low. -Ability to create spectrum holes: BF-OFDM [28] has been designed so that entire sub-bands power can be dynamically set to zero. This enables/improves the implementation of RRM coordination schemes, dynamically allocating sub-bands to cells of different BS (gNB, eNB) sharing the same band (both NTN and TN cells). -Numerology (sub-carrier spacing in the 5G terminology) can be set in different sub-bands, with a unique filtering stage.	Technique to be further used in the Waveform Design task (T4.1) part of WP4 in the 6G-NTN project.

8.7 NTN INTERFERENCE MITIGATION TECHNIQUES CONCLUSION

As previously mentioned, synchronisation strategies based on ICIC are not currently considered for NTN. However, the preliminary study has highlighted other potential techniques such as FFR (Fractionary Frequency Reuse), beam steering, polarisation, scheduling and MMSE-IRC. These techniques are summarized in ***Table 31***.

Table 31: *NTN interference mitigation techniques for different equipment types and frequency bands*

Equipment type	Band	Interference mitigation technique	Comments
NTN SAN	C-band	FFR (Fractionary Frequency Reuse), see Figure 18 with FRF = 2 or 3 Beam steering, Side lobe limitation Beam/cell scheduling (RB, BWP, Power, Channel, MCS (Modulation and Coding Scheme), etc.), Inter-satellite scheduling	Potentially investigate: DL/UL band inversion with respect to TN, GSO/NGSO coordination
	Q/V-bands	FFR (Fractionary Frequency Reuse), see Figure 18 with FRF = 2 or 3 Beam steering, Side lobe limitation Beam/cell scheduling (RB, BWP, Power, Channel, MCS, etc.), Inter-satellite scheduling Circular polarisation (Left-Handed and Right-Handed Circular Polarisation (LHCP, RHCP))	
NTN UE	C-band	FFR (Fractionary Frequency Reuse), see Figure 18 with FRF = 2 or 3 MMSE-IRC receivers	
	Q/V-bands	FFR (Fractionary Frequency Reuse), see Figure 18 with FRF = 2 or 3 Circular polarisation (LHCP, RHCP) Pointing accuracy, Antenna off-axis limits Self-power reduction/shutdown (based on spectrum allocation/ regional requirements)	Investigate potential feasibility of MMSE-IRC receiver in Q/V-band in next sections

Figure 15 shows different frequency reuse factors (FRFs) applied to a cluster of beams. Fractionary Frequency Reuse (FFR) systems use different FRFs to divide available bandwidth into sub-bands.

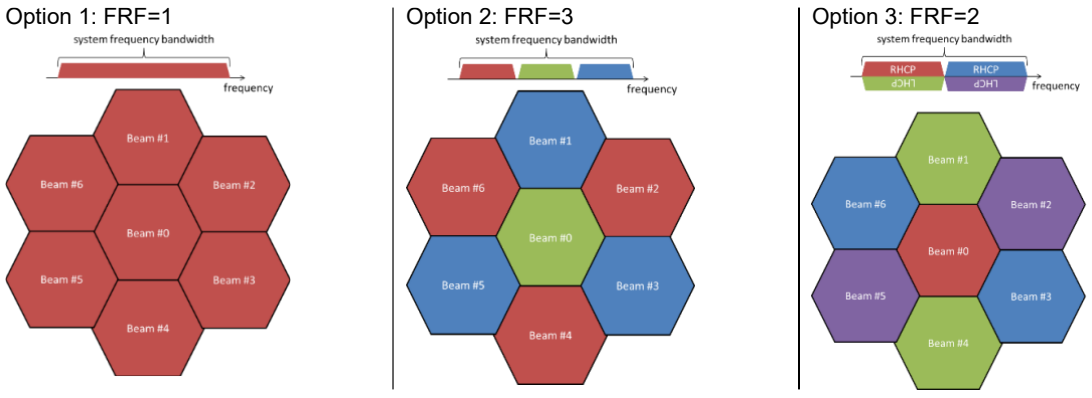

Figure 15: *different Frequency reuse factors applied to a cluster of beams – extracted from [7]*

9 INTRODUCTION ON THE NTN AND TN CALIBRATION PURPOSE

In this section, we first provide in section 9.1 some comments related to the parameters introduced in the previous sections. We then explain in section 9.2 the principles and the objectives of the calibration of the simulators developed by the different partners. We finally detail in section 9.3 the metrics considered to assess the calibration.

9.1 COMMENTS RELATED TO PARAMETERS

Two comments with respect to previous parameters from previous sections related to VSAT and Satellite Access Node are in order:

- The size of SAN antenna, antenna gain and/or satellite EIRP used for calibration simulations (in D4.7) could be further changed/increased for the coexistence simulations (in D4.8) in order to compensate the reduced size of VSAT UE antenna (e.g. 15 cm x 15 cm size, reduced from initially considered 60 cm antenna aperture diameter, for better integration with vehicles and drones).
- The system channel bandwidth / resource allocation for the satellite system may also be reduced, potentially only for UL transmission since the satellite will probably require using the whole channel bandwidth whereas each UE may only use a reduced portion of the bandwidth with the granularity of one RB.

9.2 PRINCIPLES AND OBJECTIVES OF THE CALIBRATION

Performing the coexistence studies requires that each partner implement a simulator for both NTN and TN communications. These different simulators are developed independently, but should follow the same procedure provided in the relevant TR (i.e. [7] for NTN and [14] for TN) and summarized in the present document for the computation of *i*) the link budget and *ii*) the interference level. It is thus of interest to check that they provide similar results on some reference scenarios before performing the coexistence studies. This first step is called the *calibration* of the simulators in the 3GPP terminology, and consists in simulating only NTN or TN links as depicted in ***Figure 16*** under interferences in different topologies generated through Monte Carlo simulations to collect metrics. Then, the Cumulative Distribution Function (CDF) of the metrics collected by the different partners are compared to assess whether the simulators provide similar results or not. The calibration methodology related to NTN (resp. TN) communications is detailed in section 10 (resp. section 11). The metrics used to assess the calibration of the simulators are detailed in section 9.3.

Remark: ***Figure 16*** differs from

Figure 4 and ***Figure 5*** due to the presence of the blue ellipses that highlight that, during the TN (resp. NTN) calibration, only TN (resp. NTN) links are simulated.

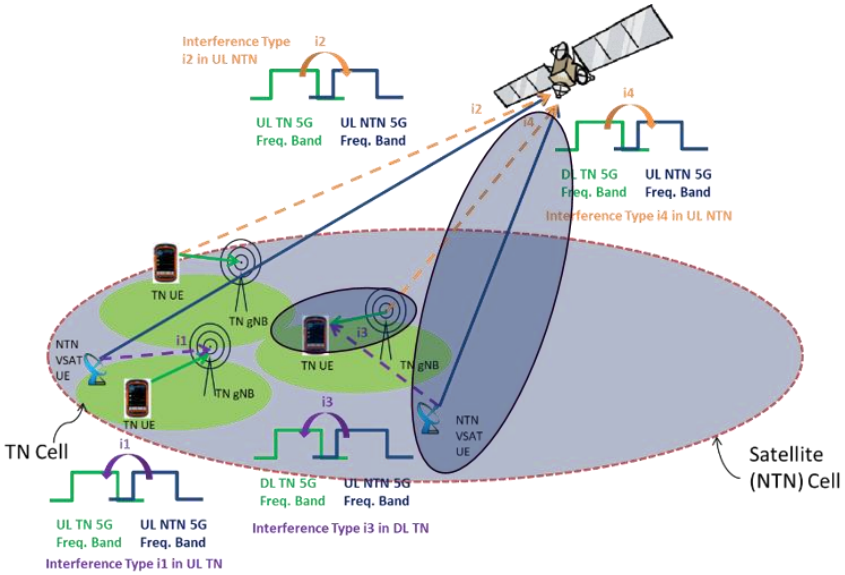

(a) DL TN and UL NTN.

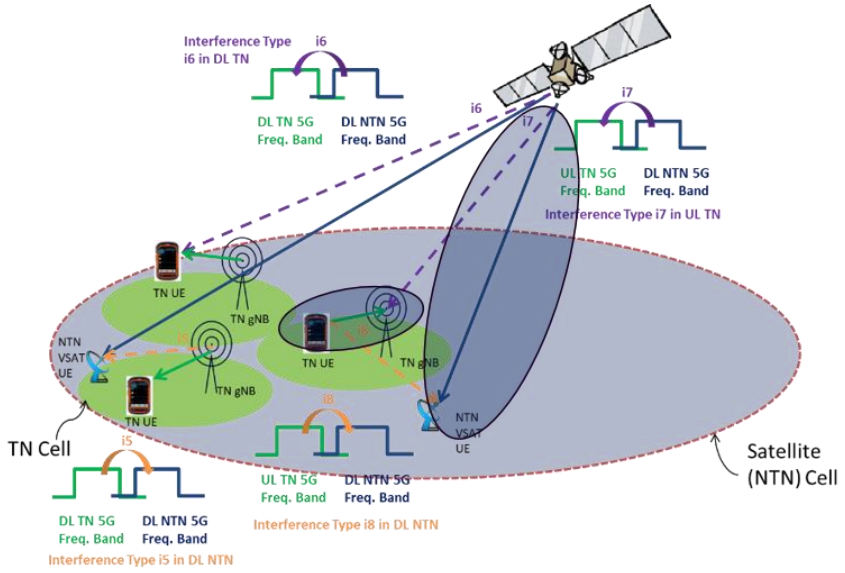

(b) UL TN and DL NTN.

Figure 16: *high level illustration of the calibration procedure for NTN and TN communications. Unlike for the coexistence studies, Only NTN or TN links are simulated for the calibration, as illustrated by the blue ovals*

9.3 CONSIDERED METRICS FOR THE CALIBRATION

The CDF following two metrics are considered for the simulators calibration (more mathematical details are provided latter in this section):

1. The Coupling Loss (CL), defined as the difference between the received and the transmit power for the useful signal. This metric is useful to assess the implementation of *i*) the propagation loss, and *ii*) the antennas gain of the transmitter and the receiver.

2. The Signal to Interference plus Noise Ratio (SINR), defined as the ratio between the received power from the useful signal and the sum of the noise power and the interference level. This metric is useful to assess the computation of the interference level.

Mathematically, the CL between a transmitter T_X and a receiver R_X can be written as:

$$CL = P_{T_X} - P_{R_X}$$

where P_{T_X} and P_{R_X} are the transmit and the received power, respectively, which are linked by the following equation that holds for both NTN and TN communications:

$$P_{R_X} = P_{T_X} + G_{T_X} + G_{R_X} - P_L,$$

where G_{T_X} and G_{R_X} are the antenna gains at the transmitter and the receiver side, respectively, and P_L is the path loss. The computations of P_{T_X} , G_{T_X}, G_{R_X}, and P_L differ between NTN and TN communications. For NTN, the computation of P_L is detailed in section 2.3 which is extracted from [7] whereas P_{T_X}, G_{T_X}, and G_{R_X} are computed according to section 6. It is worth mentioning that we used for the shadowing the standard deviation values provided in [6] for the Ka-band. These values could be modified in future works if more appropriate values are proposed for the Q/V or the C frequency bands. For TN communications, the computation of P_L is detailed in section 2.4 whereas P_{T_X}, G_{T_X}, and G_{R_X} are computed according to sections 5 and 7.

It comes from the previous discussion that the CL can be written as:

$$CL = P_L - (G_{TX} + G_{RX}).$$

Thus, a good match between the CL of two different simulators provides good hint that the implementation of the path loss and the antenna gains is similar.

On the other hand, the SINR in a communication subject to N_{itf} interferers can be mathematically written as:

$$SINR = \frac{P_{R_X}}{10^{0.1N_F}N_0 + \sum_{i=1}^{N_{itf}} P_{R_X}^i}$$

where N_F [dB] is the noise figure whose value is provided in ***Table 13***, for NTN UE, in section 5 for TN BS and UE, and in ***Table 22*** for SAN at different satellite orbit, N_0 is the noise power (that depends on the allocated bandwidth), and $P_{R_X}^i$ is the received power from the ith interferer. $P_{R_X}^i$ is computed using the same equation as P_{R_X} with different values for the path loss and antenna gains since each interferer is at a different location than the transmitter of the useful signal (except for the DL of NTN as it will be detailed in section 10.1.3).

A good match of the SINR of two different simulators provides hint that the computation of the interference level is similar.

10 NTN CALIBRATION

We first detail the calibration methodology for both the UL and the DL of NTN communications in Section 10.1. Then, we provide calibration results for the UL and the DL in the Q/V-band in Section 10.2.

Remark: calibration in the Q/V band had been performed assuming the following EIRP values for the DL of the different orbits: 3 dBW/MHz for LEO-600 km, 8 dBW/MHz for LEO-1200 km, and 38 dBW/MHz for GEO.

10.1 CALIBRATION METHODOLOGY

10.1.1 General hypotheses

The following hypotheses are made for both the calibration of the UL and the DL, as for the RAN4 assumptions starting from release 17:

1. The satellite is at nadir, i.e. its elevation is 90 degree with respect to the central beam.
2. The FRF is set to one, i.e. the same frequency is used by the satellite across the beams for communicating (DL and UL) with the users (see also Figure 18). This enables to validate the implementation of the interference from adjacent beams.
3. The metrics are computed for UE(s) in the central beam that will also be referred to as reference beam in the sequel.
4. The interference is caused by the six direct adjacent beams. The interference coming from further beams is neglected.
5. The UEs antennas are pointing to the satellite and thus UEs' antenna gain is maximal in the direction of the satellite.

10.1.2 UL calibration

The calibration methodology for the UL of NTN communications is illustrated in ***Figure 17*** which is extracted from [7], Figure 6.1.3.2-2, and can be explained as follows. 10 UEs are randomly placed in the reference beam as well as in each of the six adjacent beams at each Monte Carlo simulation. The useful received power at the satellite side comes from the UEs in the central beams whereas the UEs in the adjacent beams create interference.

The bandwidth allocated to each UE in each beam corresponds to the total bandwidth divided by 10, and the frequencies allocated to the different UEs in a given beam are orthogonal (i.e. we do not consider intra beam interference). As a consequence, there is one UE in each adjacent beam that uses the same frequency band as each UE from the central beam, thus creating interferences at the satellite side.

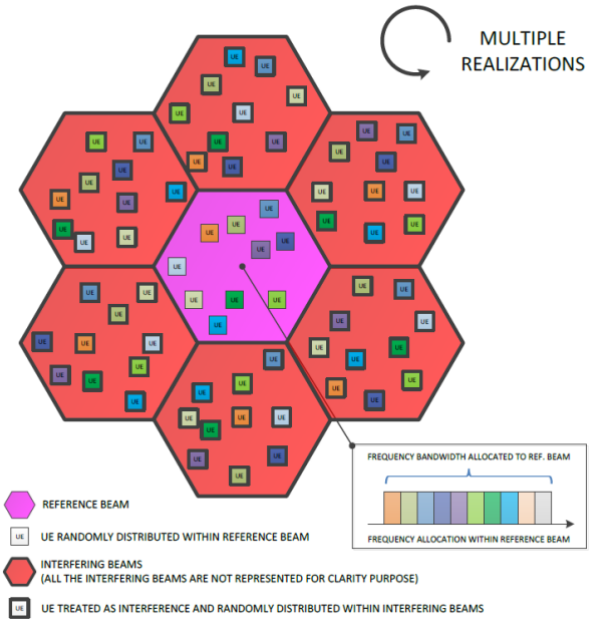

Figure 17: *Illustration of the methodology for UL calibration of NTN communications*

10.1.3 DL calibration

The calibration methodology for the DL of NTN communications is illustrated in ***Figure 18*** which is extracted from [7], Figure 6.1.3.2-1, and can be explained as follows. NTN UE is randomly dropped into the central reference beam at each Monte Carlo simulation. The full channel bandwidth is allocated for communications. The useful received power at the UE corresponds to the power transmitted by the satellite to the central beam, whereas the interference comes from the transmission from the satellite to the adjacent beams on the same frequency (since the satellite beams are slightly overlapping at -3 dB from the beam peak value). It is worth mentioning that in this case, the path loss of the interferer in the SINR computation is the same as for the useful signal since the interfering signal comes from the satellite as well.

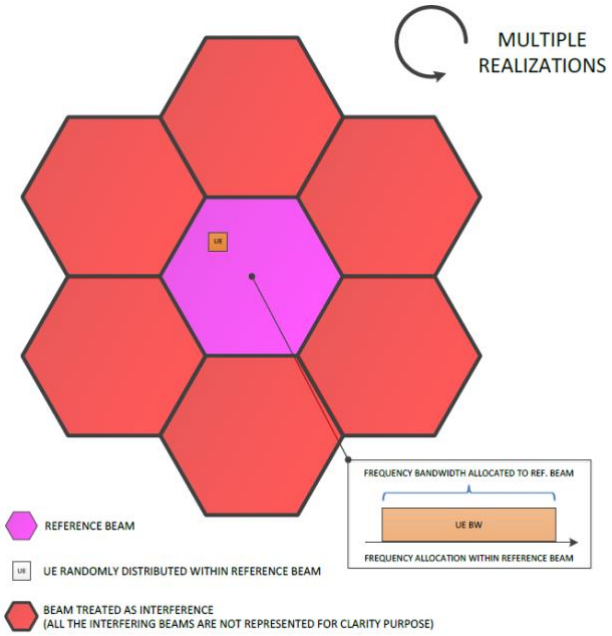

Figure 18: *Illustration of the methodology for DL calibration of NTN communications*

10.2 NTN Q/V-BAND

The calibration results for the UL and the DL are provided in sections 10.2.1 and 10.2.2, respectively.

10.2.1 NTN UL Q/V-band

The CDF of the CL for the UL of NTN communications in the Q/V-band at 47 GHz are provided in ***Figure 19*** for GEO (left) and LEO-600km (right) satellites. We can observe a good match between the partners' results with less than 2 dB difference between the CDF of the CL for both satellite orbits.

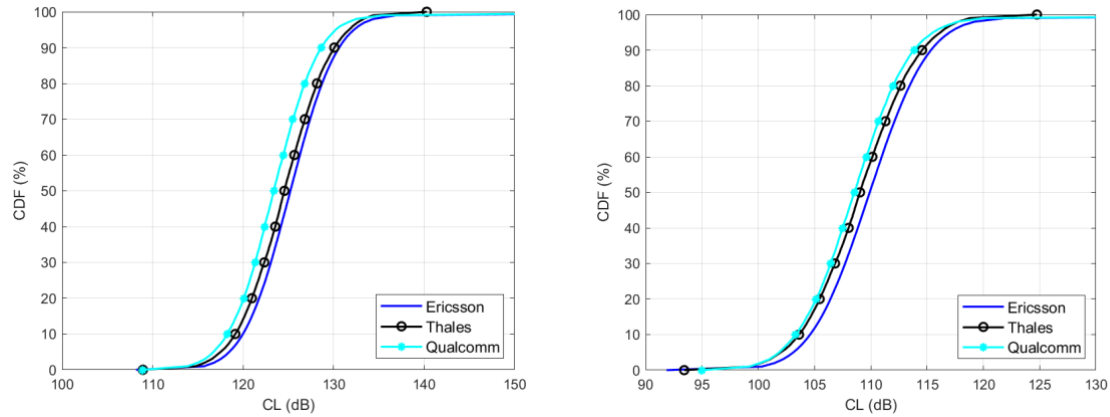

Figure 19: *CDF of the CL for the UL of NTN communications in the Q/V-band at 47 GHz for GEO (left) and LEO-600km (right) satellites*

The CDF of the SINR for the UL of NTN communications in the Q/V-band at 47 GHz are provided in ***Figure 20*** for GEO (left) and LEO-600km (right) satellites. We can see that there is a good agreement between the results obtained by the three partners for both satellite orbits.

We can also observe that the obtained SINR (reported in current deliverable D4.7 for calibration phase) are quite low, especially for GEO satellite for which half of the obtained values are below 0 dB. This is due to *i*) the assumption that FRF=1, resulting in a high interference level, and *ii*) the small antenna aperture of the UE that results in a small antenna gain at the UE side towards (and from) the satellite.

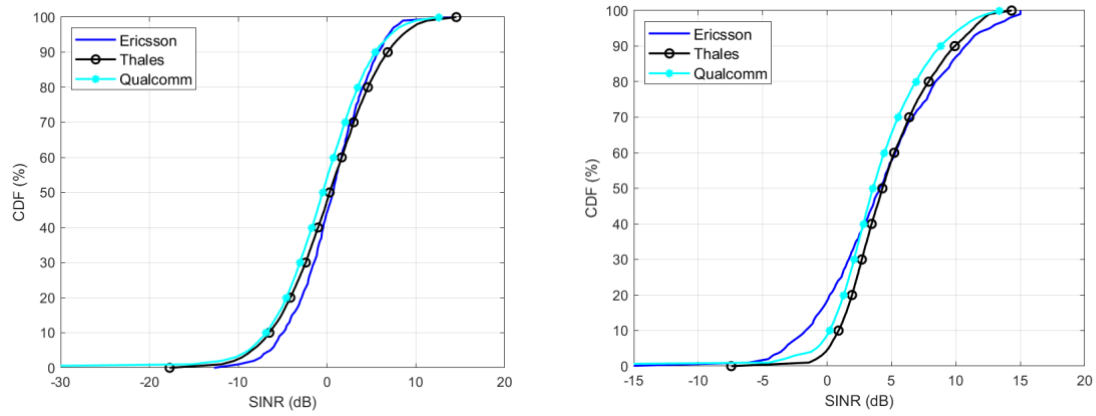

Figure 20: *CDF of the SINR for the UL of NTN communications in the Q/V-band at 47 GHz for GEO (left) and LEO-600km (right) satellites*

10.2.2 NTN DL Q/V-band

The CDF of the CL for the DL of NTN communications in the Q/V-band at 37 GHz are provided in ***Figure 21*** for GEO (left) and LEO-600km (right) satellites. We can observe a good match between the different results with less than 0.5 dB (resp. 1 dB) difference between the CDF for GEO (resp. LEO-600km) satellites.

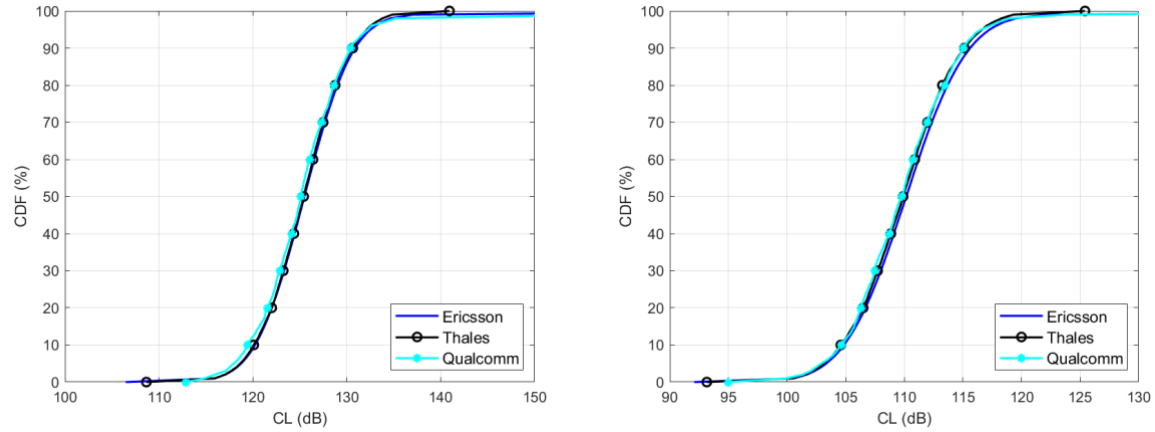

Figure 21: *CDF of the CL for the DL of NTN communications in the Q/V-band at 37 GHz for GEO (left) and LEO-600km (right) satellites*

The CDF of the SINR for the DL of NTN communications in the Q/V-band at 37 GHz are provided in ***Figure 22*** for GEO (left) and LEO-600km (right) satellites. As for the CL, we can observe a good agreement between the three SINR CDF. Similarly to the UL, we can see that the resulting SINR are low, which is due to the same reason as for the UL.

As a matter of fact, increasing antenna size of the satellite (for increased antenna gain) is not necessary a viable option for mainly two reasons: 1/ (from the system point of view) due to

lower beam footprint on ground which may have an impact on the number of handovers and also satellite capacity to deliver higher number of beams over the same area; 2/ (from the launching point of view) the antenna size has to remain compatible with the cost of the launch and the launcher capacity. On the other hand, satellite transmit power is limited and thus energy saving strategy and/or beam switching must be considered in order to decrease the number of beams used at the same time. The selection of these satellite parameters will therefore take into account D3.5 6G-NTN project results related to available satellite transmission power and constraints such as satellite power dissipation.

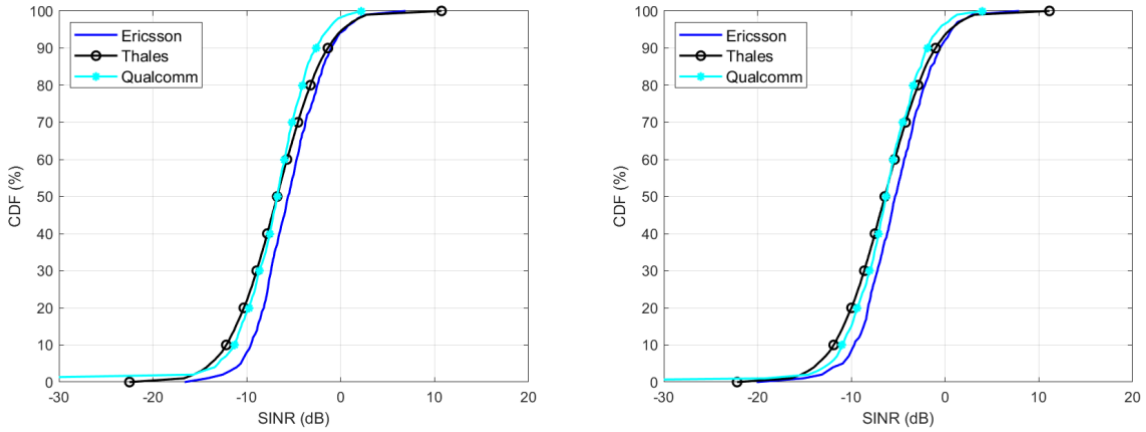

Figure 22: *CDF of the SINR for the DL of NTN communications in the Q/V-band at 37 GHz for GEO (left) and LEO-600km (right) satellites*

11 TN CALIBRATION

In this section, we first detail the calibration methodology for both the UL and the DL of TN communications in section 11.1. Then, we provide calibration results for the UL and the DL in the Q/V-band in section 11.2.

11.1 CALIBRATION METHODOLOGY

As for the NTN calibration procedure described in 10.1, the calibration for the TN is performed by assuming that FRF=1. The network layout is illustrated in ***Figure 23*** which is extracted from [29], Figure 1. It is composed of 19 tri-sector BSs resulting in a total of 57 sectors also referred to as cells in the sequel. TN UE is randomly placed in each cell at each Monte Carlo simulation. The association the BSs and the UEs is performed based on the CL as recommended in [14], section 5.3. The calibration is then performed once the association is done.

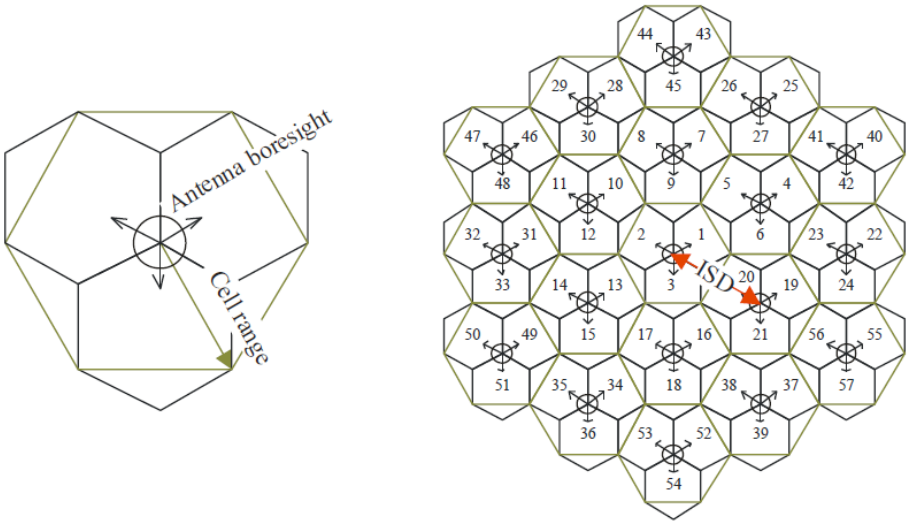

Figure 23: *Illustration of the simulated network layout*

The UL calibration is performed by computing the CL and the SINR at each BS. The SINR is computed by assuming that each UE transmit using the same frequency band due to the FRF=1 assumption, creating thus interference.

The DL calibration is performed by computing the CL and the SINR at each UE by assuming that all the BS use the same frequency band, creating thus interference.

It is worth mentioning that the interference induced by the FRF=1 assumption is mitigated thanks to the use of directive antennas as well as the use of beamforming (see section 7).

11.2 TN Q/V-BAND

11.2.1 TN UL Q/V-band

The CDF of the CL for the UL of TN communications in the Q/V-band is provided in ***Figure 24*** for 37 GHz (left) and 47 GHz (right). We can observe a good match between the CL obtained by the different partners. We can also see that the CL at 47 GHz is slightly higher than at 37 GHz which was expected since the path loss (and thus the CL) increases with the carrier frequency.

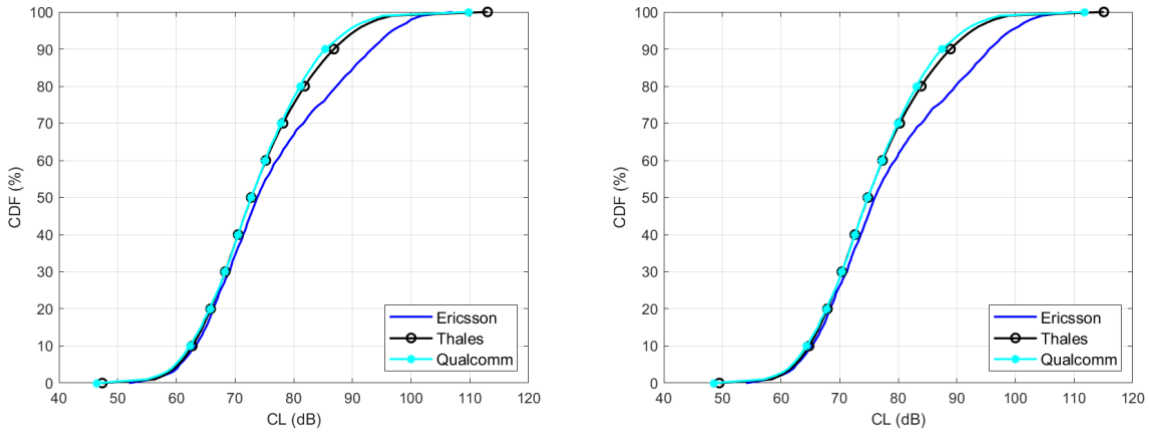

Figure 24: *CDF of the CL for the UL of TN communications in the Q/V-band at 37 GHz (left) and 47 GHz (right)*

The CDF of the SINR for the UL of TN communications in the Q/V-band is provided in ***Figure 25*** for 37 GHz (left) and 47 GHz (right). Firstly, we can see that the different curves have the same behaviour, with a vertical asymptote at SINR=15 dB which can be explained by the transmit power control mechanism described in section 5.3. Secondly, we can see a good match (only a few dB difference) between the SINR values obtained by the different partners. More precisely, the curves from TH-SIX and QC are almost superimposed, whereas there is a few dB shift between Ericsson results and the other ones.

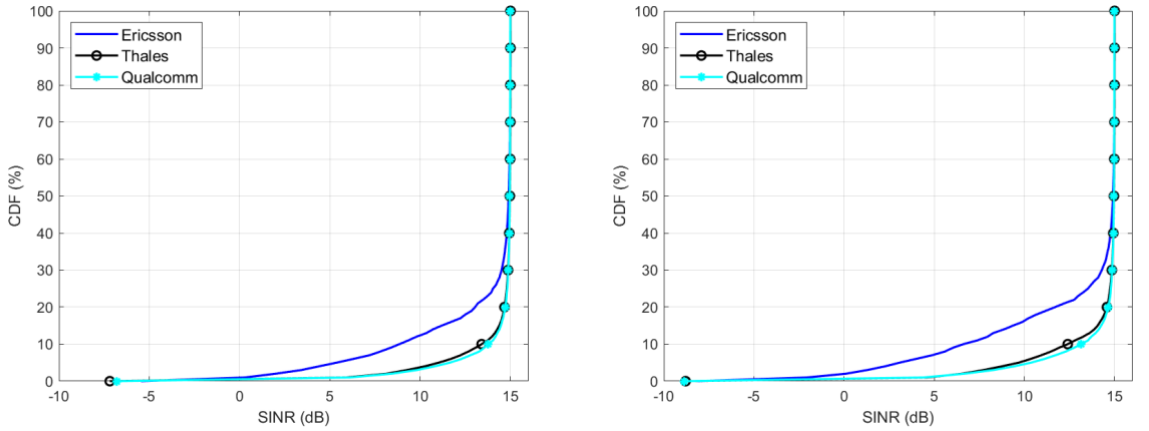

Figure 25: *CDF of the SINR for the UL of TN communications in the Q/V-band at 37 GHz (left) and 47 GHz (right)*

11.2.2 TN DL Q/V-band

The CDF of the CL for the DL of TN communications in the Q/V-band is provided in ***Figure 26*** for 37 GHz (left) and 47 GHz (right). These results are provided for the sake of completeness since they are as expected to be identical to the CL depicted for the UL in ***Figure 24***, and thus the same comments apply.

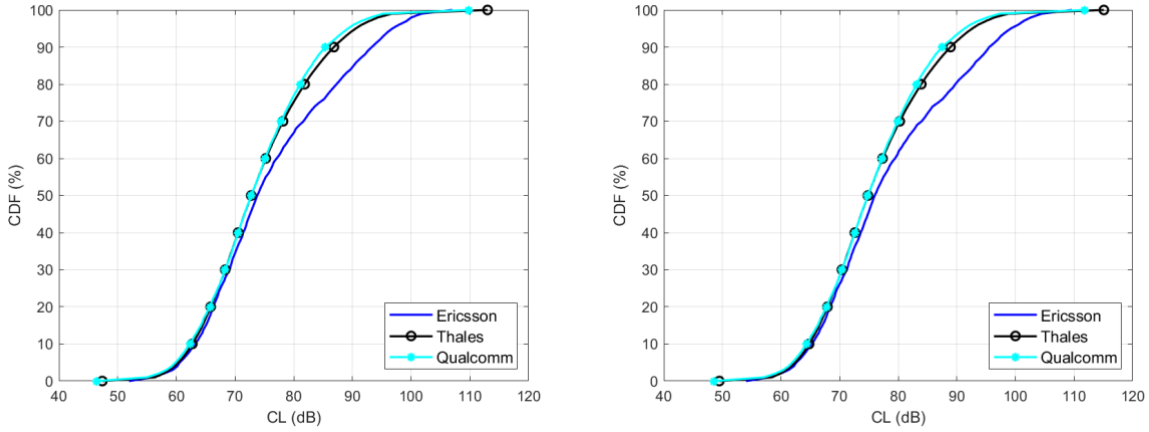

Figure 26: *CDF of the CL for the DL of TN communications in the Q/V-band at 37 GHz (left) and 47 GHz (right)*

The CDF of the SINR for the DL of TN communications in the Q/V-band is provided in ***Figure 27*** for 37 GHz (left) and 47 GHz (right). We can observe a good agreement between the SINR obtained by the different partners.

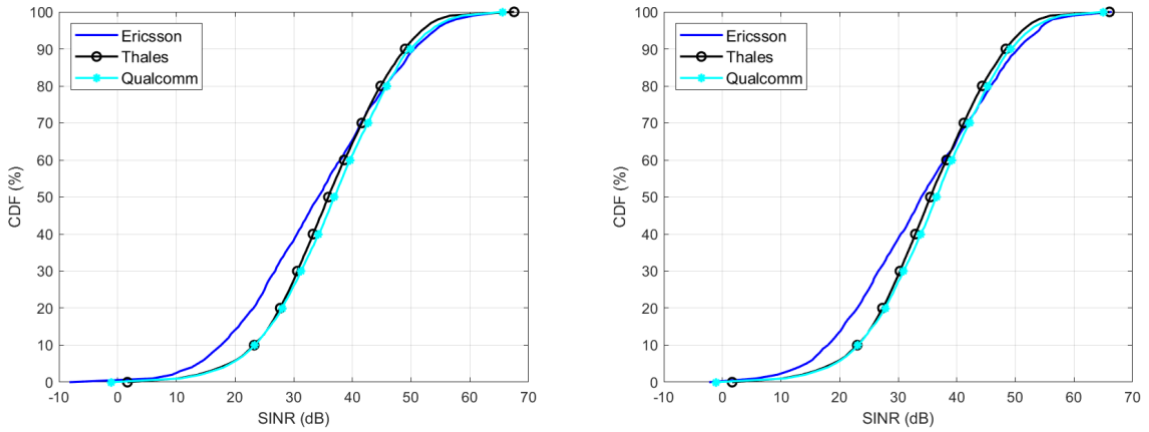

Figure 27: *CDF of the SINR for the UL of TN communications in the Q/V-band at 37 GHz (left) and 47 GHz (right)*

12 FURTHER DETAILS FOR COEXISTENCE SIMULATIONS

Cellular cell structure is considered for both NTN and TN network layout. As in [16], the ACIR is modelled as flat, i.e. the same ACIR is used for all RB in both DL and UL.

12.1 COORDINATE SYSTEM

Referring to TR 38.811 Section 6.3 and Annex A, a 3D global coordinate system is considered (Earth-Centred Earth Fixed) for simulating NTN beams direction and location on the earth surface. It means the NTN beam location, TN randomly dropping location are generated with a set of three parameters (x,y,z).

12.2 SIMULATION METHODOLOGY

The simulations for NTN-TN coexistence study can be performed by following the steps below.

1. Generate aggressor and victim networks.
   - FRF=2 with two polarisations (RHCP, LHCP) (see Figure 15, Option 3)
     - Do not consider interference leakage from adjacent beams for coexistence study.
     - For example, in Figure 15 for FRF = 2, do not consider the interference leakage from green, blue and purple beams when study SINR for the red beam.
   - Deployment of TN network (19 cells with wraparound) refers to ***Table 32***.
2. UE associations.
   - TN UEs are generated randomly inside the TN network. We must ensure that enough TN UEs are associated to each TN sectors based on coupling loss.
   - We consider the following approach for the deployment of NTN UE and satellite.
     a) The Satellite should be generated in the visible area/sky of NTN UE;
     b) NTN UEs point to the satellite accurately;
     c) The position of the satellite should guarantee that NTN UE vertical angle is towards the satellite;
        - For calibration, we used 90 degree (see section 10.1).
        - We consider 30, 45 and 90 degree elevation (computed from the centre of the beam) for coexistence simulation.
3. Once association is done, round robin scheduling is used. BF weights are adjusted to point to the LOS direction between BS-UE. This is done for both victim and aggressor networks.
4. Throughput is computed in the victim systems without considering ACI (adjacent channel interference) as below:

   - $Thput_{\text{NO ACI}}[\text{bpshz}] = f(SNR_{\text{NO ACI}}) = f\left(\frac{S}{N}\right)$, where N is the noise power, and $f(.)$ is a truncated form of the Shannon bound, as described in [16].

5. Throughput is computed considering ACI as below:

   - $\text{Thput}_{\text{ACI}}[\text{bpshz}] = f(SINR_{\text{ACI}}) = f\left(\frac{S}{N+I_{\text{ACI}}}\right)$, where I_{ACI} is the adjacent channel interference.

6. RF parameters are determined based on the degradation caused by ACI as below:

   - $Loss_{\text{ACI}} = 1 - \frac{Thput_{\text{ACI}}}{Thput_{\text{NO ACI}}}$

Scaling factor (SF) can be used to simplify the simulation of interference from TN to NTN UL for e.g. coexistence scenarios 2 and 4. Section 13.4.2.2 provides more details regarding the usage and computation of SF.

Table 32 further describes different coexistence scenarios that are studied in the next sections of the present deliverable.

Table 32: *coexistence scenarios*

No.	Aggressor	Victim	Elevation	NTN cell to observe	UE to observe	Which TN/UE to observe?	Which TN cells in a TN to observe?
1	NTN UL	TN UL	90 degrees (SAN at Nadir point); 30 degrees	N/A	NTN UEs randomly dropped in TN clusters	TN randomly placed in this NTN beam	Only the active TN clusters which contain NTN UE(s)
2	TN UL	NTN UL	90 degrees (SAN at Nadir point)	Observe NTN central beam for SINR*	NTN UEs randomly dropped in TN clusters	Consider an active rate of 20% for TN	All active TN cells in central NTN beam
3	NTN UL	TN DL	90 degrees (SAN at Nadir point); 30 degrees	N/A	NTN UEs randomly dropped in TN clusters	TN clusters randomly placed in this NTN beam	Only the active TN clusters which contain NTN UE(s)
4	TN DL	NTN UL	90 degrees (SAN at Nadir point)	Observe NTN central beam for SINR*	NTN UEs randomly dropped in TN clusters	Consider the active rate of 20% for TN	All active TN cells in central NTN beam
5	TN DL	NTN DL	90 degrees (SAN at Nadir point); 30 degrees	Observe NTN central beam for SINR*	NTN UEs randomly dropped in TN clusters	One cluster with 19 TN cells (57 sectors) randomly placed in the central NTN beam	Only the active TN clusters which contain the NTN UE(s)
6	NTN DL	TN DL	90 degrees (SAN at Nadir point);	N/A	No NTN UE needed	One cluster with 19 TN cells (57 sectors) randomly placed in the central NTN beam	All in central NTN beam**
7	NTN DL	TN UL	90 degrees (SAN at Nadir point);	N/A	No NTN UE needed	TN clusters randomly placed in this NTN beam	Only the active TN clusters which contain NTN UE(s)***

8	TN UL	NTN DL	90 degrees (SAN at Nadir point); 30 degrees	Observe NTN central beam for SINR*	NTN UEs randomly dropped in TN clusters	Consider the active rate of 20% for TN	All active TN cells in central NTN beam

*6 adjacent beams for inter-beam interference can be mitigated with deployment strategies such as FRF=2 and LHCP/RHCP (the latter is not considered as assumption for TN configuration).

**To be further discussed: the interference impact of NTN adjacent beams using circular polarisation to TN UE using linear polarisation.

***To be further discussed: the interference impact of NTN adjacent beams using circular polarisation to TN BS using linear polarisation.

13 COMPLETE DESCRIPTION OF THE COEXISTENCE SIMULATIONS

This section provides a complete overview of the methodology for the coexistence simulations by synthetizing and complementing different elements from the previous sections. The goal is to ensure a self-contained section before providing the coexistence simulation results between TN and NTN in Section 14 for the Q/V-band and in Section 15 for C-band.

13.1 ASSUMPTIONS ON THE FREQUENCY AND BANDWIDTH

Table 33 summarizes the assumptions regarding the considered carrier frequencies. The carrier frequencies in the C-band have been decided after discussions with WP3 partners.

Table 33: *Assumptions on the carrier frequencies for coexistence simulations*

System	Q/V-band (GHz)	C-band (GHz)
NTN DL	47	3.4
NTN UL	37	3.9
TN DL	37 or 47 (depends on scenario)	3.4 or 3.9 (depends on scenario)
TN UL	37 or 47 (depends on scenario)	3.4 or 3.9 (depends on scenario)

The coexistence simulations assume that the satellite operates using the FRF=2 configuration with two polarisations, as depicted in ***Figure 15***, in order to achieve better SINR target since lower interference between the beams/between the users in the beams. We focus on the central beam and assume that the satellite dedicates its entire power to transmit to this beam, meaning that there is no power split between the beams. ***Table 21*** and ***Table 24*** provide the satellite transmit power values for the Q/V-band and the C-band, respectively.

The satellite uses a bandwidth B_{sat} to transmit to the central beam, whereas the NTN UEs utilize a smaller fraction of B_{sat}, denoted by B_{NU}. The TN nodes (e.g. the BS and TN UEs) transmit using a bandwidth B_{TN}.

In the Q/V-band, B_{sat} is composed of 132 RBs with 12 subcarriers in each, and the subcarrier spacing is set to 120 kHz, yielding $B_{sat} = 190$ MHz. The NTN UE transmit on 1/10 of the bandwidth, thus using 13 RBs yielding $B_{NU} = 18.72$ MHz per NTN UE. Finally, we assume that $B_{TN} = B_{sat}$, i.e., the TN nodes use the same bandwidth as the satellite.

In the C-band, B_{sat} is composed of 51 RBs with 12 subcarriers in each, and the subcarrier spacing is set to 30 kHz, yielding $B_{sat} = 18.36$ MHz. The NTN UE use two RBs for transmission, yielding $B_{NU} = 0.72$ MHz per NTN UE. Finally, we assume that the bandwidth used by the TN nodes is composed of 273 RBs with the same subcarrier spacing as the satellite, yielding thus $B_{TN} = 98.28$ MHz.

Table 34 summarizes the above assumptions.

Table 34: *Assumptions on the bandwidth for coexistence simulations*

Parameter	Q/V-band	C-band
SCS (kHz)	120	30
# RBs in B	132	100
B (MHz)	190	18
# RBs in B_{NU}	13	6
B_{NU} (MHz)	18.72	1.08

13.2 UPDATE OF SOME PARAMETERS IN THE C-BAND

We updated some parameters in the C-band for the sake of consistency with WP3. ***Table 35*** provides the new parameters for the TN and NTN UE and replace those from the UE related column in ***Table 17***, whereas

Table 36 provides the new parameters for the SAN and replace their old values from ***Table 24***.

Remark: The updated parameters are different from those provided in [15], and were chosen after discussion with WP3. Section 18.3 provides the complete study related to this discussion.

Table 35: *updated parameters for the UEs in the C-band*

Parameter	Value
Antenna gain (dBi)	-2
Transmit power (dBm)	26
Noise figure NTN UE (dB)	7
Noise figure TN UE (dB)	5.5

Table 36*: updated parameters for the satellite in the C-band*

Parameter	Value
LEO 600 antenna gain (dBi) – Nadir	35
LEO 1200 antenna gain (dBi) – Nadir	35
GEO antenna gain (dBi) – Nadir	50.5
LEO 600 antenna gain (dBi) – Lower elevation	33
LEO 1200 antenna gain (dBi) – Lower elevation	33
GEO antenna gain (dBi) – Lower elevation	48.5
Noise figure (dB)	2

13.3 CONSIDERED ELEVATION

Table 32 mentioned that some scenarios should be performed at Nadir and at 30° elevation. According from input provided from WP3, **the minimum elevation angle of interest is 45° elevation**, and thus the main priority will be to ensure coexistence at Nadir and 45° elevation. For the sake of completeness, the coexistence simulations have also been performed at 30° elevation as per 3GPP work asumption.

13.4 DETAILED SIMULATION METHODOLOGY

Table 32 describes the eight considered coexistence scenarios between TN and NTN, which can be classified in the following four categories in which TN nodes represent either TN BS or TN UEs:

1. Category 1 – TN nodes aggressing NTN DL, which includes:
    a. Scenario 5, in which the aggressor is the TN BS.
    b. Scenario 8, in which the aggressor is the TN UE.
2. Category 2 – TN nodes aggressing NTN UL, which includes:
    a. Scenario 2, in which the aggressor is the TN UE.
    b. Scenario 4, in which the aggressor is the TN BS.
3. Category 3 – NTN DL aggressing TN nodes, which includes:
    a. Scenarios 6, in which the victim is the TN UE.

   b. Scenario 7, in which the victim is the TN BS.
4. Category 4 – NTN UL aggressing TN nodes, which includes:
   a. Scenario 1, in which the victim is the TN BS.
   b. Scenario 3, in which the victim is the TN UE.

The following sections detail the methodology to simulate each of these categories of scenarios.

13.4.1 General assumptions

13.4.1.1 NTN UE height

Table 4 discussed different assumptions for the NTN UE height. As a final assumption, **it has been decided to focus on L-ESIM whose height is 1.5m**.

13.4.1.2 Propagation models

Table 5 provides the propagation models with respect to the inter system link type for the coexistence studies (e.g. the propagation models to compute the interference between TN and NTN).

Table 37: *Final assumptions regarding the propagation models for the coexistence simulations*

Link	Propagation model
TN – satellite	TR 38.821
NTN UE – TN BS	UMa from TR 38.901
NTN UE – TN UE	UMi from TR 38.901

13.4.1.3 Minimal distance between the communicating nodes

A minimal distance between the NTN UEs and the TN nodes is assumed. ***Table 38*** provides the values for these minimal distances.

Table 38: *Minimal Q/V-band MINIMAL distance (or attenuation) between NTN UE and TN BS/UE*

	Minimal distance (m)
NTN UE – TN BS	35
NTN UE – TN UE	No minimal distance

13.4.1.4 General assumptions regarding the communicating nodes deployment

In the rest of this document, the terminology TN cluster will refer to a network with 19 tri-sector BS with TN UEs randomly dropped in each TN cell, as considered for the TN calibration in Section 11 and illustrated in ***Figure 23***.

For the coexistence simulations, one TN cluster is randomly placed into the NTN central beam, and one NTN UE is randomly dropped into this TN cluster. The assumption that there is a single NTN UE in the considered TN cluster is mathematically justified in Section 18.1.

13.4.2 Scenarios specific assumptions

13.4.2.1 Category 1 – TN nodes aggressing NTN DL

In the Q/V-band, both the satellite (victim) and the TN nodes (aggressor) transmit on the whole bandwidth $B_{sat} = B_{TN}$ (cf. Section 13.1), meaning that the aggressor and the victim use the same bandwidth. The SINR is computed at the NTN UE side and can be written as:

$$SINR_{NU} = \frac{P_{R_X}}{10^{0.1N_F}N_0 + \sum_{i=1}^{N_{itf,TN}} I_{R_X}^i},$$

where P_{R_X} is the useful power received by the NTN UE from the satellite, N_F is the noise figure of the NTN UE in dB, N_0 is the thermal noise power, and $I_{R_X}^i$ is the interference between adjacent channel caused by the TN nodes i, whose computation is detailed in Section 13.5.

In the C-band, the TN nodes transmit on a bandwidth B_{TN} that is larger than the one of the satellite B_{sat} (cf. Section 13.1), thus, the bandwidth of the victim system (i.e., the satellite) is smaller than the one of the aggressor (i.e., the TN system). This setup is illustrated in ***Figure 28*** assuming co-channel interference, and we explain in what follows how to manage it in the simulation, i.e., how to compute the level of interference when the bandwidth of the aggressor is larger than the victim's one.

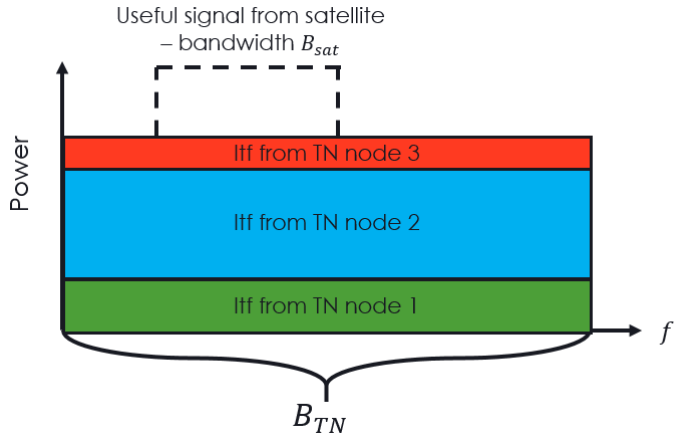

Figure 28: *ILLUSTRATION OF THE ASYMETRIC BANDWIDTH USED BY the satellite (VICTIM) AND TN NODES (AGRESSOR) in the C-band*

Let P_a be the transmit power of the TN nodes. The power $P_{a\to v}$ perceived by the NTN DL is obtained by integrating over $B_{sat} < B_{TN}$, yielding a restriction of the signal from the TN system, and thus $P_{a\to v} < P_a$. More precisely, $P_{a\to v}$ can be expressed as:

$$P_{a\to v} = P_a \frac{B_{sat}}{B_{TN}}.$$

Remark 1: the "corrective" term $\frac{B_{sat}}{B_{TN}}$ in the above equation corresponds to F_{ACLR} in section 5.1.1.4.1 of [16], and thus the provided equation is in line with [16].

Remark 2: the explanation on how to extend the above procedure to interference between adjacent channels is provided in Section 13.5.

Finally, the SINR is computed at the NTN UE side and can be expressed as:

$$SINR_{NU} = \frac{P_{R_X}}{10^{0.1N_F}N_0 + \frac{B_{sat}}{B_{TN}}\sum_{i=1}^{N_{itf,TN}} I_{R_X}^i},$$

where the variables are defined as in the Q/V-band.

13.4.2.2 Category 2 – TN nodes aggressing NTN UL

The TN nodes transmit on a bandwidth B_{TN} whereas the NTN UE uses a bandwdith $B_{NU} < B_{TN}$ (cf. Section 13.1), thus, the bandwidth of the victim system (i.e., the NTN UL) is smaller than the one of the aggressor (i.e., the TN system). Such a setup can be managed using the same procedure as the one explained for the C-band in Section 13.4.2.1 (see the explanations related to ***Figure 28***).

Moreover, as mentioned in Section 12.2, scaling factor (SF) is used to emulate the interference of all the TN clusters in the beam instead of simulating them all. The practical usage of the SF is the following one:

1. Compute the interference caused by the simulated TN cluster onto the satellite. Let $I_{TN,NU}$ be the aggregated level of interference produced by all the TN nodes (i.e., all the BS in scenario 4 and all the TN UE in scenario 2) to the satellite. We assume that $I_{TN,NU}$ takes into account the asymmetry in the bandwidth of the aggressor and the victim, i.e., it takes into account the term $\frac{B_{NU}}{B_{TN}}$.
2. The total level of interference produced by all the TN cluster in the NTN beam is then estimated as:

$$\bar{I}_{TN,NU} = S_F \times I_{TN,NU},$$

where S_F is the SF. The SF values at Nadir and 30° elevation in dB are provided in ***Table 39*** for the Q/V and the C-bands. The procedure to obtained these values is provided in the Appendix in Section 18.2.

Table 39: *Values of S_F in dB for the different orbit in the Q/V-band and the C-band*

Orbit	Band	S_F – elevation 90°	S_F – elevation 30°
LEO@600	Q/V	20.85	26.4
LEO@1200	Q/V	26.87	32.11
GEO	Q/V	36.36	39.71
LEO@600	C	16.35	21.9
LEO@1200	C	22.4	27.6
GEO	C	36.3	39.65

Finally, the SINR is computed at the satellite side, and can be written as:

$$SINR_{sat} = \frac{P_{R_X}}{10^{0.1N_F} N_0 + \bar{I}_{TN,NU}},$$

where P_{R_X} is the useful power received by the satellite from the NTN UE, N_F is the noise figure of the satellite, N_0 is the thermal noise power, and $\bar{I}_{TN,NU}$ is the total interference between adjacent channel caused by the TN nodes, that includes the SF and the corrective term $\frac{B_{NU}}{B_{TN}}$ to take into account the asymetrie of the bandwidth of the victim and the aggressor.

13.4.2.3 Category 3 – NTN DL aggressing TN nodes

In the Q/V-band, the satellite and the TN nodes transmit using the same bandwdith $B_{sat} = B_{TN}$ (cf. Section 13.1). The SINR is thus computed at the TN UE side for scenario 6, and TN BS side for scenario 7, and can be written for TN node i as:

$$SINR_{TN}^{i} = \frac{P_{R_X}^{i}}{10^{0.1N_F}N_0 + I_{TN}^{i} + I_{\text{Sat}}^{i}},$$

where $P_{R_X}^{i}$ is the useful power received by TN node i from its associated BS in scenario 6 or TN UE in scenario 7, N_F is the noise figure of the TN node, I_{TN}^{i} is the sum of the interference caused by the other TN nodes (i.e., the other BS in scenario 6 and the other TN UE in scenario 7), and $I_{R_X}^{i}$ is the interference between adjacent channel caused by the satellite received by TN node i.

In the C-band, the bandwidth used by the satellite B_{sat} (aggressor) is smaller than the bandwidth B_{TN} used by the TN nodes (victim) (cf. Section 13.1). This setup is illustrated in ***Figure 29*** assuming co-channel interference, and we explain in what follows how to manage it in the simulation (e.g., how to compute the level of interference when the bandwidth of the aggressor is narrower than the victim's one).

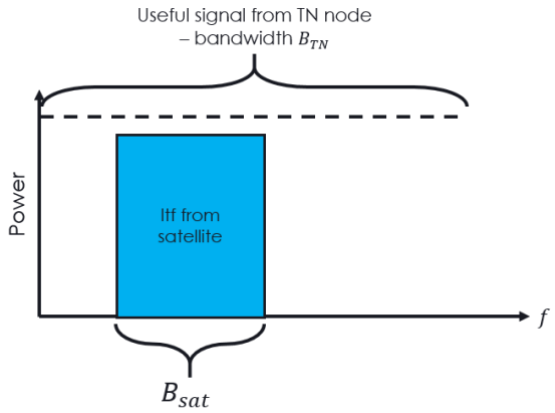

Figure 29: *ILLUSTRATION OF THE ASYMETRIC BANDWIDTH USED BY THE TN nodes (VICTIM) AND satellite (AGRESSOR) IN THE C-BAND*

Let P_a be the transmit power of the satellite. The power $P_{a\to v}$ perceived by the TN node is obtained by integrating over B_{TN} that is larger than B_{sat}, and thus the TN signal is perturbed by all the signal from the satellite. As a consequence, $P_{a\to v} = P_a$.

Remark 1: it is explained in section 5.1.1.4.2 of [16] that the case of an aggressor with smaller bandwidth than the victim can be managed the same way as the case with symmetrical bandwidth (i.e., $B_{TN} = B_{sat}$), yielding $P_{a\to v} = P_a$ as well and aligning with the previous discussion.

Remark 2: the explanation on how to extend the above procedure to interference between adjacent channels is provided in Section 13.5.

From the above discussion, we deduce that the SINR expression is the same in the Q/V and in the C-band.

13.4.2.4 Category 4 – NTN UL aggressing TN nodes

The NTN UE transmits using a bandwidth B_{NU} that is smaller than the one used by the TN nodes (cf. Section 13.1), and thus the bandwidth of the aggressor is smaller than the bandwidth of the victim. This setup can be managed using the same procedure as the one explained for the C-band in Section 13.4.2.3 (see the explanations related to ***Figure 29***), and the SINR is obtained by replacing the term I_{Sat}^{i} by the interference caused by the NTN UE in the expression provided in Section 13.4.2.3.

13.5 INTERFERENCE BETWEEN ADJACENT CHANNELS

The objective of the 6G-NTN project is to study the possible coexistence between TN and NTN using adjacent frequencies, say $f_{c,TN}$ and $f_{c,NTN}$ for TN and NTN, respectively, or between two NTN different NTN layers using adjacent frequencies. There are two contributions to interference between adjacent channels:

1. Interference due to leakage of the aggressor transmit power into the channel of the victim. The interference due to leackage expressed in dB is denoted by $I_{L,dB}$, and is characterized through the ACLR parameter of the aggressor.
2. Interference due to the imperfect channel filtering at the victim side. The interference due to this phenomenon expressed in dB is denoted by $I_{S,dB}$, and is characterized through the ACS parameter of the victim.

Figure 30 illustrates these two contributions to the adjacent channel interference on an example in which the aggressor is the TN DL and the victim is the NTN DL.

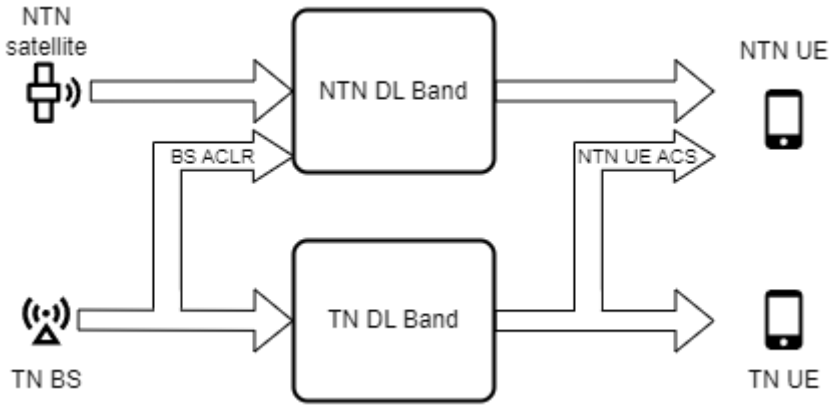

***Figure 30**: Illustration of the two contributions of the interference between adjacent channel when the aggressor is TN DL and the victim is NTN DL*

The interference terms $I_{L,dB}$ and $I_{S,dB}$ can be expressed as:

$$I_{L,dB} = \mathcal{G}_{ag,vi,dB} - \mathcal{L}_{ag,dB}$$

and

$$I_{S,dB} = \mathcal{G}_{ag,vi,dB} - \mathcal{S}_{vi,dB}$$

where $\mathcal{L}_{ag,dB}$ and $\mathcal{S}_{vi,dB}$ are the ACLR of the aggressor and the ACS of the victim in dB, respectively, and $\mathcal{G}_{ag,vi,dB}$ represents the power received by the victim from the agressor in dB that can be written as:

$$\mathcal{G}_{ag,vi,dB} \coloneqq P_{ag,dB} + G_{ag,vi,dB} + G_{vi,ag,dB} + F_{ag,vi,dB} + A_{ag,vi,dB}$$

where all the terms are expressed in dB, with $P_{ag,dB}$ the transmit power of the agressor, $G_{ag,vi,dB}$ (resp. $G_{vi,ag,dB}$) the antenna gain of the agressor (resp. victim) in the direction of the victim (resp. agressor), $A_{ag,vi,dB}$ corresponds to the other attenuation terms between the agressor and the victim (encompassing the path loss, the shadowing etc.), and $F_{ag,vi} = 10\log_{10}(\min(1, B_v/B_a))$ the term correcting the possible asymetrie between the bandwidth B_a of the agressor and the one of the victim B_v. The reasoning yielding the expression of $F_{ag,vi}$ is detailed in Sections 13.4.2.1 and 13.4.2.3.

The interference caused by the agressor to the victim can be written in the linear domain as:

$$I_{T,lin} = 10^{0.1I_{L,dB}} + 10^{0.1I_{R,dB}}$$

which can be rewritten as:

$$I_{T,lin} = 10^{0.1\mathcal{G}_{ag,vi,dB}}\left(10^{-0.1\mathcal{L}_{ag,dB}} + 10^{-0.1\mathcal{S}_{vi,dB}}\right).$$

The values of $\mathcal{L}_{ag,dB}$ and $\mathcal{S}_{vi,dB}$ for the TN communicating nodes are provided as an input for the coexistence studies, and the objective is to find ACLR and ACS values for the NTN communicating nodes (i.e., the SAN and the NTN UE) enabling to meet the 3GPP requirements detailed in section 13.6. More precisely, the ACLR and ACS of the TN communicating nodes in the Q/V-band are provided in

Table 15 whereas we propose for the C-band to use those of the S-band from Table 6.2.2.4-3 in [3] that we summarize in ***Table 40***.

Table 40: *ACLR and ACS of TN communicating nodes in the C-band*

Type of node	Parameter	Value (dB)
BS	ACLR	45
	ACS	46
UE	ACLR	30
	ACS	33

In the 3GPP framework, such coexistence studies are generally performed with respect to the so-called ACIR $\mathcal{A}$, defined in Section 5.2.6 of [14] as:

$$\mathcal{A} := \frac{1}{\frac{1}{\mathcal{L}_{ag,lin}} + \frac{1}{\mathcal{S}_{vi,lin}}}$$

where $\mathcal{L}_{ag,lin}$ and $\mathcal{S}_{vi,lin}$ are the ACLR of the agressor and ACS of the victim in the linear domain, respectively. In what follows, we explain the link between $I_{T,lin}$ and $\mathcal{A}$. Introducing $K := 10^{-0.1\mathcal{L}_{ag,dB}} + 10^{-0.1\mathcal{S}_{vi,dB}} = \frac{1}{\mathcal{L}_{ag,lin}} + \frac{1}{\mathcal{S}_{vi,lin}}$, we can write:

$$I_{T,lin} = \mathcal{G}_{ag,vi,lin}K$$

where $\mathcal{G}_{ag,vi,lin} := 10^{0.1\mathcal{G}_{ag,vi,dB}}$. Since by definition $\mathcal{A} = 1/K$, we then obtain:

$$I_{T,lin} = \frac{\mathcal{G}_{ag,vi,lin}}{\mathcal{A}}.$$

The 3GPP procedure for coexistence consists in finding an ACIR value enabling to meet the requirements detailed in the next Section 13.6, which then allows to find the correponding ACLR or ACS value for the NTN node. For instance, assume that the agressor is the TN BS and the victim if the NTN UL (scenario 4) and that the coexistence study result in a required ACIR value of $\mathcal{A}_{BS,sat}$. The ACLR $\mathcal{L}_{BS,lin}$ of the TN BS is provided as an input and thus one can deduce the required ACS of the satellite for this scenario as:

$$\mathcal{S}_{sat,lin} = \frac{1}{\frac{1}{\mathcal{A}_{BS,sat}} - \frac{1}{\mathcal{L}_{BS,lin}}}.$$

It is worth mentionning that $\lim_{\mathcal{A}\to+\infty} I_{T,lin} = 0$. As a consequence, a sufficiently high ACIR value almost vanishes the interference, and thus it is always possible to find ACIR value fulfilling the 3GPP requirements described in the next Section 13.6. However, one can see from the previous equation that $\mathcal{S}_{sat,lin} > 0$ if and only if $\mathcal{A}_{BS,sat} < \mathcal{L}_{BS,lin}$, and that $\mathcal{A}_{BS,sat} > \mathcal{L}_{BS,lin}$ results into $\mathcal{S}_{sat,lin} < 0$ which is not an admissible solution. This reasonning can be extended to all the different scenarios by remarking that $\mathcal{A} - \mathcal{L}_{ag,lin} = \mathcal{L}_{ag,lin}\left(\frac{\mathcal{S}_{vi,lin}}{\mathcal{S}_{vi,lin}+\mathcal{L}_{ag,lin}} - 1\right)$ that is lower than 0 as long as $\mathcal{S}_{vi,lin} \geq 0$, and that similarly $\mathcal{A} - \mathcal{S}_{vi,lin}$ is lower than 0 as long as $\mathcal{L}_{ag,lin} \geq 0$.

Thus, an admissible solution for the ACLR or the ACS of the NTN node exists if and only if the required ACIR value is lower than the ACLR or ACS of the TN node provided as an input. **Finding admissible ACIR value enabling coexistence between TN and NTN will be refered to as "compliance with standard" coexistence technique**.

In addition of the previously discussed "compliance with standard" coexistence technique based on ACIR, another coexistence technique that should be considered is MMSE-IRC, as mentioned in the technical annex. MMSE-IRC is a physical layer technique designed to mitigate exogeneous interference. We propose in what follows an abstraction to emulate its performance, by assuming that it can effectively reject a fixed level of interference, i.e., we assume that the interference power when using MMSE-IRC can be written in dB as:

$$P_{I,MMSE-IRC} = P_I - \mathcal{M}$$

Where P_I is the interference power without MMSE-IRC, and $\mathcal{M}$ is the level of interference that can be rejected in dB.

With this abstraction, $\mathcal{M}$ has an impact on the interference power comparable to that of the ACIR. *As a consequence, increasing $\mathcal{M}$ by mdB corresponds to a reduction of m dB in the required ACIR*.

13.6 PERFORMANCE METRIC AND REQUIREMENTS

The coexistence requirements from section 6.2.8 of [3] consist in ensuring that the average throughput loss and 5%-ile throughput loss induced by the coexistence between TN and NTN is lower than 5%.

The throughput is computed thanks to the attenuated and truncated Shannon capacity provided in section 5.2.7 of [14] whose expression is:

$$\mathbb{T}(SINR) = \begin{cases} 0 & \text{for } SINR < SINR_{\min} \\ \alpha\mathbb{S}(SINR) & \text{for } SINR \in [SINR_{\min}, SINR_{\max}] \\ \alpha\mathbb{S}(SINR_{\max}) & \text{for } SINR > SINR_{\max} \end{cases}$$

Where $SINR_{\min}$, $SINR_{\max}$ and α are parameters whose values are provided in ***Table 41***, which corresponds to Table 5.2.7-1 from [14], and $\mathbb{S}(SINR)$ is the well-known Shannon capacity that can be written as:

$$\mathbb{S}(SINR) = \log_2(1 + SINR)$$

Figure 31 illustrates the attenuated and truncated Shannon capacity using the parameters from ***Table 41***, as well as the conventional Shannon capacity, i.e., $\mathbb{S}(SINR)$.

Table 41: *Parameters for the attenuated and truncated Shannon capacity*

Parameter	DL	UL
α	0.6	0.4
$SINR_{\min}$ (dB)	-10	-10
$SINR_{\max}$ (dB)	30	22

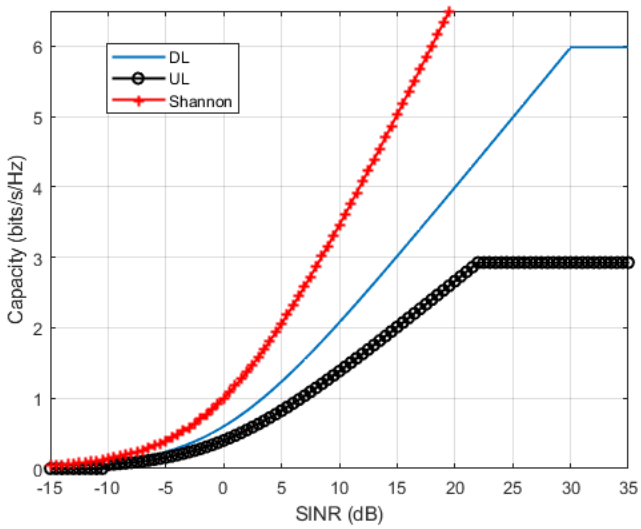

Figure 31: *Illustration of truncated Shannon capacity*

The throughput loss is then computed by first computing the throughput of the TN and NTN systems without interference between adjacent channels. Then, these interference are incorporated in the SINR, and the resulting throughput is computed. The loss between the interfered throughput and the interference free throughput is then computed. More precisely, if $\mathcal{S}_N$ and $\mathcal{S}_I$ represent the SNR (free of adjacent channel interference) and the SINR (with adjacent channel interference), respectively, then the throughput loss can be computed as:

$$\mathcal{T} \coloneqq 100\left(1 - \frac{\mathbb{T}(\mathcal{S}_I)}{\mathbb{T}(\mathcal{S}_N)}\right).$$

This throughput loss is computed for a large number of topologies, and then the average throughput loss and 5th percentile throughput loss is computed.

Remark: the throughput subject to interference between adjacent channel depends on the ACLR (resp. ACS) of the NTN system since the interference caused (resp. received) by the NTN system depends on this parameter.

14 COEXISTENCE SIMULATION RESULTS IN THE Q/V BAND

14.1 INTRODUCTION

This section provides the coexistence simulation results in the Q/V-band. Objective 9 of the technical annex mentioned that different coexistence techniques should be evaluated , and thus we propose the following methodology.

1. We first evaluate the technique referred to as “compliance with standards” in Section 8.1 and defined in Section 13.5, which consists in assessing the coexistence in the different scenarios with respect to the ACIR. This first study enables us i) to provide recommendation regarding the ACIR values allowing to fulfil the 3GPP maximum throughput loss requirement described in Section 13.6, and ii) to identify the most “difficult” scenarios, i.e. scenarios in which the required ACIR value does not enable to find admissible parameter for the NTN node (see the related detailed discussion in Section 13.5).
2. Then, we propose and evaluate other coexistence techniques for the identified difficult scenarios.

The rest of this section is structured as follows. Section 14.2 provides coexistence simulation results with respect to ACIR. Section 14.3 investigates other coexistence techniques. Finally, Section 14.4 draws conclusions and provides recommendations.

14.2 COMPLIANCE WITH STANDARDS

Sections 14.2.1, 14.2.2, 14.2.3, and 14.2.4, provide simulation results for the four category of scenarios introduced in Section 13.2. Each section presents the results for the two scenarios of the category, and a synthesis of the observations.

14.2.1 Scenarios from category 1

14.2.1.1 Scenario 5 (Aggressor: TN DL, Victim: NTN DL)

Figure 32 and ***Figure 33*** depict the average and 5th percentile throughput loss for coexistence scenario 5 in the Q/V-band for LEO@600km, LEO@1200km and GEO orbits at Nadir as a function of the ACIR. The vertical line at 26 dB represents the ACLR of the TN BS, which is an upper bound on the maximum achievable ACIR as discussed in Section 13.5. One can observe that both the average and the 5th percentile throughput loss are always larger than 5% for ACIR values lower than 26 dB for the three orbits, meaning that it is not possible to find an ACS value for the NTN UE satisfying the maximum throughput loss requirements.

For the sake of completeness, ***Figure 34*** and ***Figure 35*** (resp. ***Figure 36*** and ***Figure 37***) represent the average and 5th percentile throughput loss for coexistence scenario 5 in the Q/V-band for LEO@600km, LEO@1200km and GEO orbits at 45° (resp. 30°) elevation as a function of the ACIR. As expected, the maximum throughput loss cannot be met at lower elevation either for admissible ACIR value.

The above observations indicate the need for studying additional coexistence techniques for scenario 5.

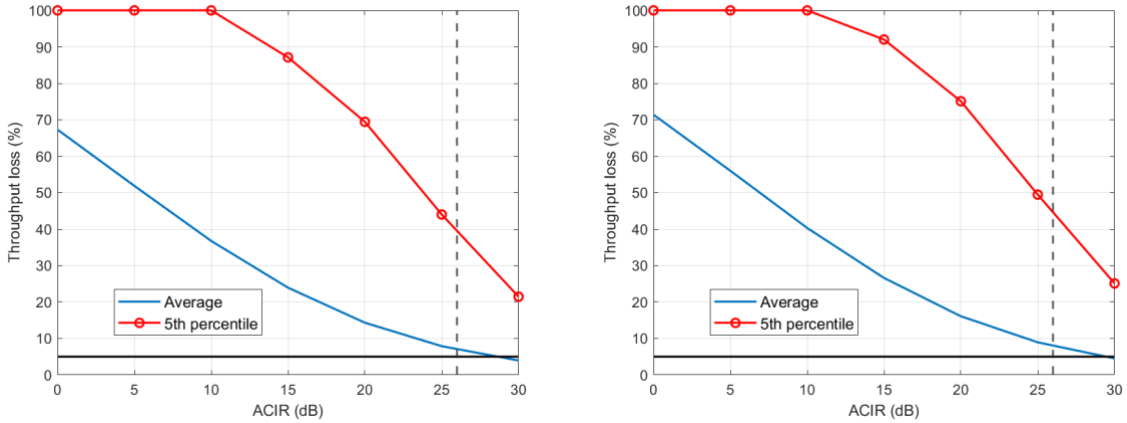

Figure 32: *AVERAGE AND 5TH PERCENTILE THROUGHPUT LOSS IN COEXISTENCE SCENARIO 5 IN THE Q/V-BAND FOR LEO@600KM (LEFT) AND LEO@1200KM (RIGHT) ORBITS AT NADIR*

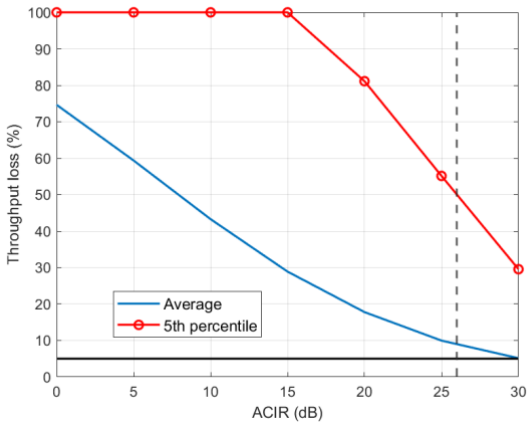

Figure 33: *AVERAGE AND 5TH PERCENTILE THROUGHPUT LOSS IN COEXISTENCE SCENARIO 5 IN THE Q/V-BAND FOR GEO ORBIT AT NADIR*

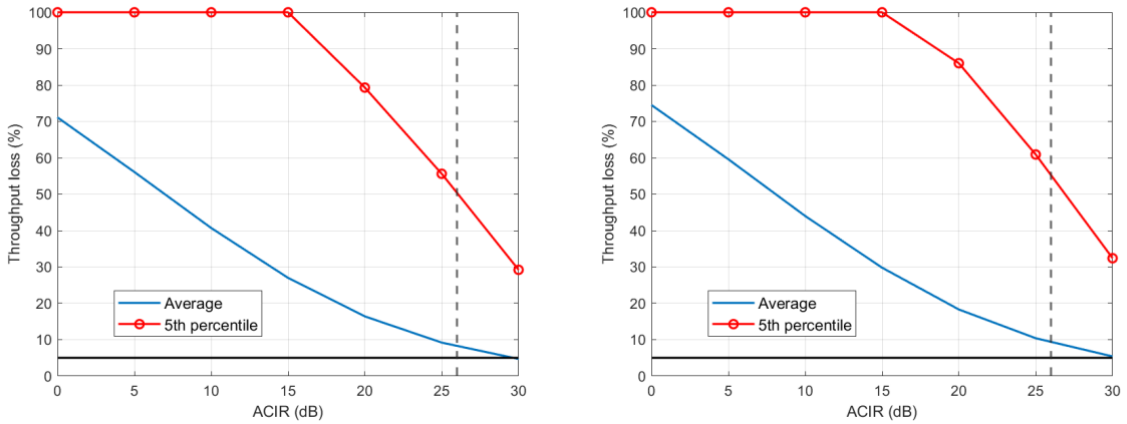

Figure 34*: AVERAGE AND 5TH PERCENTILE THROUGHPUT LOSS IN COEXISTENCE SCENARIO 5 IN THE Q/V-BAND FOR LEO@600KM (LEFT) AND LEO@1200KM (RIGHT) ORBITS AT 45° ELEVATION*

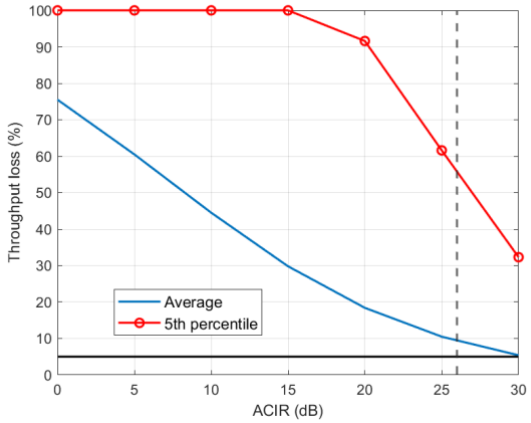

Figure 35: *AVERAGE AND 5TH PERCENTILE THROUGHPUT LOSS IN COEXISTENCE SCENARIO 5 IN THE Q/V-BAND FOR GEO ORBIT at 45° ELEVATION*

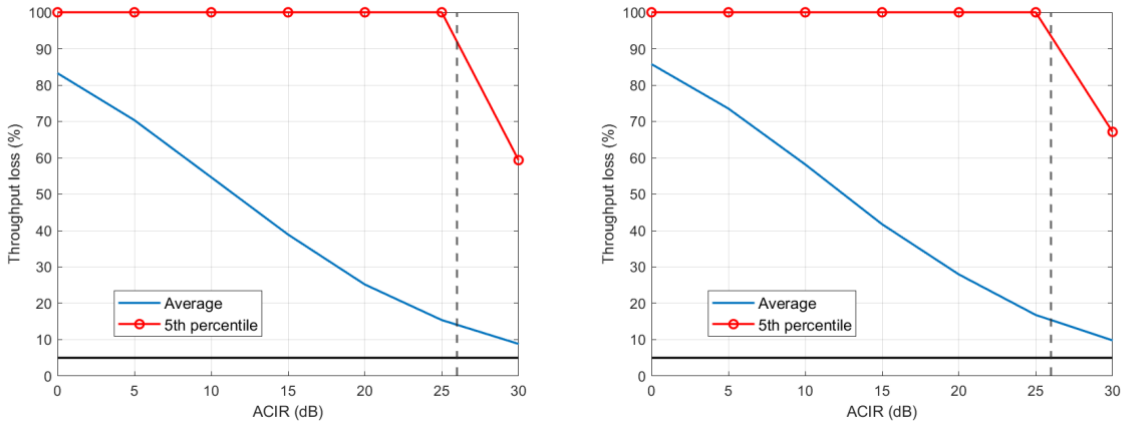

Figure 36: *AVERAGE AND 5TH PERCENTILE THROUGHPUT LOSS IN COEXISTENCE SCENARIO 5 IN THE Q/V-BAND FOR LEO@600KM (LEFT) AND LEO@1200KM (RIGHT) ORBITS AT 30° ELEVATION*

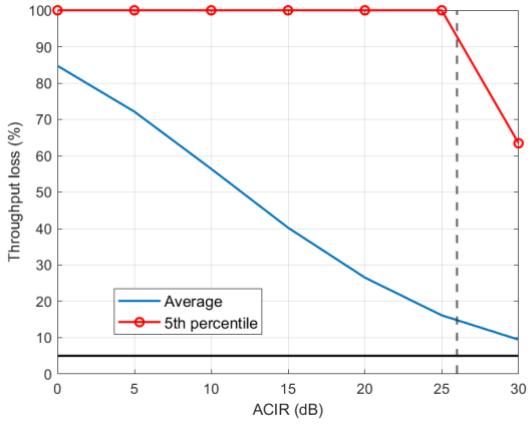

Figure 37: *AVERAGE AND 5TH PERCENTILE THROUGHPUT LOSS IN COEXISTENCE SCENARIO 5 IN THE Q/V-BAND FOR GEO ORBIT AT 30° ELEVATION*

14.2.1.2 Scenario 8 (Aggressor: TN UL, Victim: NTN DL)

Figure 38 to ***Figure 43*** depict the average and 5th percentile throughput loss for coexistence scenario 8 in the Q/V-band for LEO@600km, LEO@1200km and GEO orbits at Nadir, 45° and 30° elevation, as a function of the ACIR. The vertical line at 16 dB represents the ACLR of the TN UE, which is an upper bound on the maximum achievable ACIR. One can observe that the

maximum throughput loss requirements can be fulfilled for the three orbits and for the three considered elevations for achievable ACIR values, i.e., for ACIR values lower than the TN UE ACLR.

Table 42 provides the required ACIR and resulting ACS values for the NTN UE for scenario 8 to ensure that both the average and the 5th percentile maximum throughput loss requirements are fulfilled. **One can observe that a NTN UE ACS of 16dB enables to fulfil these requirements for the three different orbits and for the three simulated elevations**.

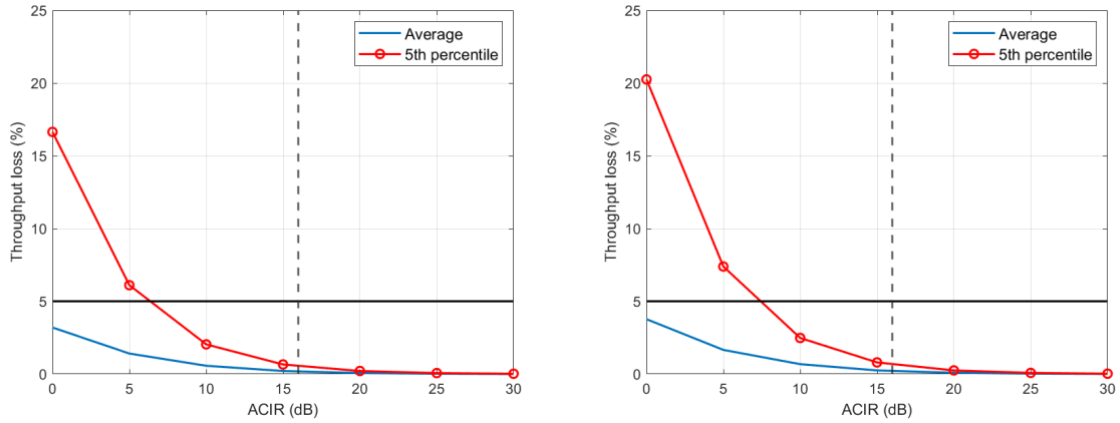

Figure 38: *AVERAGE AND 5TH PERCENTILE THROUGHPUT LOSS IN COEXISTENCE SCENARIO 8 IN THE Q/V-BAND FOR LEO@600KM (LEFT) AND LEO@1200KM (RIGHT) ORBITS AT NADIR*

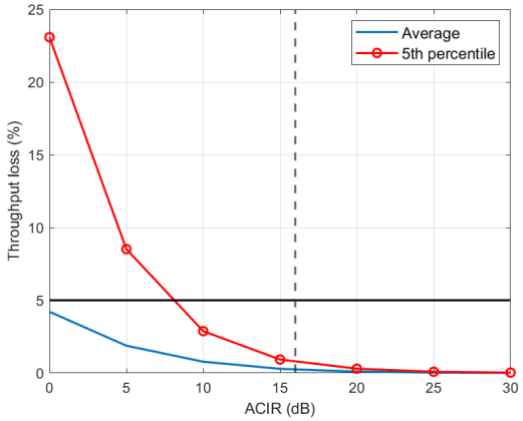

Figure 39: *AVERAGE AND 5TH PERCENTILE THROUGHPUT LOSS IN COEXISTENCE SCENARIO 8 IN THE Q/V-BAND FOR GEO ORBIT AT NADIR*

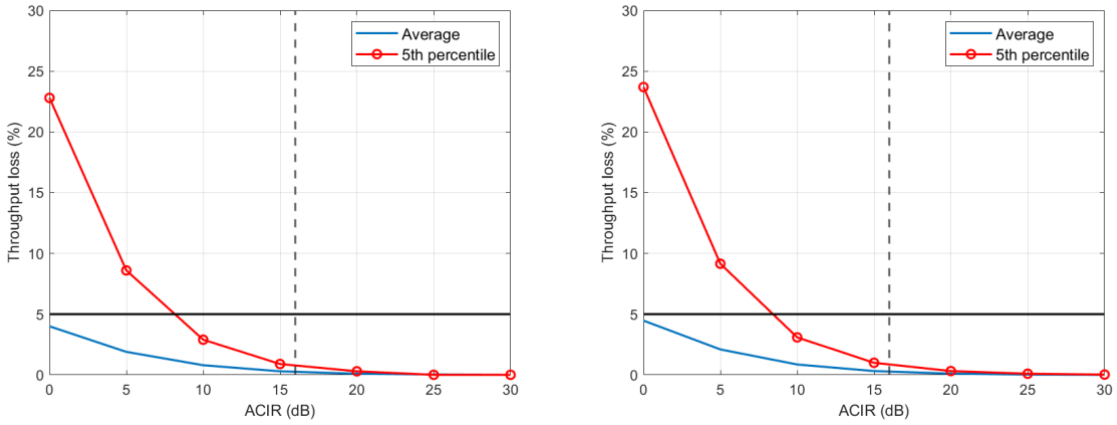

Figure 40: *AVERAGE AND 5TH PERCENTILE THROUGHPUT LOSS IN COEXISTENCE SCENARIO 8 IN THE Q/V-BAND FOR LEO@600KM (LEFT) AND LEO@1200KM (RIGHT) ORBITS AT 45° ELEVATION*

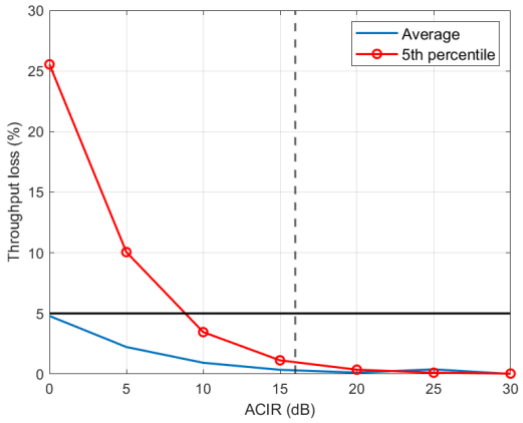

Figure 41: *AVERAGE AND 5TH PERCENTILE THROUGHPUT LOSS IN COEXISTENCE SCENARIO 8 IN THE Q/V-BAND FOR GEO ORBIT AT 45° ELEVATION*

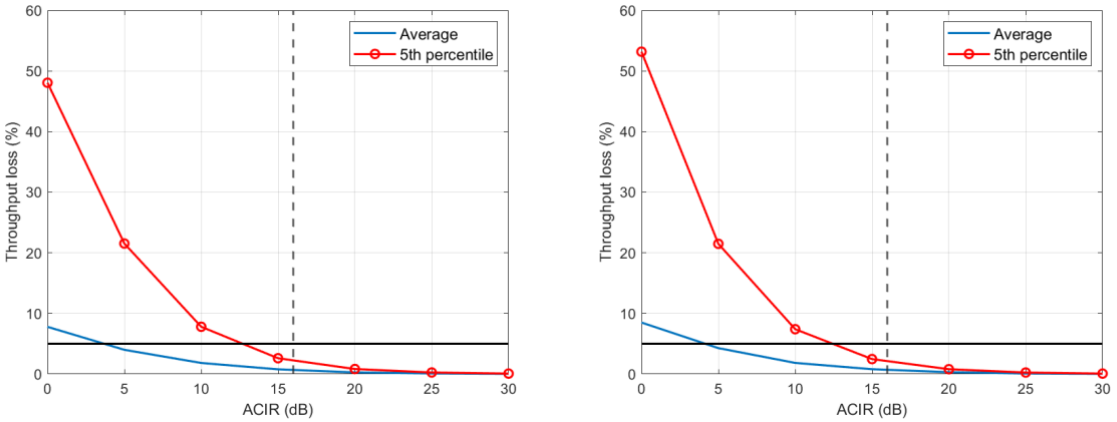

Figure 42: *AVERAGE AND 5TH PERCENTILE THROUGHPUT LOSS IN COEXISTENCE SCENARIO 8 IN THE Q/V-BAND FOR LEO@600KM (LEFT) AND LEO@1200KM (RIGHT) ORBITS AT 30° ELEVATION*

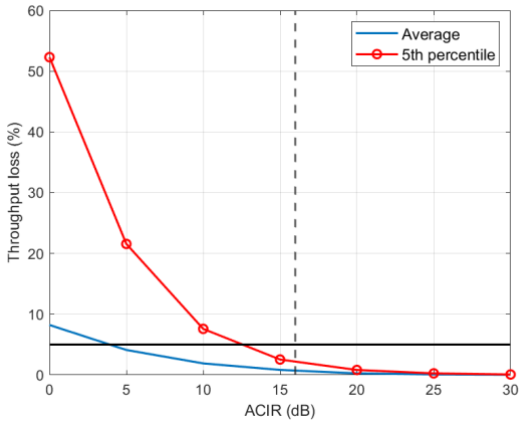

***Figure 43**: AVERAGE AND 5TH PERCENTILE THROUGHPUT LOSS IN COEXISTENCE SCENARIO 8 IN THE Q/V-BAND FOR GEO ORBIT AT 30° ELEVATION*

***Table 42:** required ACIR and resulting NTN UE ACS (both in dB) in the Q/V-band for the three orbits and the three considered elevations to fulfil the maximum throughput loss requirements for scenario 8*

Elevation	Nadir			45° elevation			30° elevation		
Orbit	LEO600	LEO1200	GEO	LEO600	LEO1200	GEO	LEO600	LEO1200	GEO
ACIR	6.4	7.5	8.2	8.2	8.5	8.9	12.7	12.5	12.6
NTN UE ACS	6.9	8.1	8.9	9	9.3	9.8	15.5	15	15.2

14.2.1.3 Synthesis

The main observations from the two previous sections can be summarized as follows:

1. The maximum throughput loss requirements cannot be met in scenario 5 for admissible ACIR value and thus additional technique should be studied to enable coexistence.
2. A NTN UE ACS value of 16dB enables to fulfil the maximum throughput loss requirements for the three different orbits and for the three simulated elevations in scenario 8.

Other coexistence techniques for scenario 5 will be studied in Section 14.3.

14.2.2 Scenarios from category 2

14.2.2.1 Scenario 2 (Aggressor: TN UL, Victim: NTN UL)

Figure 44 and ***Figure 45*** depict the average and 5th percentile throughput loss for coexistence scenario 2 in the Q/V band for LEO@600km, LEO@1200km and GEO orbits at Nadir as a function of the ACIR. One can observe that the maximum throughput loss requirements can be achieved for the three orbits for achievable ACIR values, i.e., ACIR values lower than the TN UE ACLR of 16dB.

Table 43 provides the required ACIR and resulting ACS values for the satellite for scenario 2 to ensure that both the average and the 5th percentile maximum throughput loss requirements described in Section 13.6 are fulfilled. **One can observe that a satellite ACS of the order of 15dB enables to fulfil these requirements for the three different orbits**.

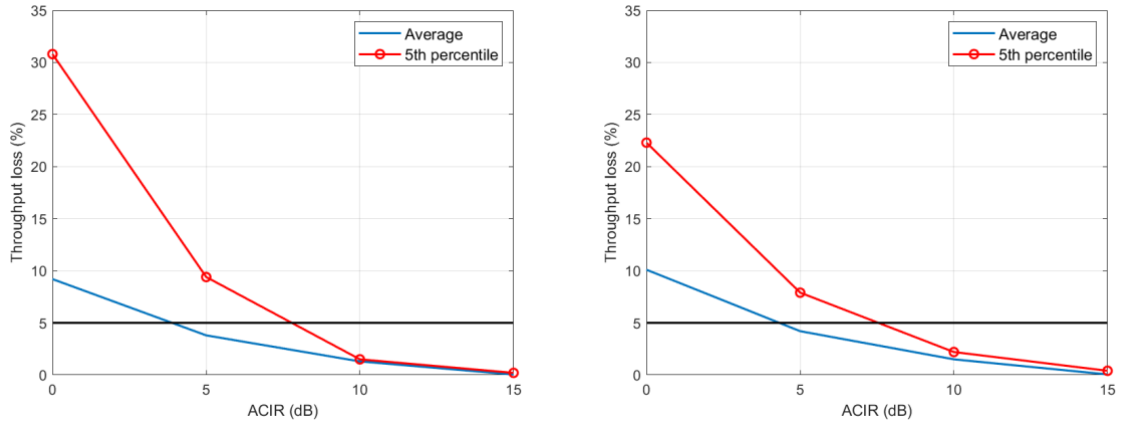

Figure 44: *AVERAGE AND 5TH PERCENTILE THROUGHPUT LOSS IN COEXISTENCE SCENARIO 2 IN THE Q/V BAND FOR LEO@600KM (LEFT) AND LEO@1200KM (RIGHT) ORBITS AT NADIR*

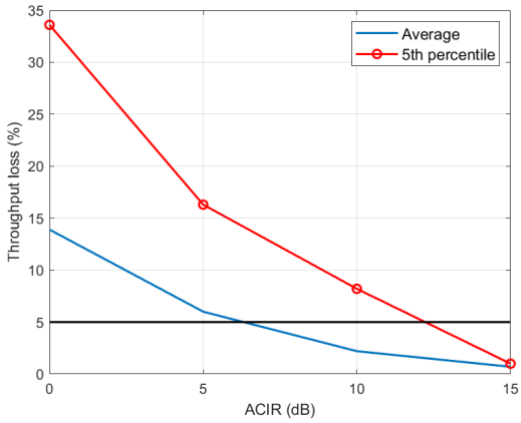

Figure 45: *AVERAGE AND 5TH PERCENTILE THROUGHPUT LOSS IN COEXISTENCE SCENARIO 2 IN THE Q/V BAND FOR GEO ORBIT AT NADIR*

Table 43: *REQUIRED ACIR AND RESULTING satellite ACS (BOTH IN DB) IN THE Q/V BAND FOR THE THREE ORBITS at nadir to fulfil the maximum throughput loss requirements FOR SCENARIO 2*

Orbit	LEO600	LEO1200	GEO
ACIR	7.8	7.6	12.3
Satellite ACS	8.5	8.3	14.6

14.2.2.2 Scenario 4 (Aggressor: TN DL, Victim: NTN UL)

Figure 46 and ***Figure 47*** depict the average and 5th percentile throughput loss for coexistence scenario 2 in the Q/V band for LEO@600km, LEO@1200km and GEO orbits at Nadir as a function of the ACIR. One can observe that the maximum throughput loss requirements can be achieved for the three orbits for achievable ACIR values, i.e., ACIR values lower than the TN BS ACLR of 26dB.

Table 44 provides the required ACIR and resulting ACS values for the satellite for scenario 4 to ensure that both the average and the 5th percentile maximum throughput loss requirements described in Section 13.6 are fulfilled. **One can observe that a satellite ACS of the order of 19dB enables to fulfil these requirements for the three different orbits**.

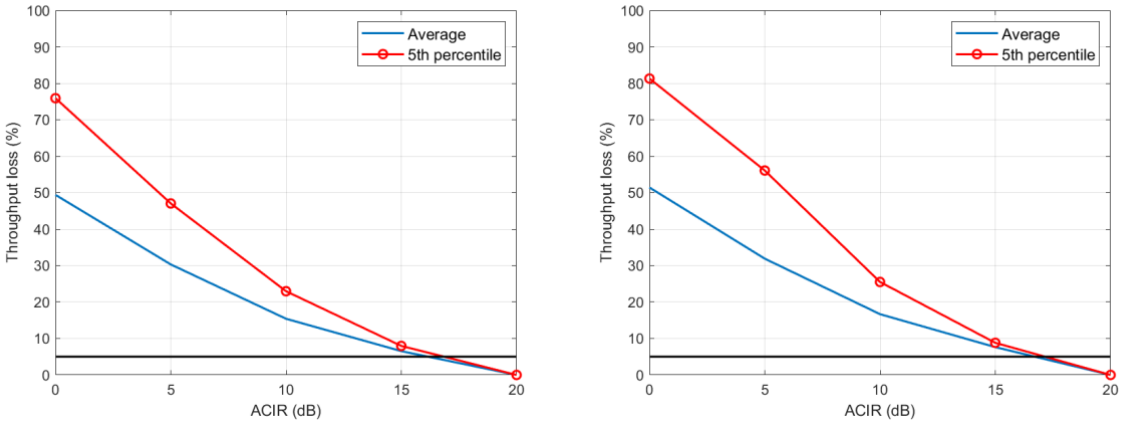

Figure 46: *AVERAGE AND 5TH PERCENTILE THROUGHPUT LOSS IN COEXISTENCE SCENARIO 4 IN THE Q/V BAND FOR LEO@600KM (LEFT) AND LEO@1200KM (RIGHT) ORBITS AT NADIR*

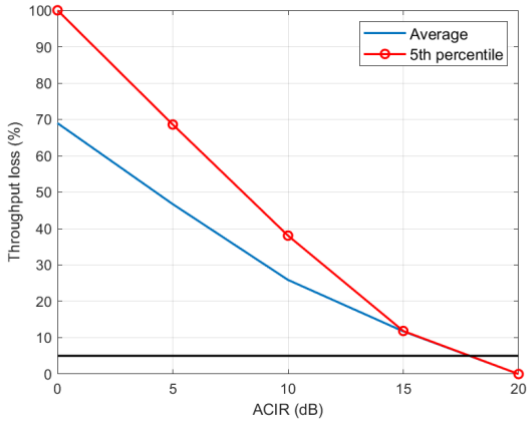

Figure 47: *AVERAGE AND 5TH PERCENTILE THROUGHPUT LOSS IN COEXISTENCE SCENARIO 4 IN THE Q/V BAND FOR GEO ORBIT AT NADIR*

Table 44: *REQUIRED ACIR AND RESULTING satellite ACS (BOTH IN DB) IN THE Q/V BAND FOR THE THREE ORBITS at nadir to fulfil the maximum throughput loss requirements FOR SCENARIO 4*

Orbit	LEO600	LEO1200	GEO
ACIR	16.9	17.2	17.9
Satellite ACS	17.5	17.8	18.7

14.2.2.3 Synthesis

The main observations from the two previous sections can be summarized as follows:

1. A satellite ACS value of 15dB enables to fulfil the 3GPP maximum throughput loss requirements for the three different orbits in scenario 2.
2. A satellite ACS value of 19dB enables to fulfil the 3GPP maximum throughput loss requirements for the three different orbits in scenario 4.

One can thus conclude that a satellite ACS value of 19dB enables coexistence between NTN UL and both TN DL and TN UL in the Q/V band.

14.2.3 Scenarios from category 3

14.2.3.1 Scenario 6 (aggressor: NTN DL, victim: TN DL)

It has been found by simulations that an ACIR equal to 0dB is enough to fulfil the 3GPP coexistence requirements detailed in Section 13.6 for the three different orbits at Nadir.

14.2.3.2 Scenario 7 (aggressor: NTN DL, victim: TN UL)

It has been found by simulations that an ACIR equal to 0dB is enough to fulfil the 3GPP coexistence requirements detailed in Section 13.6 for the three different orbits at Nadir.

14.2.3.3 Synthesis

For both scenarios 6 and 7, it has been found by simulations that an ACIR equal to 0dB is enough to fulfil the 3GPP coexistence requirements detailed in Section 13.6 for the three different orbits at Nadir.

One can thus conclude that a satellite ACLR value of 0dB enables coexistence between NTN DL and both TN DL and TN UL in the Q/V band.

14.2.4 Scenarios from category 4

14.2.4.1 Scenario 1 (Aggressor: NTN UL, Victim: TN UL)

Figure 48 to ***Figure 53*** depict the average and 5th percentile throughput loss for coexistence scenario 1 in the Q/V-band for LEO@600km, LEO@1200km and GEO orbits at Nadir, 45° and 30° elevation, as a function of the ACIR. The vertical line in the figures related to 30° elevation represents the ACS of the TN BS, which is an upper bound on the maximum achievable ACIR. One can observe that:

1. At Nadir and 45° elevation, the maximum throughput loss requirements can be fulfilled for the three orbits for achievable ACIR values, i.e., ACIR values lower than the TN BS ACS.
2. At 30° elevation:
    a. The maximum average throughput loss requirement can be fulfilled for achievable ACIR values for the three orbits.
    b. The 5th percentile throughput loss requirement cannot be fulfilled for achievable ACIR values for the three orbits.

Table 45 provides the required ACIR and resulting ACLR values for the NTN UE for scenario 1 to ensure that both the average and the 5th percentile maximum throughput loss requirements described in Section 13.6 are fulfilled, with “NV” means no value (i.e., no admissible value can be found). **One can observe that a NTN UE ACS of the order of 20dB enables to fulfil these requirements for the three different orbits at Nadir and 45° elevation, whereas no ACLR enabling coexistence at 30° elevation can be found**.

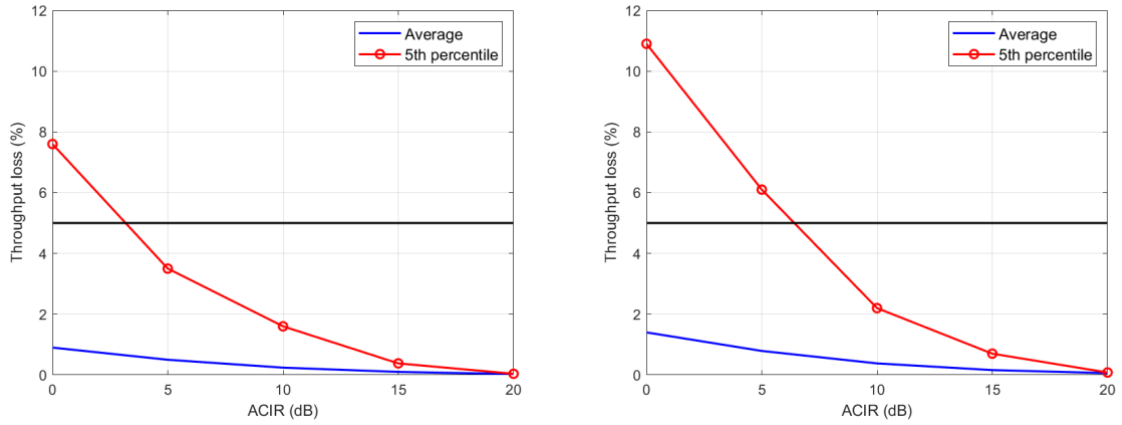

Figure 48: *AVERAGE AND 5TH PERCENTILE THROUGHPUT LOSS IN COEXISTENCE SCENARIO 1 IN THE Q/V BAND FOR LEO@600KM (LEFT) AND LEO@1200KM (RIGHT) ORBITS AT NADIR*

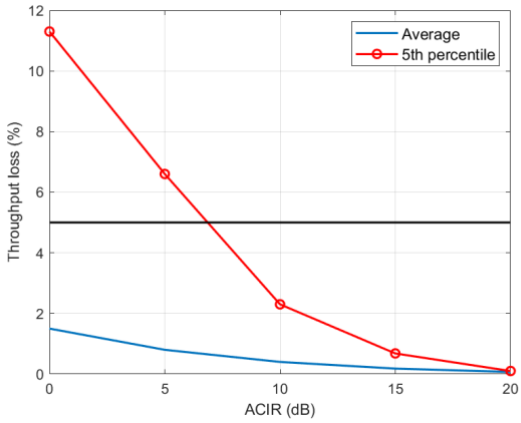

Figure 49: *AVERAGE AND 5TH PERCENTILE THROUGHPUT LOSS IN COEXISTENCE SCENARIO 1 IN THE Q/V BAND FOR GEO ORBIT AT NADIR*

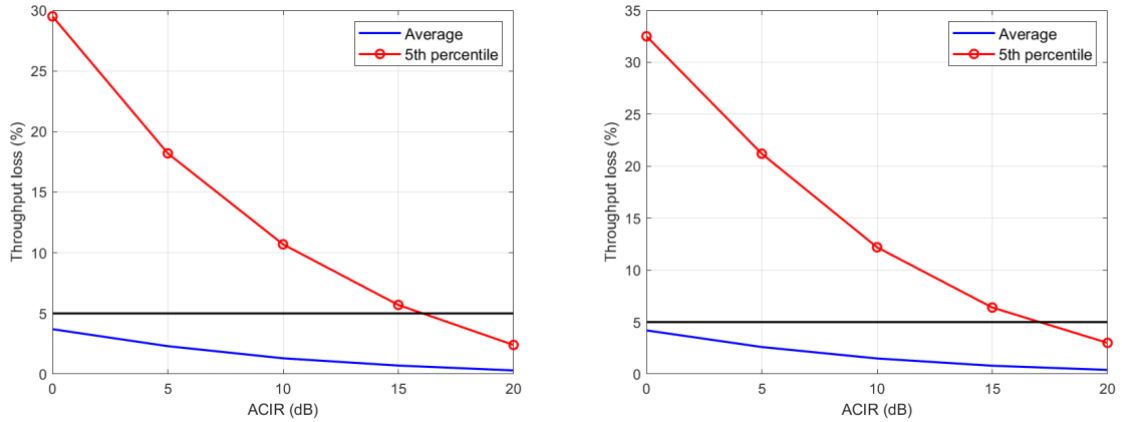

Figure 50: *AVERAGE AND 5TH PERCENTILE THROUGHPUT LOSS IN COEXISTENCE SCENARIO 1 IN THE Q/V BAND FOR LEO@600KM (LEFT) AND LEO@1200KM (RIGHT) ORBITS AT 45° ELEVATION*

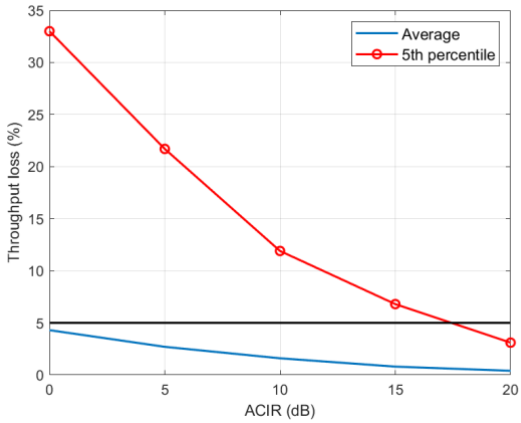

Figure 51: *AVERAGE AND 5TH PERCENTILE THROUGHPUT LOSS IN COEXISTENCE SCENARIO 1 IN THE Q/V BAND FOR GEO ORBIT AT 45° ELEVATION*

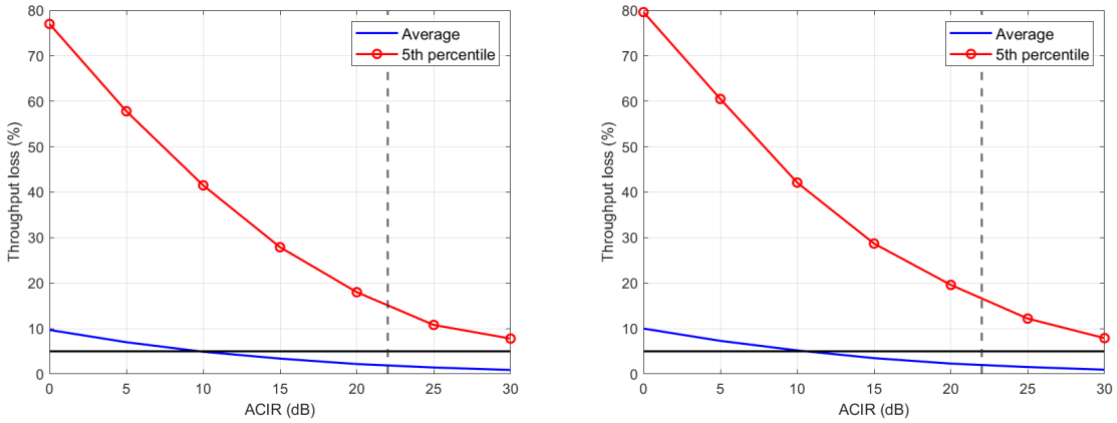

Figure 52: *AVERAGE AND 5TH PERCENTILE THROUGHPUT LOSS IN COEXISTENCE SCENARIO 1 IN THE Q/V BAND FOR LEO@600KM (LEFT) AND LEO@1200KM (RIGHT) ORBITS AT 30° ELEVATION*

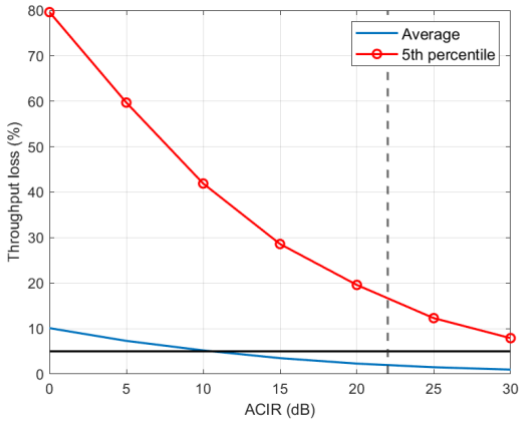

Figure 53: *AVERAGE AND 5TH PERCENTILE THROUGHPUT LOSS IN COEXISTENCE SCENARIO 1 IN THE Q/V BAND FOR GEO ORBIT AT 30° ELEVATION*

Table 45: REQUIRED ACIR AND RESULTING NTN UE ACLR (BOTH IN DB) IN THE Q/V BAND FOR THE THREE ORBITS and the three simulated elevation FOR SCENARIO 1

Elevation	Nadir			45° elevation			30° elevation		
Orbit	LEO600	LEO1200	GEO	LEO600	LEO1200	GEO	LEO600	LEO1200	GEO
ACIR	3.2	6.5	6.9	16.1	17.1	17.5	>22	>22	>22
NTN UE ACLR	3.3	6.6	7	17.4	18.8	19.3	NV	NV	NV

14.2.4.2 Scenario 3 (Aggressor: NTN UL, Victim: TN DL)

It has been found by simulations that an ACIR equal to 0dB is enough to fulfil the 3GPP coexistence requirements detailed in Section 13.6 for the three different orbits at Nadir.

14.2.4.3 Synthesis

The main observations from the two previous sections can be summarized as follows:

1. In scenario 1:
    a. A NTN UE ACLR value of 20dB enables to fulfil the 3GPP maximum throughput loss requirements at nadir and 45° elevation.
    b. At 30° elevation, it is not possible to find a NTN UE ACLR value enabling coexistence.
2. A NTN UE ACLR value of 0dB enables to fulfil the 3GPP maximum throughput loss requirements for the three different orbits in scenario 3.

These two observations suggest that:

1. A NTN UE ACLR value of 20dB enables to fulfil the 3GPP maximum throughput loss requirements at nadir and 45° elevation for scenarios 1 and 3.
2. For scenario 1, additional coexistence technique could be envisonned to enable coexistence at 30°. For instance, MMSE-IRC as discussed in Section 13.5 could enable to reduce the required ACIR to an admissible value.

Regarding the second above point, as mentioned in Section 13.3, the main priority is to ensure coexistence at 45° elevation as per WP3 architectural work, which can be achieved as discussed above through the “compliance with standard” coexistence technique. Thus, no additional coexistence technique have been investigated for scenario 1. It could be of interest to perform additional study in the future if coexistence at 30° elevation is required.

14.3 COEXISTENCE TECHNIQUES

The results presented in the previous section show that the “compliance with standard” coexistence technique enables TN-NTN coexistence in the Q/V band for all interference scenarios except for scenario 5, in which the aggressor is the TN DL and the victim is the NTN DL.

To alleviate interference from TN BS to NTN UE at 37 GHz, several coexistence techniques can be employed. They include using a frequency guard band, increasing NTN SAN transmission power, increasing the antenna gain of the NTN UE, increasing TN BS antenna gain while keeping the BS EIRP constant, e.g. by increasing the number of TN gNB antenna elements while at the same time decreasing TN gNB transmission power for a constant EIRP. Among these techniques, increasing the antenna gain of the NTN UE is investigated and its impact on improving the TN-NTN coexistence is discussed the next sections.

TH-SIX also proposed and investigated two transmit power control (TPC) algorithms for TN BS in the next sections. These theoretical coexistence techniques come with practical implementation challenges which are discussed in Section 14.3.3. They require modification on both TN BS and TN UE and additional signalling between them which are hardly acceptable by the eco system. Therefore, other coexistence techniques mentioned above should be considered in the future to enable TN-NTN coexistence for scenario 5.

The rest of this section is organized as follows. Section 14.3.1 describes the two implemented TPC algorithms and Section 14.3.2 provides the simulation results for the different coexistence techniques. Finally, Section 14.3.3 highlights the practical challenges associated with the proposed TPC techniques.

14.3.1 Description of the implemented TPC algorithms

The general idea of the proposed TPC algorithms for TN BS is to decrease the transmit power of the TN BS while satisfying a constraint on the resulting maximum TN DL throughput degradation. We implemented two TPC algorithms, a “basic” TPC algorithm (BTA), and an “advanced” TPC algorithm (ATA). In what follows, Section 14.3.1.1 describes the common idea behind the two proposed TPC algorithms. Then, Sections 14.3.1.2 and 14.3.1.3 detail the BTA and the ATA, respectively.

14.3.1.1 Common idea of the two proposed TPC algorithms

The common idea of BTA and ATA is to decrease the TN BS transmit power while ensuring that the resulting TN DL throughput degradation on each TN link is less than 5%. Both algorithms are distributed, meaning that each BS decides its own transmit power without needing a central entity with a global view on the link budget of all the TN links. Therefore there is no need for additional signalling among TN BSs. However, additional signalling between TN BS and TN UE and additional processing on both TN BS and TN UE are required which are explained below.

The underlying assumption of the proposed TPC algorithms is that the TN UE is able to compute its SINR and throughput with and without the interference from the satellite. This could be possible if i) the BS use different reference signal (RS) than the satellite, ii) the TN UE are able to decode the RS from the satellite, and iii) there exists at least one time slot during which the satellite and the TN BS transmit their RS simultaneously. More explanation and the case when such computation is not possible is addressed in the remark at the end of the present section.

Let us focus on a TN link between a BS i^t and a UE i^r. UE i^r first computes its received SINR without interference from the satellite, that will serve as a reference for the computation of the throughput degradation induced by the TPC and that can be written as:

$$SINR_{TN}^{i^r} = \frac{P_{T_X}^{i^t} G_{i^t,i^r}}{10^{0.1N_F} N_0 + \sum_{j^t=1, j\neq i^t}^{N_{itf}} P_{T_X}^{j^t} G_{j^t,i^r}},$$

where $P_{T_X}^{k^t}$ and G_{k^t,i^r} represent, for a given transmitting BS k^t, its transmit power and the loss of power between BS k^t and UE i^r, respectively. Note this function is for simulation purposes and the real throuput of the UE might be different, especially due to the usage of practical modulation and coding schemes. Then, the TN UE communicates the SINR value $SINR_{TN}^{i^r}$ to its associated BS i^t, which computes $T_{ref}^{i^r} := \mathbb{T}(SINR_{TN}^{i^r})$ where $\mathbb{T}(.)$ is the throughput function of SINR defined in Section 13.6. The throughput $T_{ref}^{i^r}$ serves as a reference for the TPC. BS i^t

then selects a transmit power $P_{T_X}^{i^t,al}$ such that the resulting $SINR_{TN,A}^{i^r}$, that can be expressed as:

$$SINR_{TN,A}^{i^r} = \frac{P_{T_X}^{i^t,al} G_{i^t,i^r}}{10^{0.1N_F} N_0 + \sum_{j^t=1,j^t\neq i^t}^{N_{itf}} P_{T_X}^{j^t,al} G_{j^t,i^r} + I_{\text{Sat}}^{i^r}},$$

yields a throughput $T_{al}^{i^r} \coloneqq \mathbb{T}(SINR_{TN,A}^{i})$ that is greater or equal to $0.95T_{ref}^{i^r}$, i.e., $T_{al}^{i^r} \geq 0.95T_{ref}^{i^r}$.

Note that the interference caused by other BSs in the denominator of $SINR_{TN,A}^{i^r}$ is lower after applying TPC due to the transmit power reduction in BSs.

The term $I_{\text{Sat}}^{i^r}$ in $SINR_{TN,A}^{i^r}$ is the interference caused by the satellite on UE i^r. Notice that $SINR_{TN,A}^{i^r}$ involves $I_{\text{Sat}}^{i^r}$ in its denominator whereas $SINR_{TN}^{i^r}$ does not. The rational is to ensure that the total throughput loss of TN UE including both interference from satellites and BS power reduction due to TPC is limited to 5%.

Remark: If i) the BS use different reference signal (RS) than the satellite, ii) the TN UE are able to decode the RS from the satellite, and iii) there exists at least one time slot during which the satellite and the TN BS transmit their RS simultaneously, the received signal at TN UE i^r can be written as:

$$Y_{i^r} = X_{i^t} + X_{sat} + I + B,$$

where X_{i^t} is the RS of the BS i^t, X_{sat} is the RS of the satellite, I represents the interference from the other BS (i.e., the sum of their respective RS), and B is the noise. If i^r knows both X_{i^t} and X_{sat}, then it is able to estimate its received SINR with and without interference from the satellite.

If such a coordination between the transmission of the RS of the two systems is not possible, other solutions need to be implemented in the TN UE to differentiate the interference from the different systems. For instance, [38] proposed machine learning algorithms to classify the source of interference among predefined sources.

The next two sections explain the two implemented TPC algorithms.

14.3.1.2 Basic TPC algorithm

In BTA, BS i^t selects its transmit power without taking into account the transmit power adaptation of the other BS. More precisely, i^t uses the following upper bound of $SINR_{TN,A}^{i^r}$ to select $P_{T_X}^{i^t,al}$:

$$\widetilde{SINR}_{TN,BTA}^{i^r} \coloneqq \frac{P_{T_X}^{i^t,al} G_{i^t,i^r}}{10^{0.1N_F} N_0 + \sum_{j^t=1,j^t\neq i}^{N_{itf}} P_{T_X}^{j^t} G_{j^t,i^r} + I_{\text{Sat}}^{i^r}} = SINR_{TN}^{i^r} \frac{P_{T_X}^{i^t,al}}{P_{T_X}^{i^t}}.$$

The denominator in $\widetilde{SINR}_{TN,BTA}^{i^r}$ does not take into account the TPC of other BSs. Therefore, $\widetilde{SINR}_{TN,BTA}^{i^r}$ is smaller than the actual SINR $SINR_{TN,A}^{i^r}$ which is expressed in previous section.

BS i^t searches for $P_{T_X}^{i^t,al}$ such that $\mathbb{T}\left(\widetilde{SINR}_{TN,BTA}^{i^r}\right) = 0.95T_{ref}^{i^r}$, which can be done e.g. using the bisection method. Since $\widetilde{SINR}_{TN,BTA}^{i^r} \leq SINR_{TN,A}^{i^r}$ and $\mathbb{T}(.)$ is non decreasing, then

$\mathbb{T}\left(\widetilde{SINR}_{TN,BTA}^{i^r}\right) = 0.95T_{ref}^{i^r} \Rightarrow \mathbb{T}\left(SINR_{TN,A}^{i^r}\right) \geq 0.95T_{ref}^{i^r}$, meaning that the BTA algorithm results into a throughput that is greater or equal to $0.95T_{ref}^{i^r}$.

14.3.1.3 Advanced TPC algorithm

Since the BTA algorithm results into a throughput that is greater or equal to $0.95T_{ref}^{i^r}$, there might be room to continue decreasing the BS transmit power. The ATA is an iterative approach designed to take advantage of this opportunity, in which each BS gradually decreases its transmit power to reach a throughput that is equal to $0.95T_{ref}^{i^r}$. Since it is an iterative approach, it needs several signalling between BS and UE and several calculations on the UE side.

The idea is to iterate between measuring the received SINR that takes into account the transmit power of the other BS and applying the BTA based on this measured SINR until convergence is reached. More precisely, at a given iteration $n > 0$, the TN UE i^r measures its received SINR as:

$$SINR_{TN,ATA}^{i^r}(n) := \frac{P_{T_X}^{i^t,al}(n-1)G_{i^t,i^r}}{10^{0.1N_F}N_0 + \sum_{j^t=1,j^t\neq i}^{N_{itf}} P_{T_X}^{j^t}(n-1)G_{j^t,i^r} + I_{\text{Sat}}^{i^r}}$$

where $P_{T_X}^{k^t,al}(0)$ is set to the initial transmit power of the BS, i.e., 43 dBm in the Q/V-band (see ***Table 15***). Then, the BS i^r selects its transmit power as in the BTA algorithm, i.e., using the following upper bound on the SINR:

$$\widetilde{SINR}_{TN,ATA}^{i^r}(n) := \frac{P_{T_X}^{i^t,al}(n)G_{i^t,i^r}}{10^{0.1N_F}N_0 + \sum_{j^t=1,j^t\neq i}^{N_{itf}} P_{T_X}^{j^t}(n-1)G_{j^t,i^r} + I_{\text{Sat}}^{i^r}} = SINR_{TN,ATA}^{i^r}(n)\frac{P_{T_X}^{i^t,al}(n)}{P_{T_X}^{i^t,al}(n-1)}.$$

As in the BTA algorithm, BS i^t searches for $P_{T_X}^{i^t,al}(n)$ such that $\mathbb{T}\left(\widetilde{SINR}_{TN,ATA}^{i^r}(n)\right) = 0.95T_{ref}^{i^r}$, which can be done e.g. using the bisection method. The ATA algorithm iterates between these two steps, i.e., measuring $SINR_{TN,ATA}^{i^r}(n)$ and finding $P_{T_X}^{i^t,al}(n)$, until convergence is reached.

The ATA is distributed since each BS decides its transmit power based on the SINR measured by its associated UE. It is expected to yield better performance in terms of coexistence than the BTA thanks to the iterative reduction of the transmit power that will yield a lower level of interference. This performance gain comes at the cost of the following two drawbacks of ATA as compared with BTA:

1. ATA requires more signalling and computation than BTA since the UE has to report multiple time its received SINR to its associated BS in the former algorithm, whereas only one reporting is required for the latter one.
2. The convergence of ATA is slower due to its iterative nature, whereas BTA is a “one shot” decision algorithm.

Remark: the signalling exchange are abstracted in the simulations, meaning that it is assumed that the signalling is instantaneous and error free. The practical challenges associated with the implementation of this additional signalling is discussed in Section 14.3.3.

14.3.2 Coexistence techniques simulation results

We first focus on the performance evaluation when the satellite is at Nadir, using the same setup as for scenario 5. ***Figure 54*** and ***Figure 55*** (resp. ***Figure 56*** and ***Figure 57***) depict the

average (resp. 5th percentile) throughput loss for coexistence scenario 5 in the Q/V-band for LEO@600km, LEO@1200km and GEO satellites. The vertical line in these curves represents the upper bound for the achievable ACIR, i.e., the ACLR of the BS that is equal to 26 dB. We can draw the following observations:

1. The BTA technique reduces the throughput loss, but the 5th percentile throughput loss metric still is not met with this technique.
2. NTN UE antenna diameter of 40 cm and ATA technique provide similar improvement, with a small advantage for ATA, at the cost of several iterations until convergence (between five and ten iterations in average).
3. Combining both TPC and larger antenna diameter brings more improvement than using each technique separately, however, it is not clear what is the contribution of each technique.
4. Considering the need to meet both average and the 5th percentile throughput loss metrics, one can observe that:
    a. The BTA technique alone does not enable to fulfil the requirements for admissible ACIR value.
    b. Setting the antenna diameter of the NTN UE to 40 cm enables the TN-NTN coexistence for scenario 5 for LEO600 and LEO1200 satellites, and is very close for GEO satellite.
    c. The other coexistence techniques, i.e., ATA, D=40+BTA, and D=40+ATA, enable to fulfil the requirements for admissible ACIR values at the cost of additional signalling between TN BS and TN UE.

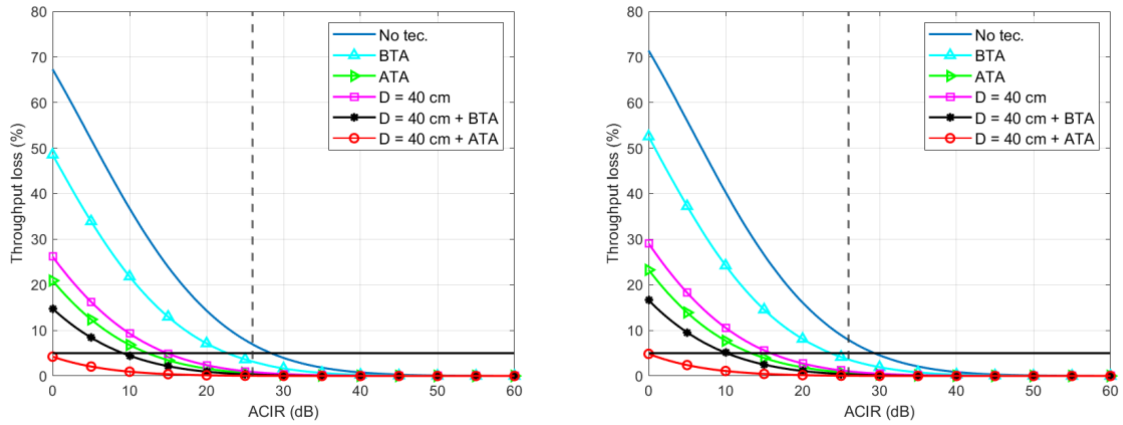

Figure 54: *Average throughput loss for the different coexistence techniques evaluated for scenario 5 at Nadir for IEO600 (left) and LEO 1200 (right) satellites*

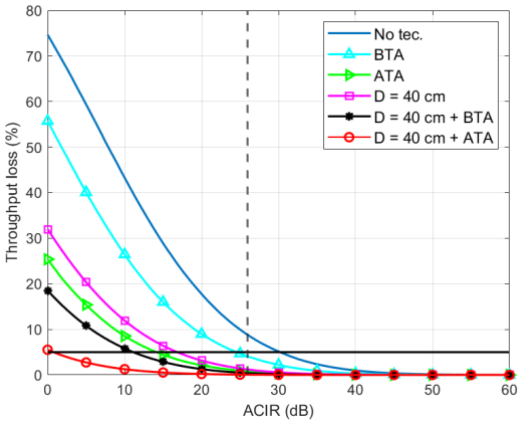

Figure 55: *average throughput loss for the different coexistence techniques evaluated for scenario 5 at nadir for GEO satellite*

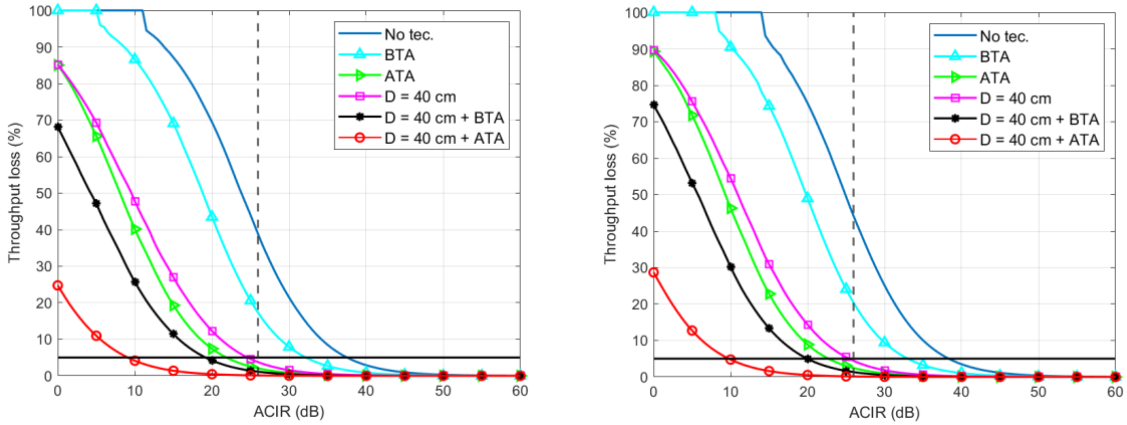

Figure 56: *5th percentilE throughput loss for the different coexistence techniques evaluated for scenario 5 at Nadir for lEO600 (left) and LEO 1200 (right) satellites*

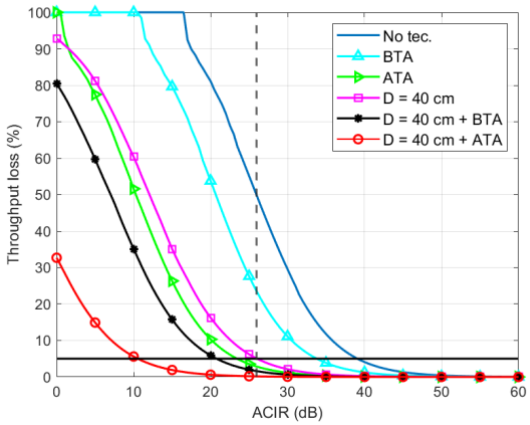

Figure 57: *5th percentile throughput loss for the different coexistence techniques evaluated for scenario 5 at nadir for GEO satellite*

We now focus on the performance evaluation when the satellite is at 45° elevation. ***Figure 58*** and ***Figure 59*** (resp. ***Figure 60*** and ***Figure 61***) depict the average (resp. 5th percentile) throughput loss for coexistence scenario 5 in the Q/V-band for LEO@600km, LEO@1200km and GEO satellites. We can draw the following observations:

1- Focusing on the average throughput loss metric, each technique enables to find an admissible ACIR value satisfying the coexistence requirement, which is not possible when no technique is used. This observation is the same as at Nadir.
2- For the 5th percentile throughput loss metric, one can observe that the two techniques enabling to find admissible ACIR values fulfilling the requirements are ATA and D=40+ATA. The other simulated techniques do not enable to fulfil the requirements for admissible ACIR.

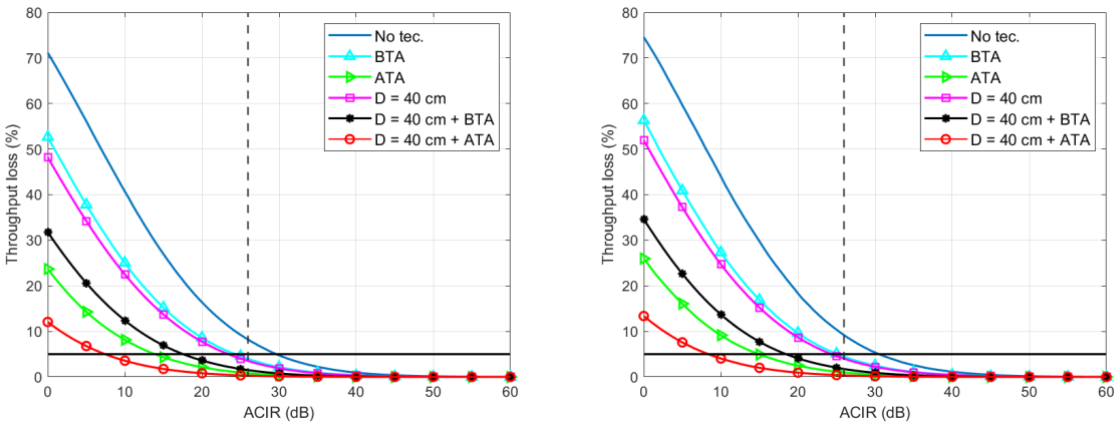

Figure 58: *Average throughput loss for the different coexistence techniques evaluated for scenario 5 at 45° elevation for IEO600 (left) and LEO 1200 (right) satellites*

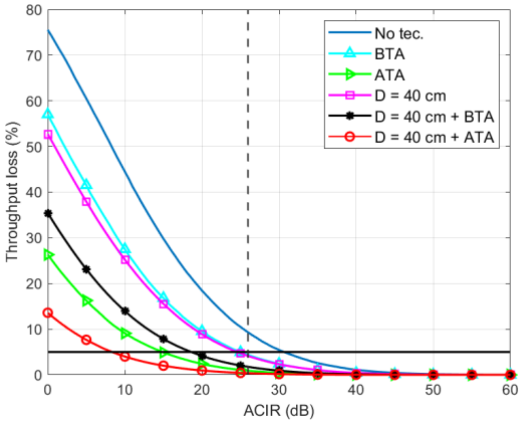

Figure 59: *average throughput loss for the different coexistence techniques evaluated for scenario 5 at 45° elevation for GEO satellite*

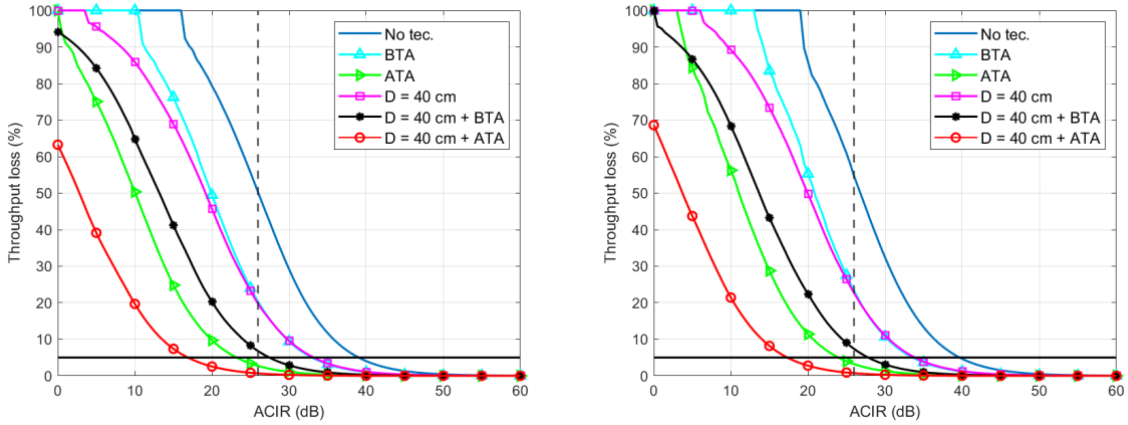

Figure 60: *5th percentilE throughput loss for the different coexistence techniques evaluated for scenario 5 at 45° elevation for IEO600 (left) and LEO 1200 (right) satellites*

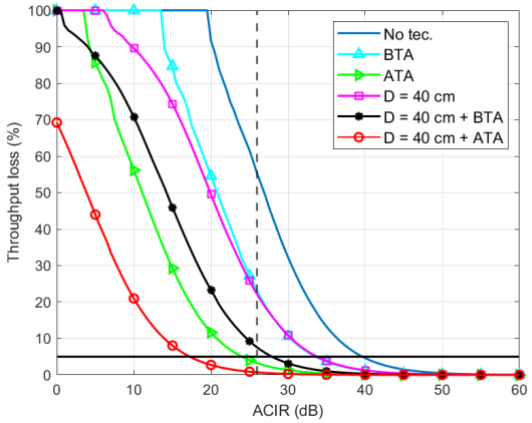

Figure 61: *5th percentile throughput loss for the different coexistence techniques evaluated for scenario 5 at 45° elevation for GEO satellite*

For the sake of completeness, we now focus on the performance evaluation when the satellite is at 30° elevation, although as discussed in Section 14.2.4.3 ensuring coexistence at 45° is sufficient. ***Figure 62*** and ***Figure 63*** (resp. ***Figure 64*** and ***Figure 65***) depict the average (resp. 5th percentile) throughput loss for coexistence scenario 5 in the Q/V-band for LEO@600km, LEO@1200km and GEO satellites. We can draw the following observations:

1- Focusing on the average throughput loss metric, the three techniques that enable finding admissible ACIR values fulfilling the requirement are ATA, D=40+BTA and D=40+ATA.
2- For the 5th percentile throughput loss metric, only the D=40+ATA technique enables finding admissible ACIR values fulfilling the requirement.

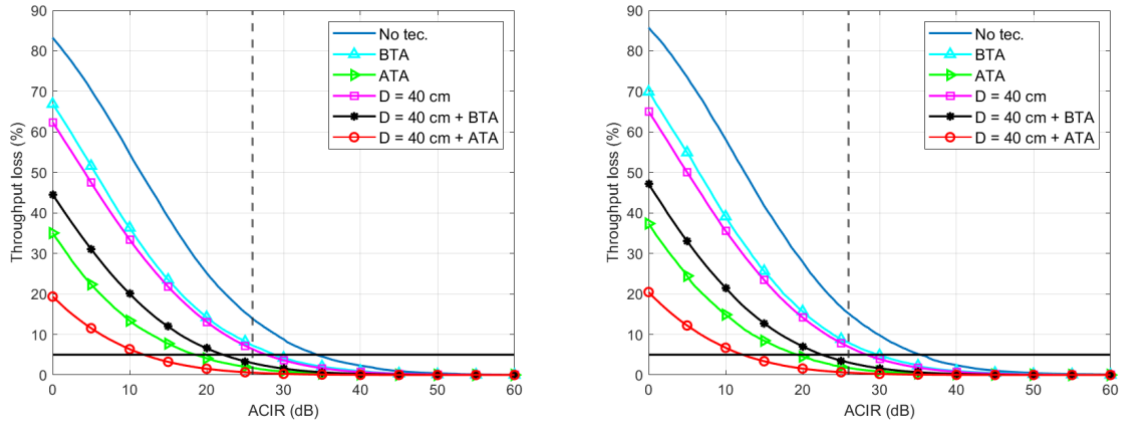

Figure 62: *Average throughput loss for the different coexistence techniques evaluated for scenario 5 at 30° elevation for IEO600 (left) and LEO 1200 (right) satellites*

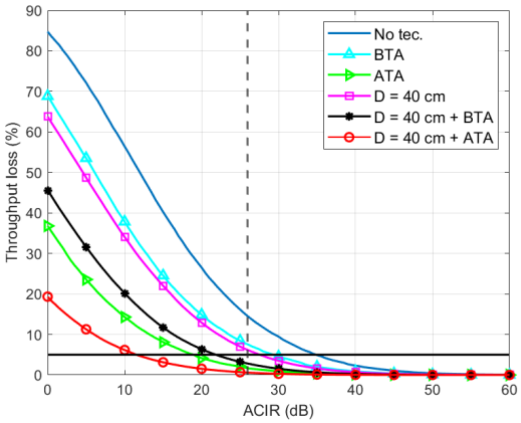

Figure 63: *average throughput loss for the different coexistence techniques evaluated for scenario 5 at 30° elevation for GEO satellite*

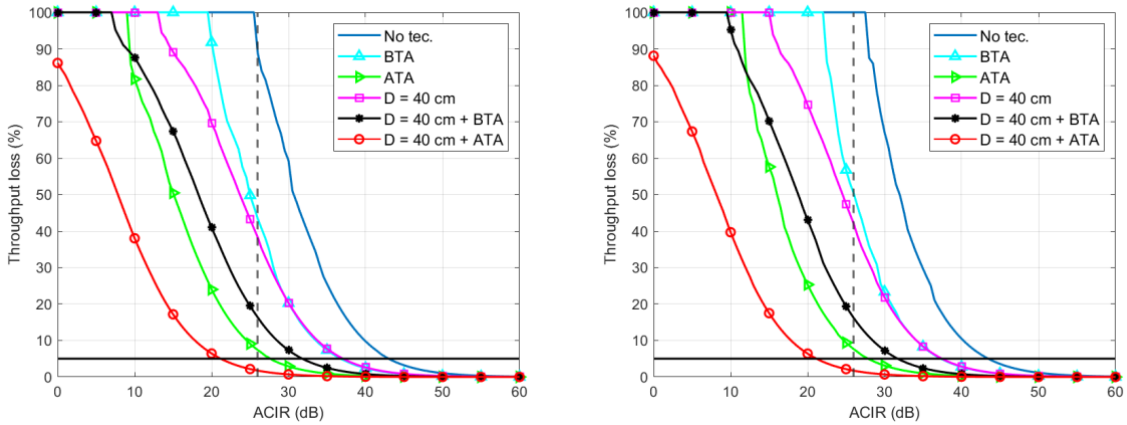

Figure 64: *5th percentilE throughput loss for the different coexistence techniques evaluated for scenario 5 at 30° elevation for IEO600 (left) and LEO 1200 (right) satellites*

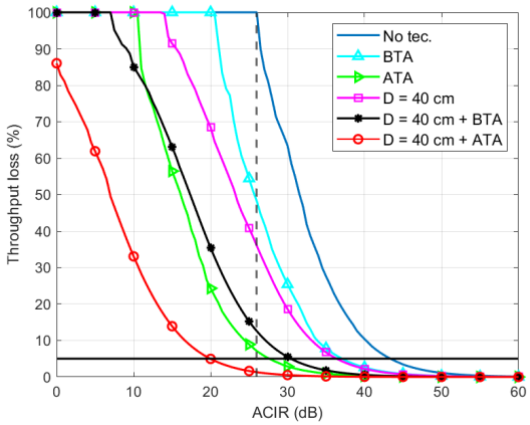

Figure 65: *5th percentile throughput loss for the different coexistence techniques evaluated for scenario 5 at 30° elevation for GEO satellite*

Table 46 and ***Table 47*** provides the required NTN UE ACS to fulfil the average and 5th percentile throughput loss requirements, respectively, for the different simulated techniques and the three orbits, and for the three simulated elevations. In these tables and in the rest of this document, NV means that no admissible value can be found. One can see that:

1- Only ATA and D=40+ATA enable coexistence at 45° for the two criteria and for the three different orbits.
2- If ATA is implemented at the BS, a NTN UE ACS of 30dB is required to enable coexistence at 45° elevation for the three different orbits.
3- If an antenna with diameter 40 cm is used for the NTN UE and ATA is implemented at the BS, a NTN UE ACS of the order of 19dB is required to enable coexistence at 45° elevation for the three different orbits.

Table 46: *Required NTN UE ACS for each orbit in scenario 5 and for each simulated technique for the average throughput loss criterion*

Elevation	Nadir			45° elevation			30° elevation		
Orbit	LEO600	LEO1200	GEO	LEO600	LEO1200	GEO	LEO600	LEO1200	GEO
No technique	NV	NV	NV	NV	NV	NV	NV	NV	NV
BTA	26	28.4	31.9	29.9	32	31.9	NV	NV	NV
ATA	12.7	13.8	14.9	14.3	15.4	15.4	20	20.6	20
D=40 cm	15.4	16.5	17.6	27.1	31.9	30.2	NV	NV	NV
D=40 cm + BTA	9.6	10.7	11.7	18.8	20	19.7	25.1	26	24.2
D=40 cm + ATA	0.6	0.6	1.1	7.6	8.6	8.5	12.2	12.7	12.2

Table 47: *Required NTN UE ACS for each orbit in scenario 5 and for each simulated technique for the 5th percentile throughput loss criterion*

Elevation	Nadir			45° elevation			30° elevation		
Orbit	LEO600	LEO1200	GEO	LEO600	LEO1200	GEO	LEO600	LEO1200	GEO
No technique	NV	NV	NV	NV	NV	NV	NV	NV	NV
BTA	NV	NV	NV	NV	NV	NV	NV	NV	NV
ATA	24.2	26	27.1	28.4	29.9	28.9	NV	NV	NV
D=40 cm	31.9	35.2	NV	NV	NV	NV	NV	NV	NV
D=40 cm + BTA	20.6	21.3	22.7	NV	NV	NV	NV	NV	NV
D=40 cm + ATA	9.6	10.2	11.1	18.2	18.2	18	23.4	23.4	21.3

As mentionned in objective 9, **these results enable to increase the throughput in NTN by 100% with respect to the case of no spectrum coexistence technique without significant degradation on the TN**. Indeed, without spectrum coexistence technique (i.e., without applying ACLR/ACS and transmit power control technique), the average (resp. 5th percentile) throughput loss of the NTN DL would be of about 67% (resp. 100%), whereas we have shown that coexistence technique enables to reduce this throughput loss below 5% for both metrics, while keeping the throughput degradation of the TN below 5%.

14.3.3 Practical challenges associated with proposed TPC algorithms

The TPC techniques described and simulated in the previous Sections enable coexistence between TN DL and NTN DL at 37 GHz (scenario 5) with the considered assumptions, but they have been validated at low technology readiness level. The practical implementation of these techniques would require addressing several key challenges:

1. **Impact on the TN throughput**. Both techniques aim to decrease the transmit power of the BS, reducing thus the TN throughput. While this degradation is kept below 5%, further investigation is needed to determine if this level of degradation is acceptable in practical scenarios.
2. **SINR estimation**. Both techniques rely on knowledge of the SINR without interference from the satellite. While we have proposed methods to estimate it, futher studies are required to assess the feasibility and accuracy of these methods in real-world context.
3. **Modulation and coding schemes**. The transmit power levels are determined based on the truncated Shannon capacity. However in practice, the BS uses practical modulation and coding schemes, which complicates the resource allocation. This requires further exploration to understand the practical implications on system performance.
4. **Dynamic user scheduling**. The current TPC procedures assume that only one UE is scheduled per cell, resulting in a fixed SINR. Extending this to a more realistic scenario with a time-varying number of scheduled UEs per cell presents significant complexity and requires additional investigation.
5. **Iterative ATA technique**. The ATA technique is iterative and requires several communication between the TN BS and TN UE, leading to potential latency and signalling overhead. Further studies are needed to quantify whether these increases in latency and overhad are acceptable in practical systems.

14.4 CONCLUSION

This section provided coexistence results between TN and NTN in the Q/V-band. We identified that:

1- The “compliance with standard” technique enables to fulfil the 3GPP maximum throughput loss requirements for seven scenarios out of the eight.
2- For scenario 5 in which the aggressor is the TN BS and the victim is the NTN DL, additional coexistence technique is required to define a finite value for NTN UE ACS.

We thus evaluated five additional coexistence techniques for this scenario. These techniques include increasing the NTN UE antenna diameter, and transmit power control of the BS. Each technique has been simulated for the three different orbits and three elevations for scenario 5, yielding a total number of simulations of $\#\text{simulation} = 48 + 5 * 3 * 3 = 93$, in which the first term in the sum (e.g. 48) corresponds to the fact that we simulate for the “compliance with standards technique” four scenarios for one elevation and four scenarios with three elevations, each for three different orbits, resulting into 3(4+4*3)=48 simulations for this technique.

These studies enabled us to find ACLR and ACS values for the satellite and NTN UE to fulfil the 3GPP requirements, that are summarized in ***Table 48***, in which NV means that no admissible value can be found. The required NTN UE ACS depends on the implemented coexistence technique:

1- If no coexistence technique is used, then there is no finite NTN UE ACS value enabling coexistence because of scenario 5.
2- If the ATA algorithm described in Section 14.3.1.3 is implemented and the NTN UE antenna diameter is set to 15cm, a NTN UE ACS of 30dB could be chosen.
3- If the ATA algorithm is implemented and the NTN UE antenna diameter is set to 40cm, then a NTN UE ACS of 19dB could be chosen.

Remark 1: using a 15 cm antenna aperture result in an ACS of 30 dB when ATA is implemented. The reason why we try to find a viable solution to decrease ACS is because the implementation of the VSAT UE is more costly when the ACS is too high, due to the required extra filtering. One solution to decrease the required ACS is to increase UE antenna aperture, as observed in 2.

Remark 2: WP3 assumes a 20 by 10 cm NTN UE antenna, resulting into an area of 200 cm². The assumption of a circular antenna of 15 cm diameter in the present document corresponds to an area of $(7.5)^2\pi = 178$ cm², which is close to the assumption from WP3.

Remark 3: the satellite ACLR value resulting from the coexistence study between TN and NTN is 0dB. However, in practice, this ACLR should be set to a higher value to account for interference when e.g. two satellites operate on adjacent bands. For instance, we observed in Section 16 that a strictly positive ACIR is required to enable coexistence between a GEO and a LEO satellite, yielding a strictly positive ACLR value for the satellite, equal to $ACLR = \frac{1}{\frac{1}{ACIR} - \frac{1}{ACS}}$.

The requirements provided in ***Table 48*** could be lowered by applying MMSE-IRC, as mentioned in Section 13.5. For instance, if the NTN UE implements MMSE-IRC with a rejection capability of 5dB, then the required NTN UE ACS could be 5dB lower.

Table 48: *required ACLR and ACS for the satellite and the NTN UE to enable TN-NTN coexistence in the Q/V-band*

	Value result for TN-NTN coexistence
Satellite ACLR	0
Satellite ACS	19
NTN UE ACLR	20
NTN UE ACS	NV if no technique is used 30dB if ATA is used at the BS and NTN UE antenna diameter is 15 cm 19dB if ATA is used at the TN BS and NTN UE antenna diameter is 40cm

15 COEXISTENCE SIMULATION RESULTS IN THE C-BAND

15.1 INTRODUCTION

This section provides the coexistence simulation results for scenarios 7 and 8 in the C-band, that were identified as “high priority” scenario in ***Table 9***. As it will be seen, none of these scenarios require additional coexistence technique, i.e., the “compliance with standards” technique from Section 8.1 coexistence technique enables finding admissible ACIR values fulfilling the maximum throughput loss requirement.

The rest of this section is organized as follows. Section 15.2 provides the coexistence results with respect to ACIR, and section 15.3 provides the conclusions.

15.2 COMPLIANCE WITH STANDARDS

In what follows, Section 15.2.1 and Section 15.2.2 provide the coexistence simulation results for scenario 7 and 8, respectively.

15.2.1 Scenario 7 (Aggressor: NTN DL, Victim: TN UL)

It has been found by simulations that an ACIR equal to 0dB is enough to fulfil the 3GPP coexistence requirements detailed in Section 13.6 for the three different orbits and the three different elevations.

15.2.2 Scenario 8 (Aggressor: TN UL, Victim: NTN DL)

Figure 66 to ***Figure 71*** depict the average and 5th percentile throughput loss for coexistence scenario 8 in the C-band for LEO@600km, LEO@1200km, and GEO orbits, at Nadir, 45° and 30° elevation, as a function of the ACIR. The vertical line at 30 dB represents the ACLR of the TN UE in the C-band provided in ***Table 40***, which is an upper bound on the maximum admissible ACIR as discussed in Section 13.5. One can observe that the maximum throughput loss requirements can be achieved for the three orbits and for the three considered elevations for admissible ACIR values, i.e., for ACIR values lower than the TN UE ACLR.

Table 49 provides the required ACIR and resulting ACS values for the NTN UE for scenario 8 ensuring that both the average and the 5th percentile maximum throughput loss requirements are fulfilled. **One can observe that a NTN UE ACS of 22.1dB enables to fulfil these requirements for the three different orbits and for the three simulated elevations**.

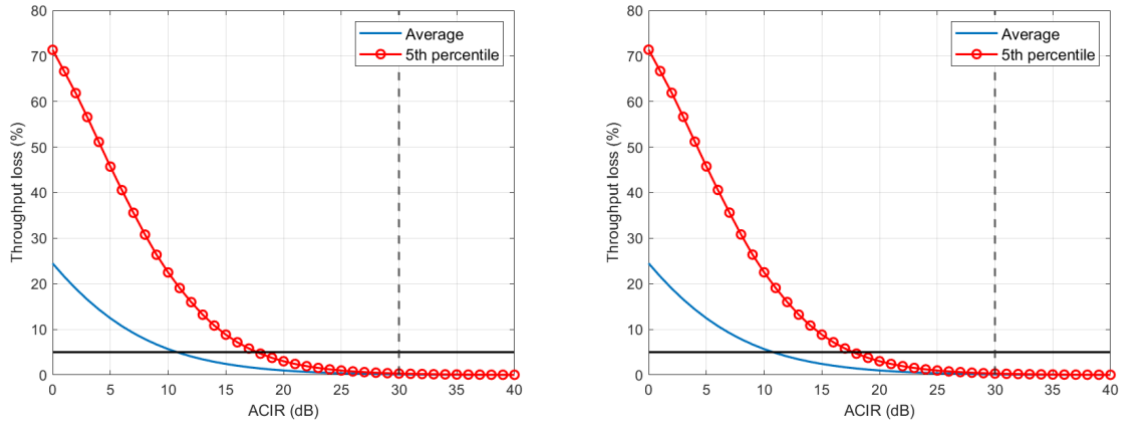

Figure 66: *AVERAGE and 5th percentile THROUGHPUT LOSS in coexistence SCENARIO 8 in the C-band FOR LEO@600 (LEFT) AND LEO@1200 (RIGHT) orbits at nadir*

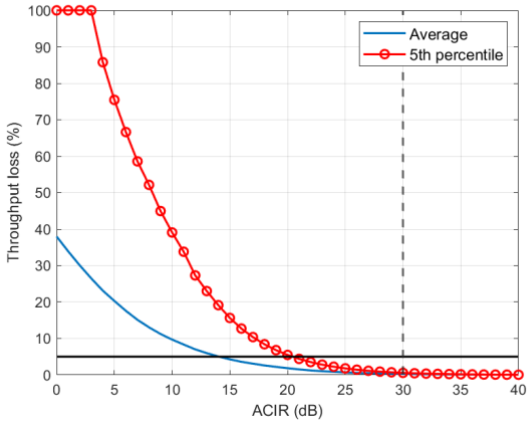

Figure 67: *AVERAGE AND 5TH PERCENTILE THROUGHPUT LOSS IN COEXISTENCE SCENARIO 8 IN THE C-BAND FOR GEO ORBIT AT NADIR*

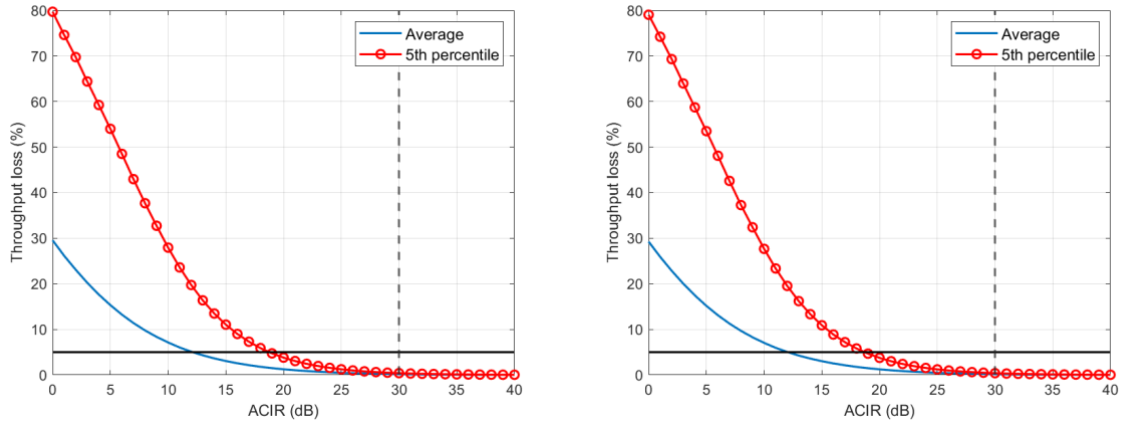

Figure 68: *AVERAGE AND 5TH PERCENTILE THROUGHPUT LOSS IN COEXISTENCE SCENARIO 8 IN THE C-BAND FOR LEO@600 (LEFT) AND LEO@1200 (RIGHT) ORBITS AT 45° ELEVATION*

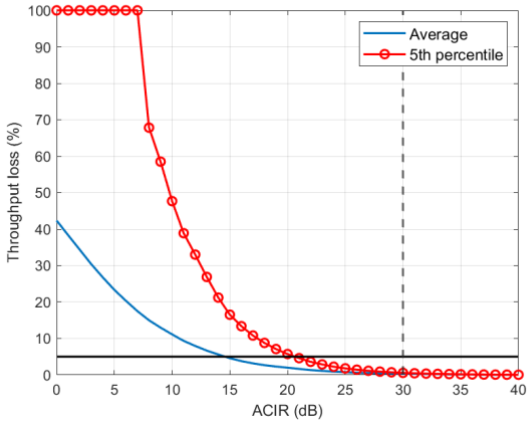

Figure 69: *AVERAGE AND 5TH PERCENTILE THROUGHPUT LOSS IN COEXISTENCE SCENARIO 8 IN THE C-BAND FOR GEO ORBIT AT 45° ELEVATION*

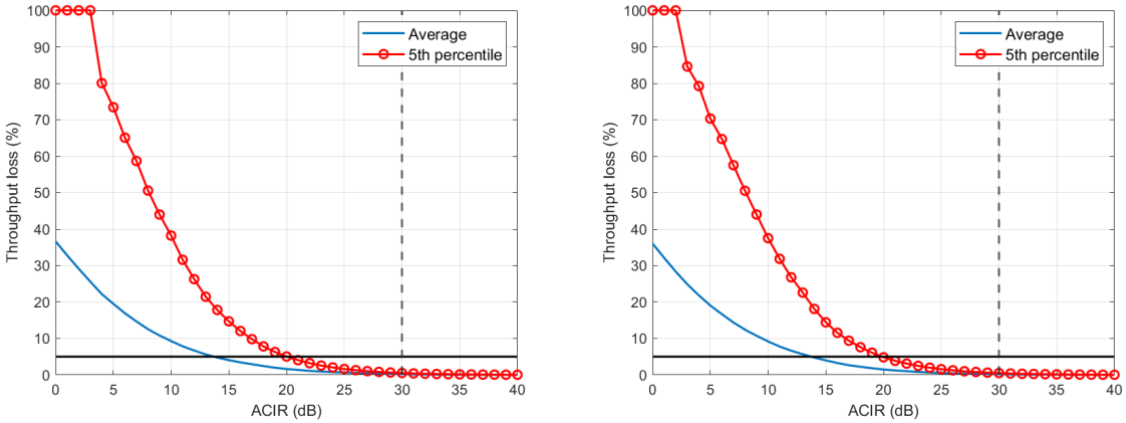

Figure 70: *AVERAGE AND 5TH PERCENTILE THROUGHPUT LOSS IN COEXISTENCE SCENARIO 8 IN THE C-BAND FOR LEO@600 (LEFT) AND LEO@1200 (RIGHT) ORBITS AT 30° ELEVATION*

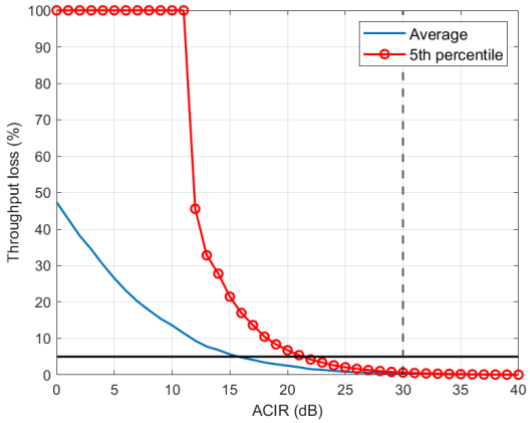

Figure 71: *AVERAGE AND 5TH PERCENTILE THROUGHPUT LOSS IN COEXISTENCE SCENARIO 8 IN THE C-BAND FOR GEO ORBIT AT 30° ELEVATION*

Table 49: *Required acir and resulting ntn ue acs (both in db) in the c-band for the three orbits and the three considered elevations for scenario 8*

Elevation	**Nadir**			**45° elevation**			**30° elevation**		
Orbit	LEO600	LEO1200	GEO	LEO600	LEO1200	GEO	LEO600	LEO1200	GEO
ACIR	17.7	17.7	20.5	18.8	18.7	20.7	20	19.9	21.4
NTN UE ACS	18	18	21.1	19.2	19.1	21.3	20.5	20.4	22.1

15.2.3 Intermediate conclusion

The main observations from the two previous sections can be summarized as follows:

1. A satellite ACLR value of 0dB enables to fulfil the maximum throughput loss requirements in scenario 7.
2. A NTN UE ACS value of 22.1dB enables to fulfil the maximum throughput loss requirements in scenario 8.

Furthermore, using the same reasoning as in Section 14.3.2, one can highlight that as mentioned in objective 9, these results enable to increase the throughput in NTN by 100% with respect to the case of no spectrum coexistence technique without degradation for the TN.

15.3 CONCLUSION

This section provided coexistence results between TN and NTN in the C-band for scenarios 7 and 8. Both these scenarios have been simulated for three different orbits and three different elevations, yielding in total $\#\text{simulations} = 3 * 2 * 3 = 18$.

We identified that the “compliance with standard” technique is enough to fulfil the 3GPP maximum throughput loss requirements for both scenarios.

Table 50 provides the required satellite ACLR and NTN UE ACS in dB enabling coexistence for scenarios 7 and 8 in the C-band. To define final ACLR and ACS values of satellite and NTN UE to ensure TN-NTN coexistence for all interference scenarios in C-band, the study of other coexistence scenarios and combining all the results is required.

Table 50: *required satellite ACLR and NTN UE ACS in the C-band to enable coexistence for scenarios 7 and 8*

Parameter	Value
Satellite ACLR	0
NTN UE ACS	22.1

The requirements provided in ***Table 50*** could be lowered by applying MMSE-IRC, as mentioned in Section 13.5. For instance, if the NTN UE implements MMSE-IRC with a rejection capability of 5dB, then the required NTN UE ACS could be 5dB lower.

16 TWO LAYERS SATELLITE STUDY

16.1 INTRODUCTION

This section studies the coexistence between a GEO and a LEO@600 satellite operating in the Q/V-band, considering both cochannel interference and interference between adjacent channels.

One conventional approach to enable spectrum sharing between satellites in different orbital layers is to define an exclusion angle [32]. This angle represents the minimum separation between the boresight of the GEO and LEO satellites below which interference leads to significant performance degradation for either system. Also known as “GEO arc avoidance” in the literature [35], determining an appropriate exclusion angle is crucial prior to deploying new LEO satellite constellations alongside existing GEO satellites. This section aims to define exclusion angles that ensure coexistence between GEO and LEO@600 satellites by considering the 3GPP maximum throughput loss requirements from Section 13.6 as the performance metric.

While conventional studies in the literature have primarily focused on exclusion angles for cochannel interference, this section expands the analysis to include adjacent channel interference, thus yielding an exclusion angle which is a function of the ACIR.

Remark: other coexistence techniques such as beam steering [33] or coordinated beam hopping [34] could be used to improve the coexistence between GEO and LEO satellite, but they are beyond the scope of the present study.

The rest of this section is organized as follows. Section 16.2 describes the considered coexistence scenario. Section 16.3 is dedicated to numerical results. Finally, Section 16.4 provides conclusions. Part of the material presented in this section has been published in [37].

16.2 SCENARIO DESCRIPTION

16.2.1 General considerations

We study the coexistence between a GEO satellite located at Nadir and a LEO@600 satellite with elevation α. We assume that the two satellites are pointing towards the same point on the Earth surface, i.e., the coordinates of the center of the beam of each satellite is the same. We assume that each satellite is associated with a different NTN UE, whose location on the surface of the Earth is discussed in the next Section 16.2.2.

16.2.2 NTN UE location

We consider the following two hypothesis regarding the two NTN UE location:

1- The two NTN UE are collocated at the center of the beam. Such an assumption is also considered in [35] and corresponds to a worst case scenario in terms of interference. This assumption will be referred to as “deterministic UE location” (DUEL) in the rest of this section.

2- Each NTN UE is randomly located inside the beam of its associated satellite, i.e., the NTN UE associated with the GEO (resp. the LEO) satellite is randomly dropped in the GEO (resp. the LEO) beam. This assumption will be referred to as “random UE location” (RUEL) in the rest of this section.

The DUEL assumption with the two NTN UE collocated at the center of the beam is depicted on the left in ***Figure 72***, wheras the RUEL assumption is illustrated on the right in the same figure. We also illustrated in the right of the figure that the center of the two beams are collocated, regardless of the NTN UE locations.

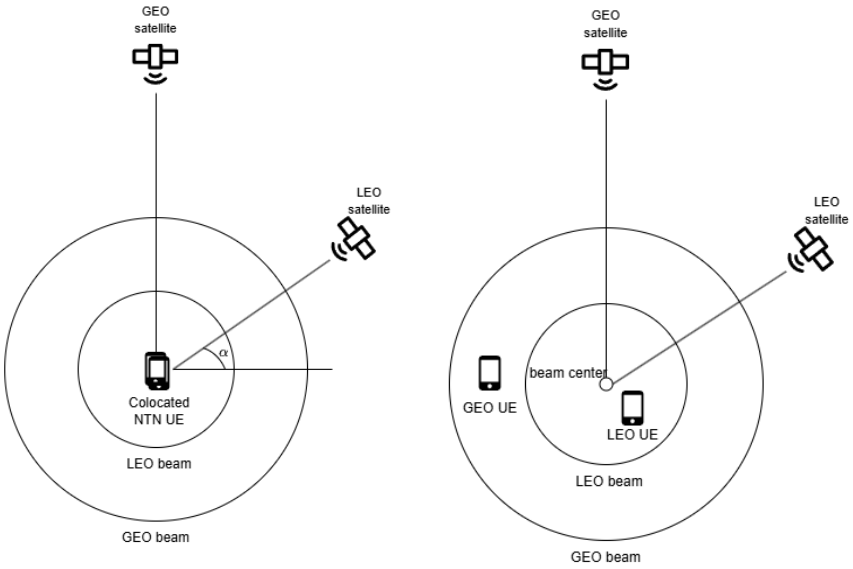

Figure 72: *Illustration of the coexistence scenario for DUEL (left) and RUEL (right) assumptions*

16.2.3 Objectives of the study

The “exclusive angle strategy” consists in defining a minimal separation angle $\phi_{\min}$ between the boresight of both satellites to mitigate the level of inter system interference. Since we assume that the GEO satellite is located a Nadir, defining $\phi_{\min}$ is equivalent to defining a maximum elevation $\alpha_{\max}$ for the LEO satellite and then deduce $\phi_{\min} = \frac{\pi}{2} - \alpha_{\max}$ (see ***Figure 72***).

This study has two objectives:

1. Establishing the exclusion angle that allows both satellite to operate using the same communication channels.
2. Establising the exclusion angle that allows both satellite to operate using adjacent communication channels.

For the second above objective, the exclusion angle $\phi_{\min}$ is influenced by the ACIR since a higher ACIR corresponds to reduced interference between adjacent channels, thereby allowing a smaller $\phi_{\min}$.

We propose using the performance metrics from Section 13.6 to define $\phi_{\min}$, ensuring that it is defined such that the average and 5th percentile throughput loss caused by inter systems interference remains below 5%.

Table 51 lists the four coexistence scenarios explored in this study in terms of aggressor and victim.

Table 51: *simulated coexistence scenarios in the multi layer satellite context*

Scenario	Aggressor	Victim
S1	LEO DL	GEO DL
S2	GEO DL	LEO DL
S3	LEO UL	GEO UL
S4	GEO UL	LEO UL

16.3 NUMERICAL RESULTS

In what follows, Section 16.3.1 provides the setup of the simulations. Section 16.3.2 and Section 16.3.3 are devoted to the simulation results in the co-channel and adjacent channel interference scenarios, respectively.

16.3.1 Setup

We use the parameters provided in Section 13 for the bandwidth and for the parameters of the satellite and the NTN UE, except that we simulated two values for the NTN UE antenna aperture:

1. $D_1 = 15$ cm.
2. $D_2 = 40$ cm.

Moreover, we performed the simulations with and without the TPC for the UL described in Section 5.3, to study the impact of this mechanism on the coexistence.

16.3.2 Co-channel interference context

In what follows, Sections 16.3.2.1 to 16.3.2.4 provide the simulation results for the four scenarios from ***Table 51***, and Section 16.3.2.5 synthetizes the results.

16.3.2.1 Scenario S1

Figure 73 shows the average and 5th percentile throughput loss versus the LEO satellite elevation for scenario S1 and for both the DUEL and the RUEL assumptions in the cochannel interference context. The left (resp. right) part of the figure represents the loss for NTN UE antenna aperture of $D_1 = 15$ cm (resp. $D_2 = 40$ cm). One can draw the following observations:

1. For the DUEL assumptions, the throughput loss is not a monotonic function of the LEO satellite elevation. The loss curves intersect the 5% line multiple times, suggesting that several values for exclusion angle could be envisonned. **We propose in this study to define the exclusion angle as the angle at which the throughput loss curves first exceeds 5%.**
2. The throughput loss is generally lower under the RUEL assumption than under the DUEL one.
3. Larger antenna result in lower throughput loss, except for LEO elevation close to Nadir. For instance, at 85° elevation for the LEO, the average throughput loss with 15 cm aperture is 11.3% whereas it is almost zero with 40 cm aperture.

The first above observation can be explained due to the fluctuating nature of the Bessel antenna diagram of the NTN UE, see Section 4.3.

The second observation is mainly attributed to the difference in the beam sizes of the two satellites, linked directly to the antenna gain of the LEO satellite decreasing much faster than that of the GEO one when moving away from the center of the beam (as a reminder, the contour of the satellite beam corresponds to the area where the power is halved compared to its center). Thus, the interference level received by a GEO NTN UE located outside the LEO beam is significantly attenuated compared to a GEO NTN UE inside the LEO beam. We quantify in what follows the probability that a GEO NTN UE is located outside the LEO beam, denoted as p_{GIL}, corresponding to setups where its received level of interference is attenuated.

The GEO NTN UE is randomly dropped inside the GEO beam under the RUEL hypothesis, yielding:

$$p_{GIL} = 1 - \frac{A_r^{LEO}}{A_r^{GEO}}$$

where A_r^{GEO} (resp. A_r^{LEO}) is the area of the GEO (resp. LEO) beam. Plugging the values from ***Table 20*** into the above equation yields:

$$p_{GIL} = 1 - \frac{9.85^2}{58.85^2} \approx 0.97$$

There is thus a high probability that the GEO NTN UE under the RUEL hypothesis receives a low level of interference from the LEO satellite, justifying the lower throughput loss under the RUEL hypothesis.

Finally, the third observation can be explained by noting that larger antennas are more directive. Therefore, the throughput loss is generaly lower when the angle between the boresight of the two satellites is sufficiently large. Conversely, when the elevations of the two satellites are very close, the antenna gain approaches its maximum value, which is higher for larger antenna, yielding in the considered setup to a higher throughput loss.

Table 52 provides the exclusion angle for scenario S1 for the two simulated NTN UE antenna diameter and the two assumptions for the NTN UE location. As already observed in ***Figure 73***, larger antennas yield lower exclusion angle, and the exclusion angles under the RUEL assumption are significantly lower than under the DUEL one.

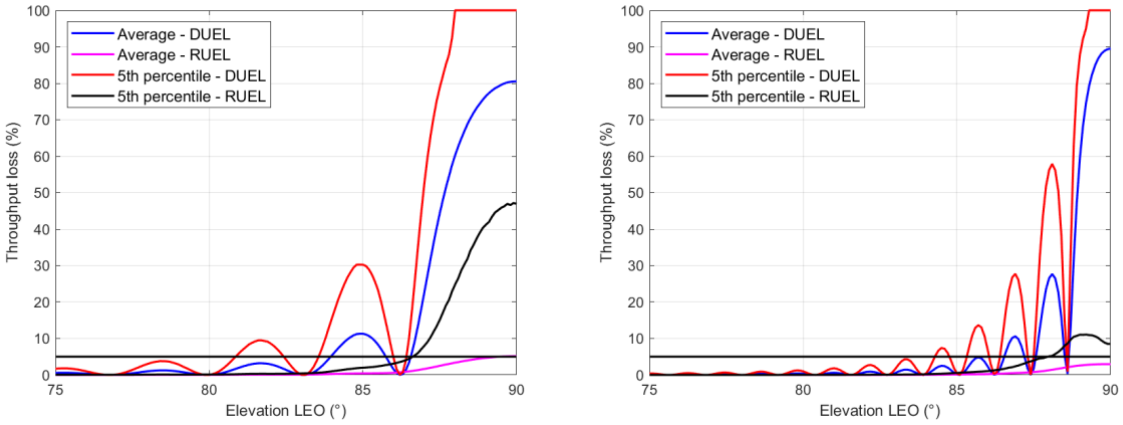

Figure 73: *Average and 5th percentile throughput loss versus the LEO satellite elevation for scenario S1 with NTN antenna aperture of 15cm (left) and 40 cm (right)*

Table 52: exclusion angle ϕ_{min} for scenario S1 for the two simulated NTN UE antenna aperture

Antenna aperture	NTN UE location	ϕ_{min} (°)
D_1	DUEL	9.2
	RUEL	3.4
D_2	DUEL	5.8
	RUEL	2.1

16.3.2.2 Scenario S2

Figure 74 shows the average and 5th percentile throughput loss versus the LEO satellite elevation for scenario S2 and for both the DUEL and the RUEL assumptions in the cochannel interference context. The left (resp. right) part of the figure represents the loss for NTN UE antenna aperture of $D_1 = 15$ cm (resp. $D_2 = 40$ cm). One can observe that unlike in scenario S1 in Section 16.3.2.1, the throughput loss in scenario S2 is not necessarily lower under the RUEL hypothesis than under the DUEL hypothesis. This can be explained because the LEO NTN UE is necessarily dropped inside the GEO beam since the LEO beam is included inside the GEO one, and thus the antenna gain of the GEO satellite involved in the computation of the level of interference is high in the whole LEO beam area (especially since, as discussed in the previous Section 16.3.2.1, the antenna gain of the LEO satellite decreases faster than the GEO one when moving away from the center of the beam).

Table 53 provides the exclusion angle for scenario S2 for the two simulated NTN UE antenna diameter and the two assumptions for the NTN UE location. One can see that the exclusion angle under both assumptions for the NTN UE location are similar. One can also see that, as expected, larger antenna yields once again lower exclusion angles.

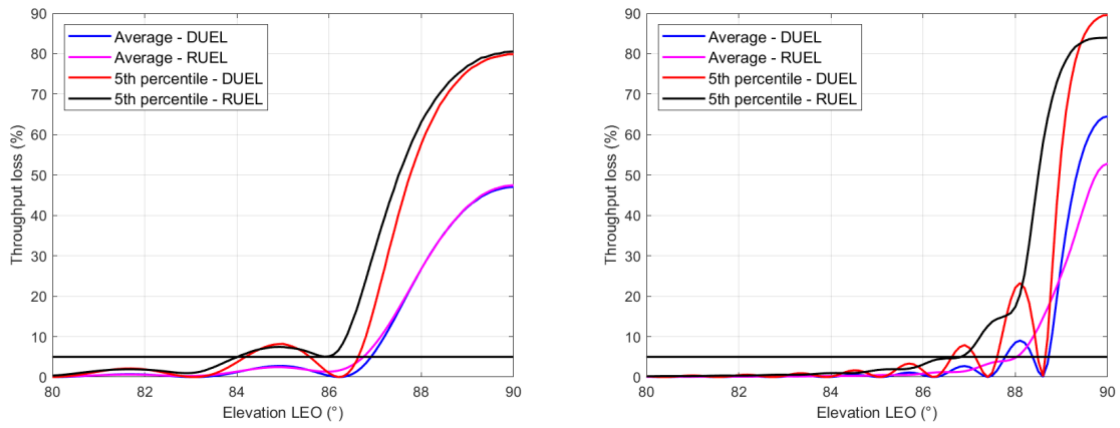

Figure 74: AVERAGE AND 5TH PERCENTILE THROUGHPUT LOSS VERSUS THE LEO SATELLITE ELEVATION FOR SCENARIO S2 WITH NTN ANTENNA APERTURE OF 15CM (LEFT) AND 40 CM (RIGHT)

Table 53: exclusion angle ϕ_{min} for scenario S2 for the two simulated NTN UE antenna aperture

Antenna aperture	NTN UE location	ϕ_{min} (°)
D_1	DUEL	5.9
	RUEL	6
D_2	DUEL	3.4
	RUEL	3.2

16.3.2.3 Scenario S3

Figure 75 shows the average and 5th percentile throughput loss versus the LEO satellite elevation for scenario S3 and for both the DUEL and the RUEL assumptions, with and without TPC, in the cochannel interference context. The plain (resp. dot) curves correspond to the setup without (resp. with) TPC. The left (resp. right) part of the figure represents the loss for NTN UE antenna aperture of $D_1 = 15$ cm (resp. $D_2 = 40$ cm). One can observe that the TPC reduces the throughput loss in the different simulated setups, which can be explained because the LEO NTN UE is located close to the center of the beam and thus creates a high level of interference, which is mitigated when using TPC. In addition, the LEO@600 satellite is much closer to the Earth than the GEO satellite, and thus the LEO satellite reduces its transmit power much more than the GEO NTN UE, reducing thus the level of interference.

Table 54 provides the exclusion angle for scenario S3 for the two simulated NTN UE antenna diameter and the two assumptions for the NTN UE location, with and without TPC. As previously discussed, the use of TPC reduces the exclusion angles. One can also observe that the exclusion angles under DUEL and RUEL hypothesis are close.

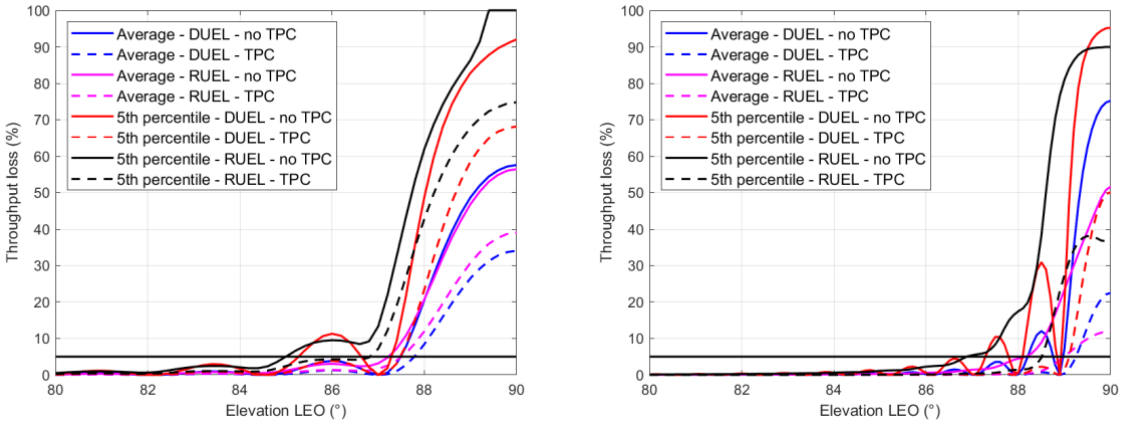

Figure 75: *AVERAGE AND 5TH PERCENTILE THROUGHPUT LOSS VERSUS THE LEO SATELLITE ELEVATION FOR SCENARIO S3 WITH NTN ANTENNA APERTURE OF 15CM (LEFT) AND 40 CM (RIGHT)*

Table 54: *exclusion angle ϕ_{min} for scenario S3 for the two simulated NTN UE antenna aperture, with and without TPC*

Antenna aperture	NTN UE location	TPC	ϕ_{min} (°)
D_1	DUEL	NO	4.8
		YES	2.6
	RUEL	NO	5.1
		YES	3.2
D_2	DUEL	NO	2.8
		YES	0.9
	RUEL	NO	3.2
		YES	1.5

16.3.2.4 Scenario S4

Figure 76 shows the average and 5th percentile throughput loss versus the LEO satellite elevation for scenario S4 and for both the DUEL and the RUEL assumptions, with and without TPC, in the cochannel interference context. The left (resp. right) part of the figure represents the loss for NTN UE antenna aperture of $D_1 = 15$ cm (resp. $D_2 = 40$ cm). One can observe that unlike for scenario S3 in Section 16.3.2.3, using TPC is counterproductive since it increases the throughput loss. This can be explained because i) the distance with the GEO satellite is large and thus the transmit power reduction of the GEO NTN UE is low, and ii) as discussed in the previous Section 16.3.2.3, the transmit power reduction of the LEO NTN UE

is much more important. As a consequence of (ii), the reference throughput of the LEO UL (i.e., the throughput without the interference from the GEO UL) is lower when using TPC, and interference are more detrimental in the low throughput regime due to the logarithmic nature of the Shannon capacity. Moreover, the level of interference with and without TPC is almost the same due to (i), thus explaining why TPC is counterproductive in this scenario.

Table 55 provides the exclusion angle for scenario S4 for the two simulated NTN UE antenna diameter and the two assumptions for the NTN UE location, with and without TPC. One can see that the exclusion angles are much lower under the RUEL hypothesis than under the DUEL hypothesis, which is due to the GEO NTN UE that might be located outside the LEO beam, producing thus a lower level of interference on the LEO UL in these cases.

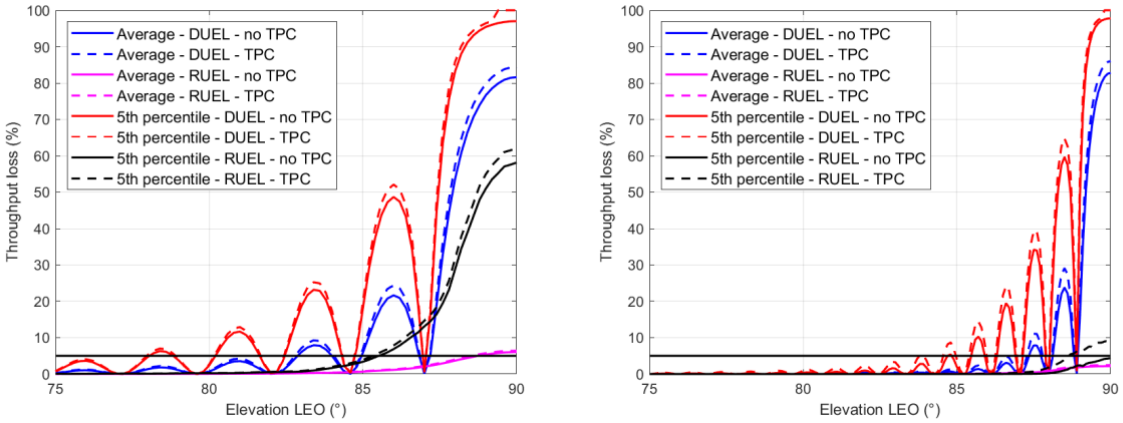

Figure 76: *AVERAGE AND 5TH PERCENTILE THROUGHPUT LOSS VERSUS THE LEO SATELLITE ELEVATION FOR SCENARIO S4 WITH NTN ANTENNA APERTURE OF 15CM (LEFT) AND 40 CM (RIGHT)*

Table 55: *exclusion angle ϕ_{min} for scenario S4 for the two simulated NTN UE antenna aperture, with and without TPC*

Antenna aperture	NTN UE location	TPC	$\phi_{\min}$ (°)
D_1	DUEL	NO	12
		YES	12.1
	RUEL	NO	4.5
		YES	4.7
D_2	DUEL	NO	5.4
		YES	6.3
	RUEL	NO	0
		YES	1.4

16.3.2.5 Synthesis

The main observations from the previous sections can be summarized as follows:

1. Larger antenna enables to chose lower value for the exclusion angle.
2. The RUEL assumption yields lower value for the exclusion angle, which was expected since the DUEL assumption is a worst case in terms of interference.
3. The TPC enables to chose lower value for the exclusion angle in scenario S3, but not in S4.

Table 56 provides the exclusion angles enabling to fulfil the maximum throughput loss requirements for the two considered NTN UE antenna aperture, for the two assumptions for the NTN UE location, with and without TPC. For each configuration, the table provides in the last column the scenario driving the found value for the exclusion angle, i.e., the scenario with

the highest exclusion angle for a given tuple (antenna aperture, NTN UE location assumption, TPC UL).

Table 56: *summary of the found exclusion angles*

Antenna aperture	NTN UE location	TPC UL	$\phi_{\min}$ (°)	Driven by
D_1	DUEL	NO	12	S4
		YES	12.1	
	RUEL	NO	6	S2
		YES	6	
D_2	DUEL	NO	5.7	S1
		YES	6.3	S4
	RUEL	NO	3.2	S2/S3
		YES	3.2	S2

16.3.3 Adjacent channel interference context

In what follows, Sections 16.3.3.1 to 16.3.3.4 provide the simulation results for the four scenarios from ***Table 51***, and Section 16.3.3.5 synthetizes the results.

16.3.3.1 Scenario S1

Figure 77 shows the maximum value of the LEO satellite elevation at which the maximum throughput loss requirements are fulfilled as a function of the ACIR for scenario S1 and for both the DUEL and the RUEL assumptions in the adjacent channel interference context. The left (resp. right) part of the figure provides the results for NTN UE antenna aperture of $D_1 = 15$ cm (resp. $D_2 = 40$ cm). One can draw the following observations:

1. As expected, the higher the ACIR, the higher the maximum LEO elevation.
2. For a given elevation, the required ACIR is lower under the RUEL assumption than under the DUEL one. This can be explained using the same reasoning regarding the size of the beam as in the co-channel interference context in Section 16.3.2.1.
3. For ACIR=0dB, one can retrieve the same results as for the co-channel interference context provided in Section 16.3.2.1, i.e., the maximum elevation for e.g. D_1 under the DUEL assumption is 80.8°, which is in agreement with the results provided in ***Table 52***.
4. The curves related to D_1 (left) and D_2 (right) cross each other under the DUEL assumption, which is illustrated in ***Figure 78*** in which we plot the maximum value of the LEO satellite elevation at which the maximum throughput loss requirements are fulfilled as a function of the ACIR for scenario S1 under the DUEL assumption and for both NTN UE antenna aperture. This behaviour can be explained using the same reasoning as in Section 16.3.2.1 in the co-channel interference context: larger antenna are more directive and thus lower ACIR is required when the LEO elevation is sufficiently far from the Nadir. On the other hand, when the LEO satellite is close to nadir, the level of interference experienced by the NTN UE increases with the NTN UE antenna size, and thus larger ACIR is required.

Such curves should be of interest for system designer, for instance assuming that the satellite and NTN UE hardware imposes a maximum value of 5 dB for the ACIR, then one can observe that, under the DUEL assumption, the maximum value of the LEO satellite elevation is about 84° for D_1 cm and 86.9° for D_2.

To explain the stepwise behavior of the curves, we plot as an example in ***Figure 79*** the required ACIR versus the LEO satellite elevation for scenario S1 and with NTN UE antenna

aperture of D_1. One can infer that the maximum elevation gradually increases from 80.8° to 81.6° for ACIR between 0 and 3.1 dB for the 5th percentile metric. Then, the maximum elevation jumps to 83.7° as soon as the ACIR is greater than 3.2 dB, explaining the behaviour observed in ***Figure 77***.

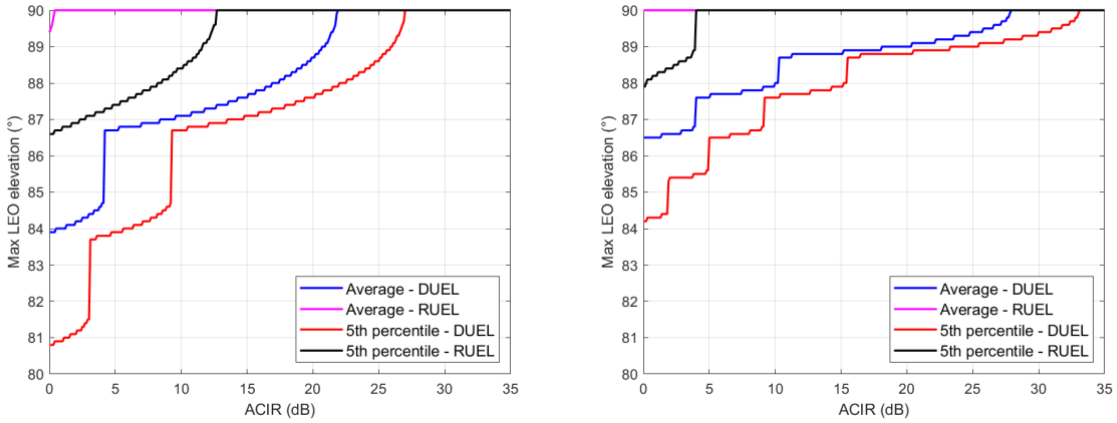

Figure 77: *LEO maximum elevation value at which the maximum throughput loss requirements are fulfilled as a function of the ACIR FOR SCENARIO S1 WITH NTN ANTENNA APERTURE OF 15CM (LEFT) AND 40 CM (RIGHT)*

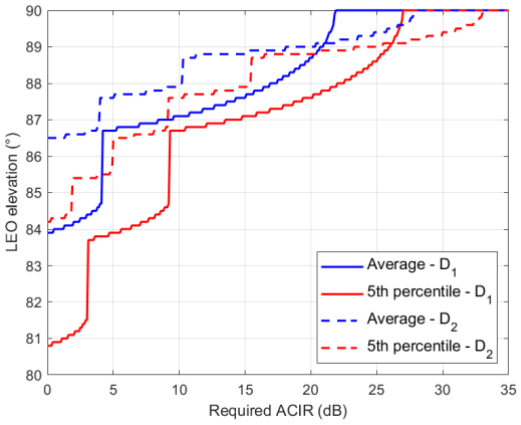

Figure 78: *superposing the LEO MAXIMUM ELEVATION VALUE AT WHICH THE MAXIMUM THROUGHPUT LOSS REQUIREMENTS ARE FULFILLED AS A FUNCTION OF THE ACIR FOR SCENARIO S1 for both NTN ANTENNA APERTURE under the duel assumption*

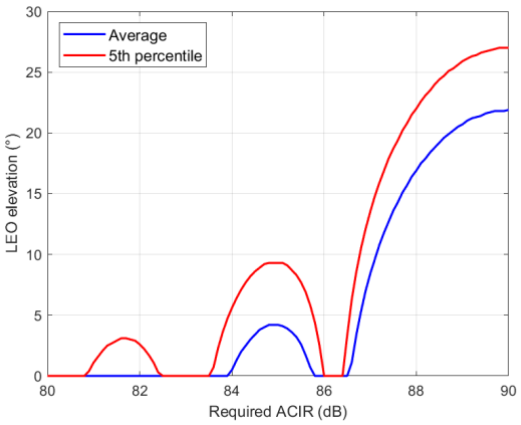

Figure 79: *ACIR value ensuring that the maximum throughput loss requirements are fufilled for scenario S1 with NTN UE antenna aperture of 15cm*

Table 57: REQUIRED ACIR TO FULFIL THE MAXIMUM THROUGHPUT LOSS REQUIREMENTS when the LEO satellite is AT NADIR FOR SCENARIO S1

Antenna aperture	NTN UE location	ACIR (dB)
D_1	DUEL	27
	RUEL	12.7
D_2	DUEL	33.1
	RUEL	4

16.3.3.2 Scenario S2

Figure 80 shows the maximum value of the LEO satellite elevation at which the maximum throughput loss requirements are fulfilled as a function of the ACIR for scenario S1 and for both the DUEL and the RUEL assumptions in the adjacent channel interference context. The left (resp. right) part of the figure provides the results for NTN UE antenna aperture of $D_1 = 15$ cm (resp. $D_2 = 40$ cm). As observed for the co-channel interference setup in Section 16.3.2.2, one can see that there is no clear performance difference between the DUEL and the RUEL assumptions for this scenario since the different curves cross each other several times.

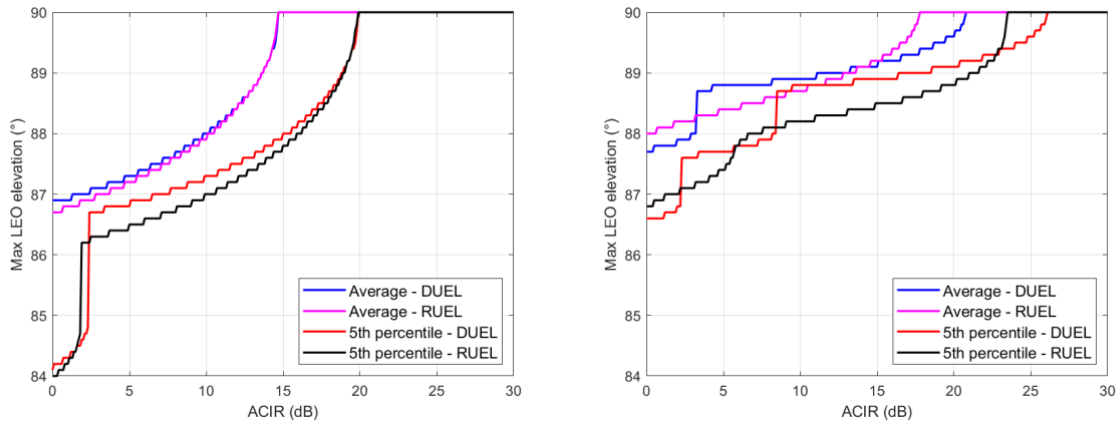

Figure 80: LEO maximum elevation value at which the maximum throughput loss requirements are fulfilled as a function of the ACIR FOR SCENARIO S2 WITH NTN ANTENNA APERTURE OF 15CM (LEFT) AND 40 CM (RIGHT)

Table 58: REQUIRED ACIR TO FULFIL THE MAXIMUM THROUGHPUT LOSS REQUIREMENTS when the LEO satellite is AT NADIR FOR SCENARIO S2

Antenna aperture	NTN UE location	ACIR (dB)
D_1	DUEL	19.9
	RUEL	19.9
D_2	DUEL	26.1
	RUEL	23.5

16.3.3.3 Scenario S3

Figure 81 shows the maximum value of the LEO satellite elevation at which the maximum throughput loss requirements are fulfilled as a function of the ACIR for scenario S1 and for both the DUEL and the RUEL assumptions in the adjacent channel interference context. The left (resp. right) part of the figure provides the results for NTN UE antenna aperture of $D_1 = 15$ cm (resp. $D_2 = 40$ cm). One can observe that TPC reduce the required ACIR value for a given LEO elevation, or conversaly, that for a given ACIR value, the maximum elevation at which the LEO can transmit is larger. This observation can be explained using the same reasoning as in the cochannel interference setup in Section 16.3.2.3.

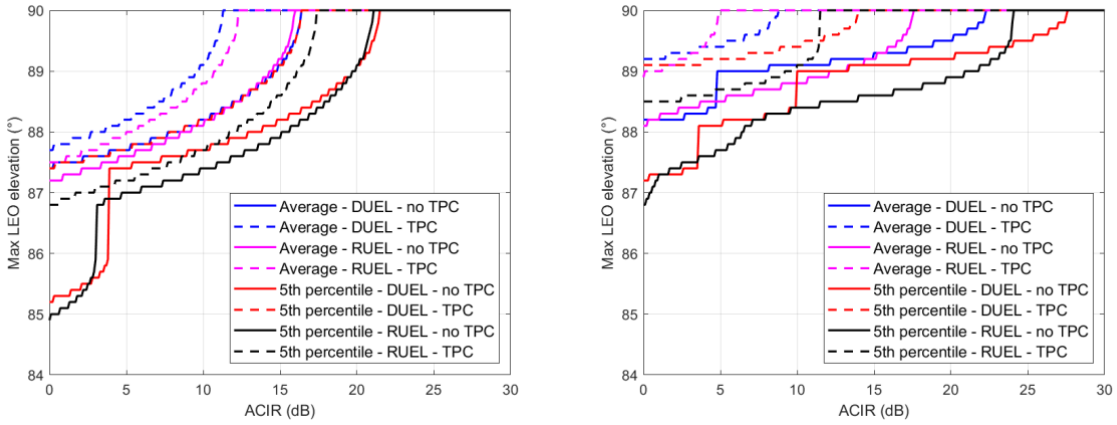

Figure 81: *LEO MAXIMUM ELEVATION VALUE AT WHICH THE MAXIMUM THROUGHPUT LOSS REQUIREMENTS ARE FULFILLED AS A FUNCTION OF THE ACIR FOR SCENARIO S3 WITH NTN ANTENNA APERTURE OF 15CM (LEFT) AND 40 CM (RIGHT)*

Table 59: REQUIRED ACIR TO FULFIL THE MAXIMUM THROUGHPUT LOSS REQUIREMENTS when the LEO satellite is AT NADIR FOR SCENARIO S3

Antenna aperture	NTN UE location	TPC	ACIR (dB
D_1	DUEL	NO	21.5
		YES	16.4
	RUEL	NO	21.1
		YES	17.4
D_2	DUEL	NO	27.6
		YES	14
	RUEL	NO	24.1
		YES	11.5

16.3.3.4 Scenario S4

Figure 82 shows the maximum value of the LEO satellite elevation at which the maximum throughput loss requirements are fulfilled as a function of the ACIR for scenario S1 and for both the DUEL and the RUEL assumptions in the adjacent channel interference context. The left (resp. right) part of the figure provides the results for NTN UE antenna aperture of $D_1 = 15$ cm (resp. $D_2 = 40$ cm)

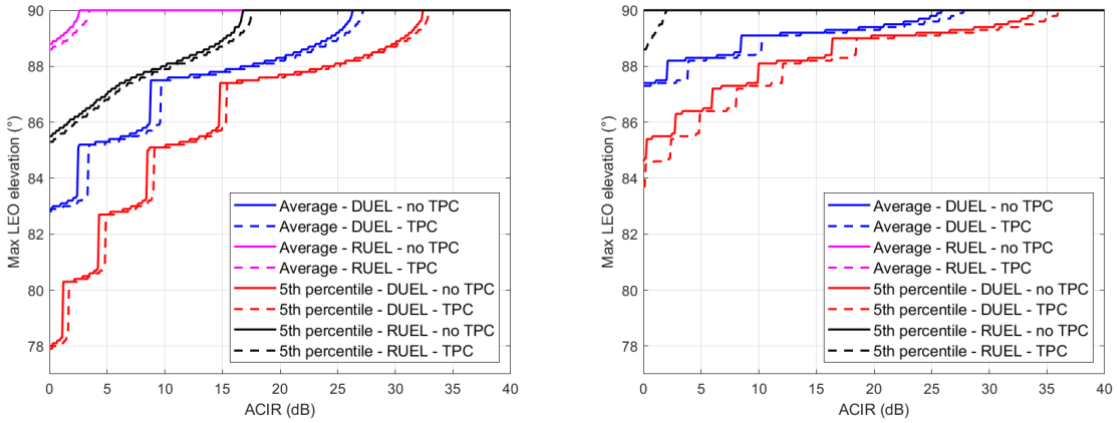

Figure 82: *LEO MAXIMUM ELEVATION VALUE AT WHICH THE MAXIMUM THROUGHPUT LOSS REQUIREMENTS ARE FULFILLED AS A FUNCTION OF THE ACIR FOR SCENARIO S4 WITH NTN ANTENNA APERTURE OF 15CM (LEFT) AND 40 CM (RIGHT)*

Table 60: REQUIRED ACIR TO FULFIL THE MAXIMUM THROUGHPUT LOSS REQUIREMENTS when the LEO satellite is AT NADIR FOR SCENARIO S4

Antenna aperture	NTN UE location	TPC	ACIR (dB
D_1	DUEL	NO	32.4
		YES	32.9
	RUEL	NO	16.8
		YES	17.7
D_2	DUEL	NO	33.9
		YES	36
	RUEL	NO	0
		YES	2

16.3.3.5 Synthesis

The main observations from the previous sections are similar to those in the adjacent channel interference setup. These simulations enabled us to deduce the exclusion angle for a given ACIR value. For instance, if the hardware impose a constraint on the maximum achievable ACIR, then these curves enable to deduce the corresponding exclusion angle.

16.4 CONCLUSION

This section provided coexistence results between GEO and LEO@600 satellites in the Q/V-band in both the co-channel interference and the interference between adjacent channel setups. We simulated four different scenarios dependending on the aggressor and the victim. For each scenario, we simulated two different NTN UE antenna aperture, and two assumptions for the NTN UE location. Moreover, for the two UL scenarios, we performed simulations with and without TPC. Thus, the total number of performed simulations for each value of the LEO elevation angle is $\#\text{simulations} = 2 * (2 + 4) = 12$, and we simulated all the LEO elevation between 75 and 90 degrees by step 0.1 degree.

The simulations in the co-channel interference setup enabled us to provide recommendations for the exclusion angles ensuring that the maximum throughput loss requirements of the 3GPP are fulfilled for the four different scenarios.

The simulations in the adjacent channel interference setup provide a matching between the ACIR value and the corresponding exclusion angle. The higher the ACIR, the lower the exclusion angle, and the longer the LEO satellite can transmit, thus increasing its throughput. As a consequence, it is of interest to choose the lowest exclusion angle depending on the achievable ACIR.

All these results should be of interest for system designers, to chose appropriate exclusion angle prior to deploying new LEO constellations on top of existing GEO ones.

17 CONCLUSION

The first version of this deliverable, i.e., D4.3, provided an initial set of parameters for both TN and NTN. The next version, i.e., D4.7, provided calibration results of the simulators implemented independently by the different partners from the task. D4.7 also provided a new VSAT model for phased array system, and updates for the SAN parameters. The present and final version of the deliverable, i.e., D4.8, provided coexistence simulation results between TN and NTN, and between two NTN layers for two frequency bands.

For the coexistence between TN and NTN on adjacent channels:

1. In the Q/V-band, we simulated eight different coexistence scenarios. We observed through simulations that:

    a. The maximum throughput loss requirements for coexistence can be fulfilled in seven out of the eight considered scenarios using the “compliance with standard” coexistence technique, i.e., by defining appropriate ACLR and ACS values for the NTN UE and satellite.

    b. However, one scenario has been identified as more difficult than the other ones, i.e., scenario 5 in which the aggressor is the TN DL and the victim is the NTN DL. The “compliance with standard” coexistence technique did not enable to fulfill the maximum throughput loss requirements for this scenario, and thus additional coexistence techniques were required. We proposed different coexistence techniques to resolve the issue:

        i. We investigated a coexistence technique that increases NTN UE gain by increasing the NTN UE antenna aperture and demonstrated a great improvement to enable meeting the coexistence requirements for scenario 5.

        ii. We also proposed and simulated two theoretical-based TPC algorithms for the TN BS whose practical feasibility needs to be investigated. These techniques enabled defining ACS values for the NTN UE fulfilling the 5th percentile maximum throughput loss requirements at the cost of need for modifications on both TN UE and TN BS and additional signalling between them. The impact of the additional signalling on the TN DL throughput needs to be further investigated.

2. In the C-band, we simulated two different coexistence scenarios, identified as “high priority” earlier in the project. These simulations enabled us to define the satellite ACLR and NTN UE ACS to achieve coexistence for those two interference scenarios in the C-band. The final ACLR and ACS values of satellite and NTN UE to ensure TN-NTN coexistence for all interference scenarios in C-band can be defined after studying other coexistence scenarios and combining all the results.

For the coexistence between two NTN layers, we focused on the Q/V-band, and considered the coexistence between a GEO and a LEO 600km satellite. We simulated two different setups for inter-layer NTN coexistence:

1. Co-channel interference, in which both satellites use the same communication channel. These simulations enabled us to obtain exclusion angle, i.e., a minimum separation

between the boresight of the GEO and the LEO satellites such that the 3GPP maximum throughput loss requirements is fulfilled.

2. Interference between adjacent channels. These simulations enabled us to obtain the exclusion angle as a function of the ACIR. Indeed, the higher the ACIR, the lower the exclusion angle, and thus the longer the LEO satellite can transmit.

The results provided in this deliverable should serve as a basis for system designers to chose appropriate ACLR and ACS values for the satellites and the NTN UE, and for the exclusion angles, to enable coexistence between TN and NTN, and between several NTN layers, in the studied bands.

Finally, it is worth mentioning that part of the material presented in this document has been published in [36], which provides results for link budget computation in the C-band and the Q/V-band, and in [37], which provides part of the coexistence results between GEO and LEO satellite in the Q/V-band (i.e., part of the results provided in Section 16).

18 APPENDICES

18.1 ASSUMPTION OF ONE NTN UE PER CLUSTER

Let N be the number of NTN UEs transmitting simultaneously, i.e., the number of NTN UEs scheduled in the same time slot. Let us assume that the location of each NTN UE is independent and identically distributed, following a uniform distribution into the NTN central beam. The number of NTN UEs that fall within the TN cluster of interest thus follows a binomial distribution that can be written as:

$$\Pr(k \text{ NTN UE are located in the considered TN cluster}) = \binom{N}{k} p^k (1-p)^{N-k},$$

where p is the probability that one NTN UE falls in the TN cluster that can be expressed as:

$$p = \frac{A_r^{TN}}{A_r^{NTN}},$$

where A_r^{TN} and A_r^{NTN} represent the area of the TN cluster and the area of the NTN beam, respectively. Assuming that the TN cluster can be approximated to a circle with radius $2 \times \mathrm{ISD}$ where ISD is the inter site distance yields $\mathcal{A}_{\mathrm{TN}} = \pi(2\mathrm{ISD})^2$, whereas the area of the NTN beam at nadir can be expressed as $\mathcal{A}_{\mathrm{NTN}} = \pi R_{beam}^2$ where R_{beam} is the radius of the beam. For the Q/V-band, $\mathrm{ISD} = 200\mathrm{m}$ (cf. ***Table 14***) and $R_{beam} = 19.7/2\mathrm{km}$ for LEO@600km satellite (cf. ***Table 20***) whereas for the C-band, $\mathrm{ISD} = 450\mathrm{m}$ (cf. ***Table 16***) and $R_{beam} = 26.5/2\mathrm{km}$ for LEO@600km (cf. ***Table 24***). Plugging these values in the previously derived expressions enables us to compute the probability that k among N NTN UEs falls within the TN cluster, that is depicted in ***Figure 83*** for the Q/V-band (left) and C-band (right), assuming that $N = 10$ and $N = 15$ for the Q/V and the C-band, respectively. One can see that, for both bands:

1- The probability decreases linearly in the logarithmic domain, indicating an exponentially fast decrease in the linear domain.
2- The probability that more than one NTN UE falls into the TN cluster is very small (this probability is approximately 1.2×10^{-4} and 0.002 for the Q/V and the C-band, respectively).

This computation tells us that it is unlikely that more than one NTN UE falls into the TN cluster, thus justifying the assumption of setting a single NTN UE in the TN network of interest for the coexistence simulations.

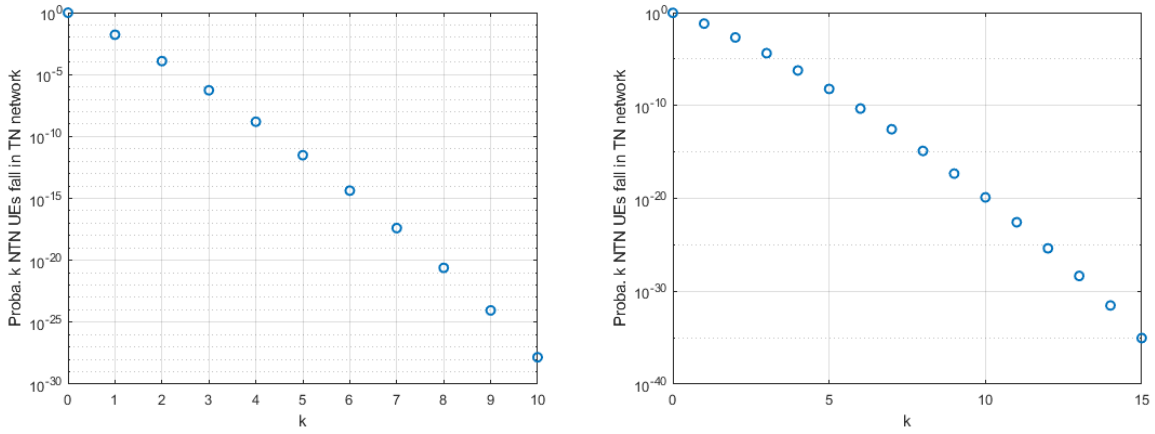

Figure 83: *Probability that k among N NTN UEs fall into a given TN cluster for the Q/V-band (left) and C-band (right)*

18.2 COMPUTATION OF THE SCALING FACTOR

The SF S_F is computed as:

$$S_F = A_F \left\lceil \frac{A_r^{NTN}}{A_r^{TN}} \right\rceil,$$

where A_F is the activity factor that is set in what follows to 0.2, and A_r^{NTN} and A_r^{TN} are defined as in section 18.1 as the areas of the NTN beam and one TN cluster, respectively. At 90° elevation, the NTN beam is a circle and thus its area can be computed as $\mathcal{A}_{\text{NTN}} = \pi R_{beam}^2$. On the other hand, the NTN beam at lower elevation is an ellipse, and additional calculations are required to compute its area. In what follows, we detail the computation of this ellipse. To do so, we extensively refer to [31] and especially to Figure 7 from this paper, that we reproduce in ***Figure 84*** for the readability.

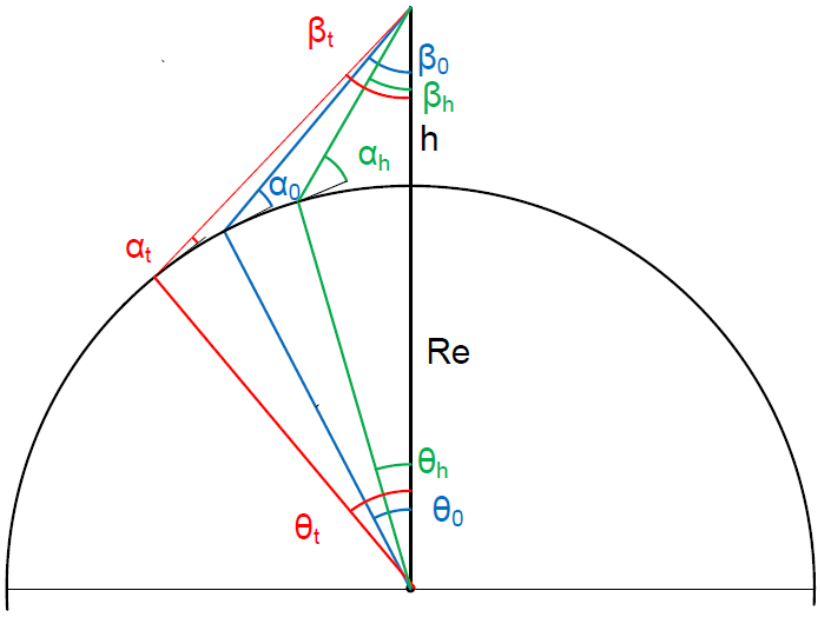

Figure 84: *extracted from [31], Figure 7. Illustration of several angles used in the computation of the ellipse area*

The area of the ellipse can be computed using Equation (19) from [31]:

$$\mathcal{A}_{\text{NTN}} = \frac{\pi}{4} F_L F_W$$

where F_L and F_W are the footprint length and footprint width, respectively, as defined in Equation (19) from [31]. To compute $\mathcal{A}_{\text{NTN}}$, we use Equation (18) from [31] that tells us:

$$F_L = R_E(\theta_t - \theta_h),$$

where R_E is the Earth radius, and θ_t and θ_h are depicted in ***Figure 84***. We can also infer from this figure and the related discussion in [31] that F_W corresponds to the diameter of the beam at nadir. We detail in what follows the computation of θ_t and θ_h.

For an elevation α_0 of the satellite with respect to the center of the beam, we compute θ_0 using Equation (4) from [31]:

$$\theta_0 = -\alpha_0 + \cos^{-1}\left(\frac{R_E}{R_E + h}\cos(\alpha_0)\right)$$

Then, one can compute β_0 according to Equation (6) from [31]:

$$\beta_0 = \frac{\pi}{2} - \alpha_0 - \theta_0.$$

One can thus deduce $\beta_h = \beta_0 - \theta_{3dB}/2$ and $\beta_t = \beta_0 + \theta_{3dB}/2$. After that, we use Equation (8) from [31] to compute $\alpha_h = \cos^{-1}\left(\frac{R_E+h}{R_E}\sin(\beta_h)\right)$ and $\alpha_t = \cos^{-1}\left(\frac{R_E+h}{R_E}\sin(\beta_t)\right)$. We can then deduce using once again Equation (4) from [31]:

$$\theta_h = -\alpha_h + \cos^{-1}\left(\frac{R_E}{R_E + h}\cos(\alpha_h)\right)$$

and

$$\theta_t = -\alpha_t + \cos^{-1}\left(\frac{R_E}{R_E + h}\cos(\alpha_t)\right)$$

For instance for LEO-600km in the Q/V band at $\alpha_0 = 30°$ elevation, one can obtain $\theta_h = 0.1286$ and $\theta_t = 0.1397$, yielding $F_L = 6371(0.1397 - 0.1286) = 70.8$ km. Moreover, since we know that the width of the beam at nadir is 19.7 km, we then obtain:

$$\mathcal{A}_{\text{NTN}} = \frac{\pi}{4} \times 19.7 \times 70.8 \text{ km}^2.$$

Finally, the obtained values for S_F in dB are provided in ***Table 39***.

18.3 DISCUSSION YIELDING NEW PARAMETERS FOR THE C-BAND

18.3.1 Introduction

This section reproduces the working paper resulting from the discussion between TF-SIX (WP4) and Thales Alenia Space (WP3) to establish a link budget analysis of a satellite access node able to support direct connectivity to a given smartphone.

It first recalls the assumptions on the targeted peak service rate, the terminals and satellite performance characteristics, the radio channel configuration and the propagation channel impairments for two satellite models considering nadir and edge cells.

Then the achievable service rate is computed thanks to the link budget calculation according to the formula in 3GPP TR 38.821 for both FDD et TDD modes.

18.3.2 Targeted service requirements

As part of the project, the targeted peak rate for a given NTN UE has been defined as:

1. DL targeted value: up to 20 Mbps.
2. UL targeted value: up to 2 Mbps.

18.3.3 Link budget assumption

18.3.3.1 Smartphone characteristics

Table 61 provides the assumptions regarding the RF parameters of the NTN UE for both TDD and FDD.

Table 61: *Assumptions for the UE RF parameters for both FDD and tdD*

UE performance in C-band (smartphone)	FDD modes		TDD modes	
	Typical	Optimized	Typical	Optimized
Antenna gain (dB)	-5	-2	-5	-2
Noise figure (dB)	7 dB		5.5 dB	
Tx power with dual antenna collocated (dBm)	26		26	

18.3.3.2 Satelitte access node characteristics

In total, four satellite configurations have been identified, all of them corresponding to a percentage of 8% active beams, with 1056 radiating elements assumption.The edge case corresponds to 45° elevation.

Case 1: FDD, $f_{Tx} = 3.4$ GHz, $f_{Rx} = 3.9$ GHz, phase-only configuration. ***Table 62*** provides the satellite parameters associated with this configuration.

Table 62: *Assumptions for the satellite parameters associated with Case 1*

Satellite parameters	Tx (DL)		Rx (UL)	
Case	Nadir	Edge	Nadir	Edge
Satellite Tx antenna gain (dBi)	35.3	33.4	NA	NA
Satellite EIRP density per radio cell, 8% active beams (dBW/MHz)	34	34	NA	NA
Satellite Rx antenna gain (dBi)	NA	NA	35.9	33.43

Satellite G/T (dB/K)	NA	NA	9.77	7.3
Satellite equivalent noise figure (dB)	NA	NA	2	2

Remark: there is a Tx loss of 1.5 dB and a Rx loss of 2 dB included in the Tx/Rx antenna gain.

Case 2: FDD, $f_{Tx} = 3.4$ GHz, $f_{Rx} = 3.9$ GHz, optimized amplitude/phase configuration with tapering. ***Table 63*** provides the satellite parameters associated with this configuration.

***Table 63**:* Assumptions for the satellite parameters associated with case 2

Satellite parameters	**Tx (DL)**		**Rx (UL)**	
Case	Nadir	Edge	Nadir	Edge
Satellite Tx antenna gain (dBi)	30.1	32.1	NA	NA
Satellite EIRP density per radio cell, 8% active beams (dBW/MHz)	34	34	NA	NA
Satellite Rx antenna gain (dBi)	NA	NA	28.73	31.84
Satellite G/T (dB/K)	NA	NA	2.6	5.71
Satellite equivalent noise figure (dB)	NA	NA	2	2

Case 3: TDD, $f_{Tx} = f_{Rx} = 3.4$ GHz, phase only configuration. ***Table 64*** provides the satellite parameters associated with this configuration.

***Table 64:** Assumptions for the satellite parameters associated with case 3*

Satellite parameters	**Tx (DL)**		**Rx (UL)**	
Case	Nadir	Edge	Nadir	Edge
Satellite Tx antenna gain (dBi)	35.8	33.9	NA	NA
Satellite EIRP density per radio cell, 8% active beams (dBW/MHz)	34	34	NA	NA
Satellite Rx antenna gain (dBi)	NA	NA	35.8	33.9
Satellite G/T (dB/K)	NA	NA	9.67	7.77
Satellite equivalent noise figure (dB)	NA	NA	2	2

Case 4: TDD, $f_{Tx} = f_{Rx} = 3.4$ GHz, optimized amplitude/phase configuration with tapering. ***Table 65*** provides the satellite parameters associated with this configuration.

Table 65: Assumptions for the satellite parameters associated with case 4

Satellite parameters	Tx (DL)		Rx (UL)	
Case	Nadir	Edge	Nadir	Edge
Satellite Tx antenna gain (dBi)	30.6	32.6	NA	NA
Satellite EIRP density per radio cell, 8% active beams (dBW/MHz)	34	34	NA	NA
Satellite Rx antenna gain (dBi)	NA	NA	30.6	32.6
Satellite G/T (dB/K)	NA	NA	4.47	6.47
Satellite equivalent noise figure (dB)	NA	NA	2	2

If all combinations of FDD UEs (two types of FDD NTN UE) with FDD satellite (four possible FDD configurations in UL/DL), and all combinations of TDD UEs (two types of TDD NTN UE) with TDD satellites (four possible TDD configurations in UL/DL) are considered, this will result in 32 different configurations (different scenarios) to be tested. More precisely, these configurations are resulted from: 2x4 combinations for FDD DL + 2x4 combinations for FDD UL + 2x4 combinations for TDD DL + 2x4 combinations for TDD UL, i.e., 32 configurations (if we consider both typical and optimized NTN UE, with cases 1/, 2/ for FDD, 3/, 4/ for TDD and both Nadir and Edge cases). We therefore focused on the most favorable configurations, i.e., Case 1/ and Case 3/ with optimized FDD/TDD NTN UE only, for both Nadir case and Edge case, which will result in only 8 scenarios to evaluate.

18.3.3.3 Radio link configuration

The assumed subcarrier spacing is 30 kHz. For the uplink, a bandwidth of 14 PRB is assumed since we found that 12 PRB are not sufficient to reach the requirements at FDD edge case or TDD at nadir. For the downlink, a bandwidth of 51 PRB is assumed.

The channel bandwidth is 20 MHz, which can be extended for a higher number of PRB.

18.3.3.4 Other parameters

We focus on LEO satellite at 600 km, and we use 6378 km for the value of the Earth radius.

18.3.4 Link budget analysis

18.3.4.1 Assesment of the achievable service requirements

FDD mode.

Table 66 provides the achievable service rate on the FDD C-band 3.9 GHz UL for LEO-600km at nadir, corresponding to 90° elevation, and edge case, corresponding to 45° elevation, in case 1, with 14 RBs and 30 kHz SCS (12 RBs not sufficient for the Edge case). One can see that the achievable uplink user peak throughput in both cases is greater that the targeted uplink max user data rate (i.e., 2 Mbps), hence the requirement is met.

Table 66: *Link budget parameters assumption and UL peak rate for C-band in FDD.*

Computed values for NTN UE located at different positions without shadowing	Nadir	Edge
Free space path loss (FSPL) (dB)	159.83	162.49
Total path loss (dB) = FSPL + other losses	159.99	162.65
Satellite figure of merit G/T (dB/K)	9.77	7.3
Rx power per PRB after Rx antenna (dBm)	-111.53	-116.66
Noise power per PRB after Rx antenna (dBm)	-116.43	-116.43
Signal to noise ratio (C/N) (dB)	4.9	-0.22
C/I (dB)	30	30
C/(N+I) (dB)	4.89	-0.23
C/(N+I) (lin)	3.08	0.95
Spectral efficiency log2(1+CINR) (bits/s/Hz)	2.03	0.96
Theoretical maximum achievable single user peak throughput (Mbps)	10.22	4.85
Single user peak throughput with imperfect coding (channel efficienty coefficient = 0.5) (Mbps)	**5.11**	**2.43**

Table 67 provides the achievable service rate on the FDD C-band 3.4 GHz DL for LEO-600km at nadir, corresponding to 90° elevation, and edge case, corresponding to 45° elevation, in case 1, with 51 RBs and 30 kHz SCS. One can see that the achievable uplink user peak throughput in both cases is greater that the targeted downlink max user data rate (i.e., 20 Mbps), hence the requirement is met.

Table 67: *LINK BUDGET PARAMETERS ASSUMPTION AND DL PEAK RATE for C-band in FDD*

Computed values for NTN UE located at different positions without shadowing	Nadir	Edge
Free space path loss (FSPL) (dB)	158.64	161.30
Total path loss (dB) = FSPL + other losses	158.80	161.45
Satellite figure of merit G/T (dB/K)	-33.62	-33.62
Rx power per PRB after Rx antenna (dBm)	-101.23	-103.89
Noise power per PRB after Rx antenna (dBm)	-111.43	-111.43

Signal to noise ratio (C/N) (dB)	10.19	7.54
C/I (dB)	30	30
C/(N+I) (dB)	10.15	7.51
C/(N+I) (lin)	10.36	5.64
Spectral efficiency log2(1+CINR) (bits/s/Hz)	3.51	2.73
Theoretical maximum achievable single user peak throughput (Mbps)	64.36	50.16
Single user peak throughput with imperfect coding (channel efficienty coefficient = 0.5) (Mbps)	**32.18**	**25.08**

Table 68 summarizes the found peak rate for both the DL and the UL at nadir and edge cell in FDD.

Table 68: *Peak rate on UL and DL for the C-band in FDD*

	UL peak rate (Mbps)	**DL peak rate (Mbps)**
Nadir	**5.11**	**32.18**
Edge	**2.43**	**25.08**

TDD mode.

Table 69 provides the achievable service rate on the TDD C-band 3.4 GHz UL for LEO-600km at nadir, corresponding to 90° elevation, and edge case, corresponding to 45° elevation, in case 3, with 14 RBs and 30 kHz SCS, and for 50% and 40% of the band for the UL. One can see that the achievable uplink user peak throughput at cell edge is lower than the targeted uplink max user data rate (i.e., 2 Mbps), hence the requirement is not met. As a consequence, we investigate in ***Table 70*** other configurations regarding the repartition between UL and DL, and regarding the number of RB. One can observe that increasing the number of RBs in UL for 50%-50% UL-DL allocation may increase the Edge cell throughput for more than 2Mbps.

Table 69: *LINK BUDGET PARAMETERS ASSUMPTION AND UL PEAK RATE FOR C-BAND IN TDD*

Computed values for NTN UE located at different positions without shadowing	**Nadir**	**Edge**
Free space path loss (FSPL) (dB)	158.64	161.30
Total path loss (dB) = FSPL + other losses	158.80	161.46
Satellite figure of merit G/T (dB/K)	9.67	7.77
Rx power per PRB after Rx antenna (dBm)	-110.44	-115.00
Noise power per PRB after Rx antenna (dBm)	-116.43	-116.43
Signal to noise ratio (C/N) (dB)	5.99	1.44

C/I (dB)	30	30
C/(N+I) (dB)	5.98	1.43
C/(N+I) (lin)	3.96	1.39
Spectral efficiency log2(1+CINR) (bits/s/Hz)	2.31	1.26
Theoretical maximum achievable single user peak throughput (Mbps)	11.64	6.34
Single user peak throughput with imperfect coding (channel efficienty coefficient = 0.5) (Mbps)	5.82	3.16
UL TDD 50% (50% in DL) frame allocation, 14 RB (Mbps)	**2.91**	**1.58**
UL TDD 40% (60% in DL) frame allocation, 14 RB (Mbps)	**2.33**	**1.27**

Table 70: *LINK BUDGET PARAMETERS ASSUMPTION AND UL PEAK RATE FOR C-BAND IN TDD for other configurations*

	Nadir	**Edge**
UL TDD 50% (50% in DL) frame allocation, 51 RB (Mbps)	**4.88**	**2.14**
UL TDD 40% (60% in DL) frame allocation, 51 RB (Mbps)	**3.91**	**1.71**
UL TDD 45% (55% in DL) frame allocation, 51 RB (Mbps)	4.39	**1.93**
UL TDD 35% (65% in DL) frame allocation, 14 RB (Mbps)	2.04	**1.11**
UL TDD 35% (65% in DL) frame allocation, 51 RB (Mbps)	3.42	**1.50**

Table 71 provides the achievable service rate on the TDD C-band 3.4 GHz UL for LEO-600km at nadir, corresponding to 90° elevation, and edge case, corresponding to 45° elevation, in case 3. One can see that the achievable downlink user peak throughput at cell edge is lower that the targeted uplink max user data rate (i.e., 20 Mbps), hence the requirement is not met. The requirement is met at nadir for 60% allocation to the DL.

Table 71: *LINK BUDGET PARAMETERS ASSUMPTION AND DL PEAK RATE FOR C-BAND IN TDD*

Computed values for NTN UE located at different positions without shadowing	**Nadir**	**Edge**
Free space path loss (FSPL) (dB)	158.64	161.30
Total path loss (dB) = FSPL + other losses	158.80	161.45
Satellite figure of merit G/T (dB/K)	-32.12	-32.12
Rx power per PRB after Rx antenna (dBm)	-101.23	-103.89

Noise power per PRB after Rx antenna (dBm)	-112.93	-112.93
Signal to noise ratio (C/N) (dB)	11.69	9.04
C/I (dB)	30	30
C/(N+I) (dB)	11.63	9.00
C/(N+I) (lin)	11.57	7.95
Spectral efficiency log2(1+CINR) (bits/s/Hz)	3.96	3.16
Theoretical maximum achievable single user peak throughput (Mbps)	74.14	59.20
Single user peak throughput with imperfect coding (channel efficienty coefficient = 0.5) (Mbps)	37.07	29.6
UL TDD 50% (50% in DL) frame allocation, 14 RB (Mbps)	**18.18**	**14.52**
UL TDD 40% (60% in DL) frame allocation, 14 RB (Mbps)	**21.82**	**17.42**

Table 72 summarizes the UL and DL peak rate at nadir and edge cell with 14 RB in UL and 51 in DL for two different allocation between DL and UL transmission time. One can observe that an allocation of 40% for the UL and 60 for the DL enables to meet the requirement of 20 Mbps at nadir. We also performed similar analysis with 78 RB in the UL and 78 RB in the UL, which is equivalent to 30 MHz of channel bandwidth with subcarrier spacing of 30 kHz. ***Table 73*** provides the obtained UL and DL peak rate at nadir and edge cell for 50-50 frame allocation between UL and DL. One can observe that in this case the minimum throughput requirements is met for both UL and DL and for both nadir and edge cell.

Table 72: *DL and UL peak rate for different UL-DL configuration in the C-band - 20 MHz CBW*

	UL peak rate (Mbps)	DL peak rate (Mbps)
50% UL - 50% DL radio frame/transmission time	**2.91 (1.58 at edge cell)**	**18.18 (14.52 at cell edge)**
40% UL - 60% DL radio frame/transmission time	**2.33 (1.27 at cell edge)**	**21.82 (17.42 at cell edge)**

Table 73: *DL AND UL PEAK RATE FOR DIFFERENT UL-DL CONFIGURATION IN THE C-BAND - 30 MHZ CBW*

	UL peak rate (Mbps)	DL peak rate (Mbps)
Nadir	**5.45**	**27.80**
Edge cell	**2.26**	**22.20**

18.3.5 Potential recommendations for improved service performance

Potential enhancements for the DL:

1. Use a lower number of beams through beam-hopping and both the power in one beam.
2. Increase the satellite antenna size and transmit power.
3. Increase the number of RB per UE.
4. Increase the NTN UE antenna gain and/or increase the number of NTN UE antennas.
5. Decrease the NTN UE noise figure.
6. Increase the satellite bandwidth, e.g. from 20 MHz to 30 MHz.

Potential enhancements for the UL:

1. Increase satellite G/T through increase satellite antenna size and lower the satellite noise figure.
2. Increase the number of RB per UE, e.g., from 14 to 51 RB, yielding a bandwidth of 20 MHz, or to 78 RB, yielding a bandwidth of 30 MHz.
3. Increase the number of transmit antennas on UE side.
4. Increase the power class on UE side, e.g., PC1.5 or PC1.

Other solutions:

1. Lower the altitudes of the satellite.
2. Increase the elevation angle of the edge cell.
3. Densify the satellite with more satellites in visibility at the same time by introducing more satellites.

18.3.6 Conclusions

The targeted service rate on both UL and DL can be met with 20 MHz channel bandwidth:

- In FDD mode for both nadir and edge cell.
- InTDD mode for nadir cell only.

The targeted service rate on both UL and DL can be met with 30 MHz channel bandwidth:

- In FDD mode for both nadir and edge cell.
- In TDD mode for both nadir and edge cell.

The range of conditions to meet the targeted service rate can be extended with possible approaches identified in Section 18.3.5, each corresponding to an increased cost of operating the constellation.

REFERENCES

[1] 3GPP TS 38.101-5, v19.2.0 (2025-09), “NR; User Equipment (UE) radio transmission and reception; Part 5: Satellite access Radio Frequency (RF) and performance requirements”, Specification # 38.101-5 (3gpp.org)

[2] 3GPP TS 38.108, v18.0.0 (2023-09), “NR; Satellite Access Node radio transmission and reception”, Specification # 38.108 (3gpp.org)

[3] 3GPP TR 38.863, v17.2.0 (2023-04), “Non-terrestrial networks (NTN) related RF and coexistence aspects”, Specification # 38.863 (3gpp.org)

[4] R4-2219076 (2022-11), “Ka-band satellite NTN band definition”, Directory Listing /ftp/tsg_ran/WG4_Radio/TSGR4_105/Docs (3gpp.org)

[5] R4-2315767, (2023-10), “Draft CR to TR 38.863 - NTN Ka band - regulatory aspects”, https://www.3gpp.org/ftp/tsg_ran/WG4_Radio/TSGR4_108bis/Docs

[6] 3GPP TR 38.811, v15.4.0 (2020-10), “Study on New Radio (NR) to support non-terrestrial networks”, Specification # 38.811 (3gpp.org)

[7] 3GPP TR 38.821, v16.2.0 (2023-04), “Solutions for NR to support Non-Terrestrial Networks (NTN)”, Specification # 38.821 (3gpp.org)

[8] 3GPP TR 38.901, v17.0.0 (2022-03), “Study on channel model for frequencies from 0.5 to 100 GHz”, Specification # 38.901 (3gpp.org)

[9] R4-2313890 (2023-08), “Simulation assumptions for NTN coexistence study in bands above 10 GHz”, Directory Listing /ftp/tsg_ran/WG4_Radio/TSGR4_108/Inbox/Drafts/[108][311]_NR_NTN_enh_Part3 (3gpp.org)

[10] ITU-R Rec. 372-16 (2022-08), P.372 : Radio noise (itu.int)

[11] ITU-R Rec. P.618-14 (2023-08), P.618 : Propagation data and prediction methods required for the design of Earth-space telecommunication systems (itu.int)

[12] R4-2312120 (2023-08), “Updates for NTN UE terminal requirements and NF in above 10 GHz”, https://www.3gpp.org/ftp/Meetings_3GPP_SYNC/RAN4/Docs/R4-2312120.zip

[13] R4-2309508 (2023-05), “Ka band UE noise figure and reference sensitivity”, https://www.3gpp.org/ftp/tsg_ran/WG4_Radio/TSGR4_107/Docs/R4-2309508.zip

[14] 3GPP TR 38.803, v14.3.0 (2022-04), “Study on new radio access technology: Radio Frequency (RF) and coexistence aspects”, Specification # 38.803 (3gpp.org)

[15] 3GPP TR 38.828, v16.1.0 (2019-10), “Cross Link Interference (CLI) handling and Remote Interference Management (RIM) for NR”, Specification # 38.828 (3gpp.org)

[16] 3GPP TR 36.942, v17.0.0 (2022-04), “Evolved Universal Terrestrial Radio Access (E-UTRA); Radio Frequency (RF) system scenarios”, Specification # 36.942 (3gpp.org)

[17] 3GPP TR 38.921, v17.1.0 (2022-05), “Study on International Mobile Telecommunications (IMT) parameters for 6.425 - 7.025 GHz, 7.025 - 7.125 GHz and 10.0 - 10.5 GHz”, Specification # 38.921 (3gpp.org)

[18] 3GPP TS 38.104, v18.2.0 (2023-06), “NR; Base Station (BS) radio transmission and reception”, Specification # 38.104 (3gpp.org)

[19] J. B. Caro et al., "Empirical study on 5G NR Adjacent Channel Coexistence," 2023 IEEE Wireless Communications and Networking Conference (WCNC), Glasgow, United Kingdom, 2023, pp. 1-6, doi: 10.1109/WCNC55385.2023.10119074.

[20] ECC Report 296, National synchronization regulatory framework options in 3400-3800

MHz: a toolbox for coexistence of MFCNs in synchronised, unsynchronised and semi-synchronised operation in 3400-3800 MHz, 2019.

[21] H. Elgendi, M. Mäenpää, T. Levanen, T. Ihalainen, S. Nielsen and M. Valkama, "Interference Measurement Methods in 5G NR: Principles and Performance," 2019 16th International Symposium on Wireless Communication Systems (ISWCS), Oulu, Finland, 2019, pp. 233-238, doi: 10.1109/ISWCS.2019.8877215.

[22] Y. Léost, M. Abdi, R. Richter and M. Jeschke, "Interference rejection combining in LTE networks," in Bell Labs Technical Journal, vol. 17, no. 1, pp. 25-49, June 2012, doi: 10.1002/bltj.21522.

[23] F. M. L. Tavares, G. Berardinelli, N. H. Mahmood, T. B. Sorensen and P. Mogensen, "On the Potential of Interference Rejection Combining in B4G Networks," 2013 IEEE 78th Vehicular Technology Conference (VTC Fall), Las Vegas, NV, USA, 2013, pp. 1-5, doi: 10.1109/VTCFall.2013.6692318.

[24] J. Wu, S. Yang, X. She, J. Wang and P. Chen, "UE MMSE-IRC Receiver for Suppressing Inter-cell and Inter-user Interference in 5G NR Standardization," 2022 IEEE 8th International Conference on Computer and Communications (ICCC), Chengdu, China, 2022, pp. 258-262, doi: 10.1109/ICCC56324.2022.10065799.

[25] ECC Report 216, Practical guidance for TDD networks synchronization, 2014, available at https://docdb.cept.org/download/1160

[26] “Reverse Spectrum Allocation for Spectrum Sharing between TN and NTN”, Hao-Wei Lee, al. , 2021 IEEE Conference on Standards for Communications and Networking (CSCN)

[27] 3GPP TR38.802 (2017-09), “Study on new radio access technology Physical layer aspects”, Specification # 38.802 (3gpp.org)

[28] Demmer, D., Zakaria, R., Doré, J. B., Gerzaguet, R., & Le Ruyet, D. (2018, October). Filter-bank OFDM transceivers for 5G and beyond. In IEEE 2018 52nd Asilomar Conference on Signals, Systems, and Computers (pp. 1057-1061).

[29] Report ITU-R M.2135-1 “Guidelines for evaluation of radio interface technologies for IMT-Advanced”

[30] *Volakis book, paragraph 1.9, Equation 1-43, R.C. Hansen “Phased Arrays” in “Antenna Engineering Handbook” by John L. Volakis, editor. McGraw Hill. 4th edition. 2007*

[31] Rainish, Doron. "Bounds on satellite system capacity and inter-constellation interference." 23rd Ka and Broadband Communications Conference,(Ka-2017), Triest, Italy. 2017.

[32] ITU-R S.1503, "Functional description to be used in developing software tools for determining conformity of non-geostationary-satellite orbit fixed-satellite service systems or networks with limits contained in Article 22 of the Radio Regulations. ", *ITU*, 2018.

[33] A. Hills, J. M. Peha, and J. Munk, “Feasibility of Using Beam Steering to Mitigate Ku-Band LEO-to-GEO Interference,” IEEE Access, vol. 10, pp. 74 023–74 032, 2022.

[34] C. Wang, D. Bian, S. Shi, J. Xu, and G. Zhang, “A Novel Cognitive Satellite Network With GEO and LEO Broadband Systems in the Downlink Case,” IEEE Access, vol. 6, pp. 25 987–26 000, 2018.

[35] M. Jalali, F. G. Ortiz-Gomez, E. Lagunas, S. Kisseleff, L. Emiliani and S. Chatzinotas, "Radio Regulation Compliance of NGSO Constellations' Interference towards GSO Ground Stations," 2022 IEEE 33rd Annual International Symposium on Personal, Indoor and Mobile Radio Communications (PIMRC), Kyoto, Japan, 2022

[36] C. Amatetti et al., "6G NTN in C and Q/V-Bands: Link Budget Analysis and Waveforms

Performance," 2024 IEEE Globecom Workshops (GC Wkshps), Cape Town, South Africa, 2024

[37] X. Leturc, D. Panaitopol, S. Tong, C. J. Le Martret, "Coexistence Study Between GEO and LEO Satellites in the Q/V-Band," 2025 IEEE 36rd Annual International Symposium on Personal, Indoor and Mobile Radio Communications (PIMRC), Istanbul, Türkey, 2025

[38] P. Henarejos, M. Á. Vázquez and A. I. Pérez-Neira, "Deep Learning For Experimental Hybrid Terrestrial and Satellite Interference Management," 2019 IEEE 20th International Workshop on Signal Processing Advances in Wireless Communications (SPAWC), Cannes, France, 2019

[39] 3GPP TR 36.102, v19.1.0 (2025-09), “Technical Specification Group Radio Access Network; Evolved Universal Terrestrial Radio Access (E-UTRA); User Equipment (UE) radio transmission and reception for satellite access”, Specification # 36.102